Table of contents

1 Riassunto dell'attività svolta

I mitocondri sono organelli essenziali per l'omeostasi cellulare. La loro funzione primaria è di produrre energia : la respirazione mitocondriale fornisce la maggior parte di ATP necessaria per le reazioni endoergoniche. Inoltre, essi regolano i livelli e i transienti di calcio citosolico e hanno un ruolo cruciale nei processi di apoptosi, invecchiamento e stress ossidativo (Jouaville et al., 1995; Wang, 2001). Il 20% della superficie mitocondriale è in stretto contatto con il reticolo endoplasmico (RE). Questa disposizione è importante per la generazione di microdomini ad alta concentrazione di calcio necessari in certe condizioni per l'attivazione dell'uniporto mitocondriale del Ca^{2+}. I siti di stretto contatto tra il RE e i mitocondri formano le cosiddette "membrane associate ai mitocondri" (MAMs), che sono cruciali per il trasporto di lipidi e Ca^{2+} tra i due organelli e hanno un ruolo anche nel processo di morte cellulare (Rizzuto et al., 1998). Sebbene i meccanismi molecolari alla base di questa stretta vicinanza tra il RE e i mitocondri siano in larga parte ignoti, si ritiene che tale interazione possa essere regolata da cambiamenti morfologici dei due organelli (Pitt set al., 1999; Simmen et al., 2005).

I mitocondri sono anche molto mobili, probabilmente allo scopo di raggiungere i siti cellulari ad alta richiesta di energia (Campello et al., 2006). Nei mammiferi il trasporto mitocondriale dipende principalmente dai microtubuli, che fungono da binari specializzati per il movimento di vari organelli, tramite l'azione di motori molecolari detti chinesine e dineine. Le chinesine regolano i movimenti anterogradi, mentre le dineine controllano il trasporto retrogrado dei mitocondri. Mentre le interazioni tra i mitocondri, l'actina e la tubulina sono state largamente caratterizzate, il ruolo dei filamenti intermedi nel controllo di movimento, forma e funzione dei mitocondri non è stato ancora chiarito. Tuttora è ignoto se l'interazione tra i filamenti intermedi e i mitocondri sia diretta o mediata da qualche proteina associata ai filamenti intermedi, fatta eccezione per l'unica proteina finora identificata, la plectina 1b (Winter et al., 2008). I filamenti intermedi potrebbero inoltre avere un ruolo nella regolazione della vicinanza tra organelli. Per esempio, in cardiomiociti privi di desmina i mitocondri perdono il loro stretto contatto con il RE (Milner et al., 2000).

Tricopleina è una nuova proteina che si lega ad un complesso costituito dalla cheratina 8 e dalla cheratina 18 (K8/K18) e che ha un basso grado di omologia con la tricoialina, la plectina e la miosina. E' stato scoperto che essa è un nuovo gene oncosoppressore, e che colocalizza con i mitocondri in cellule HeLa (Vecchione et al., 2009).

Lo scopo del mio progetto di dottorato è stato quello di studiare il ruolo della tricopleina nella morfologia e nelle dinamiche mitocondriali, e di analizzare il rapporto tra i filamenti intermedi e i mitocondri.

Per confermare l'interazione tra la tricopleina e le cheratine, abbiamo immunoprecipitato una versione della tricopleina legata all'epitopo virale V5 in cellule LnCaP che esprimessero stabilmente tale costrutto, confermando che la proteina si associa fortemente alla cheratina 8, come ci aspettavamo (Nishizawa et al., 2005). Abbiamo riscontrato che la proteina era localizzata tra i mitocondri e il complesso K8/K18 anche in cellule HeLa che overesprimessero la tricopleina. In seguito all'immunoprecipitazione della tricopleina endogena in cellule HeLa, abbiamo osservato una lieve interazione tra la proteina e l'actina. Abbiamo quindi deciso di testare se l'overespressione o il silenziamento della tricopleina potessero alterare la struttura del citoscheletro, ma non abbiamo rilevato differenze in cellule HeLa marcate con il complesso K8/K18, l'actina o la tubulina. Per confermare la parziale colocalizzazione tra la tricopleina e i mitocondri, abbiamo generato una versione della tricopleina legata alla proteina fluorescente GFP, e abbiamo analizzato se essa colocalizzasse con i mitocondri e con altri organelli quali RE, endosomi tardivi e autofagosomi, la cui forma ricordava quella del pattern puntiforme caratteristico della tricopleina. Sorprendentemente abbiamo riscontrato che la tricopleina colocalizzava parzialmente non solo con i mitocondri, ma anche con il RE. Per studiare più dettagliatamente la localizzazione submitocondriale della proteina, abbiamo generato diverse varianti della stessa legate alla GFP e di diversa lunghezza dalla porzione N-terminale della tricopleina, e ne abbiamo analizzato il grado di colocalizzazione con i mitocondri. Abbiamo riscontrato che solo l'intero costrutto di fusione tra la tricopleina e la GFP colocalizzasse parzialmente con i mitocondri. Abbiamo quindi confermato la distribuzione subcellulare dei vari costrutti di tricopleina-GFP tramite subfrazionamento cellulare e

immunoblotting.

Tramite un saggio di accessibilità alla Proteinasi K, abbiamo osservato che la tricopleina mostrava un pattern di digestione simile a quello di TOM20, una proteina localizzata sulla membrana mitocondriale esterna. Tale risultato ci ha suggerito che il dominio C.-terminale della tricopleina, fuso all'epitopo virale V5, fosse esposto verso il citoplasma. Tramite un'estrazione con carbonato, abbiamo riscontrato che la tricopleina fosse solo labilmente associata alla membrana mitocondriale esterna. Dato il suo legame con i mitocondri, ci siamo chiesti in che modo potesse avvenire l'interazione tra la tricopleina e i mitocondri. Abbiamo ipotizzato che la plectina 1b potesse essere un possibile candidato per mediare tale legame, in quanto essa aveva un basso grado di omologia con la sequenza della tricopleina, ed era stata trovata associata alla membrana mitocondriale esterna. Abbiamo silenziato la plectina 1b in cellule HeLa, e abbiamo analizzato la quantità di tricopleina associata a mitocondri isolati da tali cellule. Abbiamo osservato che l'assenza della plectina 1b diminuiva i livelli di espressione di tricopleina nei mitocondri purificati, ma non nei lisati cellulari totali. Per escludere la possibilità che l'interazione tra la plectina 1b e la tricopleina fosse indiretta e piuttosto mediata dalle citocheratine, abbiamo analizzato il pattern di localizzazione della tricopleina in linee di fibroblasti embrionari di topo (MEFs), in cui il complesso K8/K18 è assente. Abbiamo dimostrato che tale legame fosse indipendente dalla presenza delle cheratine, in quanto la distribuzione subcellulare delle varianti di tricopleina-GFP, valutata tramite subfrazionamento cellulare, si sovrapponeva perfettamente a quella ottenuta in cellule HeLa. In MEFs abbiamo riscontrato che la tricopleina frammentasse i mitocondri, come già osservato in cellule HeLa. Tale risultato ci ha suggerito che anche questa funzione della proteina fosse indipendente dal legame tra la tricopleina e il complesso K8/K18.

La distribuzione subcellulare della tricopleina ricordava quella della MFN2 (de Brito et al., 2008), tra il RE e i mitocondri. Abbiamo quindi deciso di testare se la nostra proteina fosse localizzata nelle MAMs, tramite subfrazionamento cellulare da omogenato di fegato di topo. Abbiamo riscontrato che la tricopleina fosse localizzata esclusivamente nelle MAMs. Tale compartimento è cruciale per le interazioni tra il RE e i mitocondri. Abbiamo quindi deciso di analizzare se

l'overespressione o il silenziamento di tricopleina influenzassero le interazioni tra i due organelli in cellule HeLa. Abbiamo misurato il grado di sovrapposizione tra il RE e i mitocondri tramite un approccio confocale semiquantitativo standardizzato nel nostro laboratorio, in seguito al quale abbiamo osservato che nelle cellule che overesprimevano la tricopleina la distanza tra i due organelli aumentava. Inoltre abbiamo riscontrato una riduzione dei livelli di contaminazione da RE in una frazione contenente mitocondri isolati da cellule che overesprimessero tricopleina, e un aumento da cellule in cui la proteina fosse stata silenziata. Infine abbiamo analizzato la conseguenza funzionale di questo nuovo ruolo della nostra proteina, misurando i livelli di morte cellulare indotta da vari stimoli : estrinseci, o intrinseci che non richiedessero Ca^{2+} dal RE, come tBID, che necessitassero in parte di Ca^{2+} dal RE, come la staurosporina, o che fossero completamente dipendenti da Ca^{2+} dal RE, come l'H_2O_2 (Scorrano et al., 2003). Abbiamo riscontrato che la tricopleina proteggesse cellule HeLa e MEFs da morte cellulare dipendente da Ca^{2+}. Abbiamo confermato tali dati, utilizzando cloni stabili di cellule HeLa che overesprimessero la tricopleina. Quindi abbiamo scoperto che la tricopleina, un nuovo soppressore tumorale, legata ai filamenti intermedi, è arricchita nelle MAMs, e regola negativamente l'interazione tra il RE e i mitocondri. Inoltre, la tricopleina protegge le cellule da apoptosi dipendente da Ca^{2+}. I nostri dati mostrano la rilevanza funzionale dell'interazione tra i mitocondri e i filamenti intermedi e ci inducono ad estendere la nostra analisi riguardante il rapporto tra i mitocondri e le componenti del citoscheletro.

Durante la seconda parte del mio progetto di dottorato, abbiamo quindi analizzato la funzione di TRAK1. TRAK1 è uno degli omologhi in mammifero della proteina Milton, che in Drosophila ha un ruolo essenziale per le funzioni assonali e sinaptiche, e regola il movimento mitocondriale (Stowers et al., 2002). Milton agisce formando un complesso con Miro, una Rho GTPasi, che lega la chinesina-1, tramite la sua catena pesante, alla membrana mitocondriale esterna (Glater et al., 2006). Miro ha due omologhi in mammifero, Miro-1 e Miro-2. TRAK1 colocalizza parzialmente con i mitocondri e si associa a Miro-1, Miro-2 e alla catena pesante della chinesina. Ciò suggerisce che TRAK1 possa avere una funzione simile a quella di Milton nella regolazione del movimento

mitocondriale. Abbiamo pertanto deciso di studiare la funzione di TRAK1 in vivo.

Abbiamo ottenuto dal Sanger Institute Gene Trap Resource (SIGTR) un topo in cui TRAK1 fosse stato gene-trappato (TRAK1^{gt}) tramite l'inserzione di una cassetta gene trap in una regione intronica di TRAK1, che ha causato l'ablazione di uno dei due alleli del gene TRAK1. Abbiamo amplificato la nostra colonia di topi e abbiamo ottenuto animali eterozigoti e omozigoti. I topi omozigoti sorprendentemente avevano il pelo bianco e gli occhi rossi, suggerendo un nuovo ruolo per TRAK1 nella regolazione del trasporto dei melanosomi.

2 Summary

Mitochondria are essential organelles for cellular homeostasis. Their main function is to produce energy: mitochondrial respiration provides most of the ATP required for endoergonic reactions. Furthermore, they regulate levels and transients of cytosolic calcium and are crucially involved in apoptosis, aging and oxidative stress (Jouaville et al., 1995; Wang, 2001). As much as 20% of the mitochondrial surface is in close contact with the endoplasmic reticulum (ER). This organization is important for the generation of high Ca^{2+} microdomains required to activate mitochondrial Ca^{2+} uptake under certain conditions. The sites in which ER and mitochondria are tightly bound form mitochondria-associated membranes (MAMs), that are crucial for lipid and Ca^{2+} traffic between the two organelles and are also involved in cell death (Rizzuto et al., 1998). Molecular mechanisms responsible for this ER-mitochondria juxtaposition are largely unknown, but it is thought that structural changes of either organelle could regulate the interaction (Pitts et al., 1999; Simmen et al., 2005).

Mitochondria are also very motile organelles, probably to reach cellular sites of high energy demand (Campello et al., 2006). In mammals the mitochondrial transport depends mainly on microtubules, that function as tracks for different cargoes moved by the molecular motors, kinesins and dyneins. Kinesins regulate the anterograde movements, while dyneins control the retrograde transport of mitochondria. While mitochondrial interactions with actin and tubulin have been largely characterized, the role of intermediate filaments (IFs) in controlling movement, shape and function of mitochondria is so far still unclear. Whether IFs proteins interact directly with mitochondria or the interaction is mediated by an IFs-associated protein that interacts with mitochondria is currently unknown, except for the only protein identified so far, plectin 1b (Winter et al., 2008). IFs could also be involved in regulating organelles proximity. For example, in desmin-null cardiomyocytes mitochondria lose their closeness with ER (Milner et al., 2000).

Trichoplein is a novel keratin8/18 (K8/K18)-binding protein with a low degree of homology with trichohyalin, plectin and myosin. It was found to be a novel

putative tumor suppressor gene, that partially colocalizes with mitochondria in HeLa cells (Vecchione et al., 2009).

The aim of my PhD project was to explore the role of trichoplein in mitochondrial dynamics and morphology, investigating the relationship between IFs and mitochondria.

To confirm the interaction of trichoplein with keratins, we performed an immunoprecipitation of a V5-tagged version of the protein in LnCaP cells stably expressing trichoplein-V5 and we confirmed that the protein strongly associates with keratin 8, as expected (Nishizawa et al., 2005). Also in HeLa cells, in which trichoplein was overexpressed, we found that the protein localized at the interface between K8/K18 and mitochondria. After immunoprecipitation of the endogenous trichoplein in HeLa cells, we observed also a weak interaction between the protein and actin. We therefore decided to explore the possibility that trichoplein overexpression or silencing could perturb the cytoskeleton, but we did not detect any difference in HeLa cells stained with K8/K18, actin or tubulin. To confirm that trichoplein partially colocalizes with mitochondria, we generated a GFP-version of the protein and observed if it overlapped with mitochondria and other organelles whose shape could be reminiscent of the punctuate pattern of trichoplein, like ER, late endosomes and autophagosomes. Surprisingly, we found that trichoplein partially colocalized not only with mitochondria, but also with ER. To better analyse the submitochondrial localization of the protein, we generated different GFP-variants of the protein, differing for their length from the N-terminal domain of trichoplein, and analysed their degree of colocalization with mitochondria. We found that only the full length trichoplein-GFP fusion protein partially colocalized with mitochondria. The subcellular distribution of the trichoplein-GFP constructs was further confirmed by subcellular fractionation and immunoblotting.

A Proteinase K accessibility assay showed that trichoplein displayed a digestion pattern similar to that of TOM20, a protein of the outer mitochondrial membrane. This suggested that the C-terminal domain of trichoplein, fused to the V5 epitope, is exposed to the cytoplasm. A carbonate extraction experiment showed that trichoplein is only loosely associated to the outer mitochondrial membrane. Given its binding to mitochondria, we asked how trichoplein could

interact with them. We reasoned that a possible candidate to mediate this link could be plectin 1b, that shares a low degree of sequence homology with trichoplein, and that was found associated to the outer mitochondrial membrane (OMM). We knocked-down plectin 1b in HeLa cells, and evaluated the amount of trichoplein associated with mitochondria isolated from these cells. We found that the ablation of plectin 1b decreased trichoplein expression levels in purified mitochondria, but not in total cell lysates. To rule out the possibility that plectin 1b-to-trichoplein interaction could be indirect and rather mediated by cytokeratins, we analysed the localization pattern of trichoplein in MEFs, that lack K8/K18. We could demonstrate that the binding of trichoplein is independent from the resence of keratins, since the subcellular distribution of trichoplein-GFP variants, evaluated by subcellular fractionation, was superimposable to that obtained in HeLa cells. The mitochondrial pro-fission role of trichoplein, already observed in HeLa cells, was retrieved also in MEFs, suggesting that even this function of the protein is not related to the ability of trichoplein to bind to K8/K18.

The subcellular distribution of trichoplein resembles that of MFN2 (de Brito et al., 2008), at the interface between ER and mitochondria. So we decided to analyse if also our favourite protein could localize in MAMs. When we performed a more refined subcellular fractionation of murine liver homogenates we found that trichoplein is exclusively localized in MAMs. This special compartment is crucial for interactions between ER and mitochondria. We therefore decided to analyse ER-mitochondria interactions in HeLa, after trichoplein overexpression or ablation. We measured the fraction of ER overlapping mitochondria through the confocal semiquantitative approach standardized in our laboratory, and we observed that in cells overexpressing trichoplein the distance between the two organelles increased. This effect on ER-mitochondria association was further confirmed when we detected a reduction in the amount of contaminating ER in a crude mitochondrial fraction isolated from cells overexpressing trichoplein, and an increase in cells in which trichoplein was silenced. Finally we investigated the functional consequence of this new role of our protein, analysing cellular cell death, induced by different stimuli : extrinsic or intrinsic, not requiring ER Ca^{2+}, like tBID, partially requiring

ER Ca^{2+}, like staurosporine, or completely dependent from ER Ca^{2+}, like H_2O_2 (Scorrano et al., 2003). We found that trichoplein has a protective role from Ca^{2+}-dependent cell death in HeLa cells and in MEFs, and we confirmed our data, using stable clones of HeLa cells overexpressing trichoplein. To conclude, we have found that a novel putative tumor suppressor protein, trichoplein, bound to IFs, is relatively enriched in MAMs, and negatively regulate ER-mitochondria interaction. Further, trichoplein protects cells from Ca^{2+}-dependent apoptosis. Our data indicate the functional relevance of mitochondria-IFs interaction and prompted us to extend our analysis to other linker between mitochondria and cytoskeletal components.

During the second part of my PhD project, we therefore analysed the function of TRAK1. TRAK1 is one of the mammalian orthologues of Drosophila Milton (dMilton), a protein that is essential for axonal and synaptic function and regulates the mitochondrial movement in the fruit fly (Stowers et al., 2002). dMilton functions forming a complex with Miro, a Rho GTPase, to recruit kinesin-1, via its heavy chain, to the OMM (Glater et al., 2006). Miro has two homologues in mammals, Miro-1 and Miro-2. TRAK1 partially colocalizes with mitochondria and binds to Miro-1, Miro-2 and the kinesin heavy chain. This suggests that it could have a function similar to that of dMilton, regulating the mitochondrial movement. We therefore decided to study in vivo the function of TRAK1.

We obtained from the Sanger Insitute Gene Trap Resource (SIGTR) a mouse in which TRAK1 was gene-trapped ($TRAK1^{gt}$) by inserting a gene trap cassette in an intronic region of *TRAK1*, leading to the ablation of one of the two alleles of the gene. We amplified our mice colony and we obtained heterozygous and homozygous carriers. The homozygous mice surprisingly presented a white colour coat and pink eyes, suggesting a new role for TRAK1 in the regulation of melanosomes trafficking.

3 Introduction

All eukaryotic cells are surrounded by a plasma membrane (PM), enclosing the cytosol and a variety of internal membranes and structures forming separate compartments, called organelles. Mitochondria are essential organelles for energy conversion. In addition, they contribute to the synthesis of cellular metabolites and they have been recognized as key participant in apoptosis, Ca2+ signalling, aging and oxidative stress. This functional versatility is coupled to their motility in order to rapidly arrive to sites of high energy demand, and to their morphological complexity. Mitochondria can be retrieved as independent and round-shaped organelles, or interconnected in an extended reticulum throughout the cytoplasm. Their internal structure and morphology are regulated by fusion and fission events. Mitochondria are often retrieved in close proximity with the endoplasmic reticulum. As we will discuss in further detail below, this association is pivotal in the regulation of the function of mitochondria, thereby impacting on the signalling cascades regulated by mitochondria.

We will now discuss in general the mechanisms involved in the regulation of mitochondrial shape and we will describe how the interplay between endoplasmic reticulum (ER) and mitochondria impacts on signalling cascades. We will then focus on mitochondrial motility, specifically addressing the relationship between mitochondria and intermediate filaments (IFs), so far poorly characterized.

3.1 Mitochondria

Mitochondria play a vital role in cellular maintenance and homeostasis. Most of the energy (in the form of ATP) is provided to the cell by mitochondria, placing these organelles on the center stage of many facets of cell biology and medicine. Mitochondria synthesize ATP by feeding the reducing equivalents of the main products of glycolysis, pyruvate and NADH, to two processes: the Krebs cycle and the oxidative phosphorylation.

During the Krebs cycle, enzymes present in the mitochondrial matrix remove electrons from organic compounds, generating the reduced equivalents NADH and $FADH_2$ that, together with those produced by the glycolysis, are used during oxidative phosphorylation. The electrons of NADH and $FADH_2$ are feeded to a transport chain formed by a multienzimatic complex. After several intermediate passages,these electrons are released to molecular oxygen (O_2), which is reduced and form H_2O.

To limit free energy dissipation, electrons from NADH are transferred stepwise from the inner membrane (IM)-associated respiratory chain complexes with higher redox potential to the ones with lower. Complex I (NADH dehydrogenase) catalyzes the transfer of electrons from NADH to CoQ. Complex II (succinate dehydrogenase) transfers electrons directly from succinate to CoQ. Electrons are transferred by complex III (ubiquinone-cytochrome c reductase) from reduced CoQ to cytochrome c, which in turns shuttle them to complex IV (cytochrome c oxidase). Complex IV finally catalyzes the electron transfer from cytochrome c to O_2. Electrons transfer in complexes I, III and IV is coupled to proton pumping from the matrix to the intermembrane space. The proton gradient is utilized to synthesize ATP: the F_1F_0-ATPase synthase couples the transport of these protons back across the inner membrane into the matrix with the phosphorylation of ADP to produce ATP. The synthesis of ATP from ADP and inorganic phosphate therefore employs the free energy determined by the electrical and chemical gradient generated by proton pumping across the inner mitochondrial membrane (which is highly impermeable to ions thanks to the presence of the very hydrophobic phospholipid cardiolipin). In order to efficiently operate, oxidative

phosphorylation requires a very high surface leading to maximal charge and chemical separation of protons. This is accomplished by the peculiar mitochondrial organization that we will now describe in greater detail.

3.1.1 Mitochondrial shape

In the early Fifties, George Palade recognized that mitochondria posses two lipidic membranes, reflecting their procariotic origin. He proposed that mitochondria have two very different membranes: the outer (OMM) and inner membrane (IMM). These are crucial barriers for the maintenance and integrity of two soluble compartments: the intermembrane space (IMS) and the mitochondrial matrix. This model showed that the IMM folded in ridges to the matrix from one side, and to the IMS from the other, called *cristae*, where the enzymes of respiratory chain are localized (Palade, 1952). *Cristae* increase the overall surface of the IMM, thereby maximizing the efficency of ATP synthesis. The availability of the new techniques of electron tomography, where thick samples are analyzed by a process similar to that of computer aided tomographic scanning in medical imaging, drastically changed our view of the ultrastructure of mitochondria. In particular, electron tomography showed that cristae are pleomorphic structures, shaped like bags, connected to the thin IMS through a narrow tubular junction with a diameter of about 20 nm (Frey and Mannella, 2000). This organization not only improves the surface on which the respiratory chain is developed, but also confines cytochrome c, the only soluble component of the respiratory chain, to the cristae. As we will see later, this impacts on the regulation of apoptosis.

Mitochondrial shape in living cells is very heterogeneous and can range from small spheres to interconnected tubules. (Bereiter-Hahn and Voth, 1994) (Figure 1 A, B, D). For example, mitochondria of rat cardiac muscle and diaphragm skeletal muscle appear as isolated ellipses or tubules in the embryonic stages, but then they reorganize into reticular networks in the adult (Chen et al., 2004b). The different shapes of mitochondria were already noticed

in early times by cytologists who observed this organelle under the light microscope. Noticing that mitochondrial morphology was heterogeneous, they accordingly christened this organelle ‘mitochondrion’, a combination of the Greek words for ‘thread” and “grain’. The morphological plasticity of mitochondria results from the ability of this organelle to undergo fusion and fission. Real-time imaging reveals that individual mitochondrial tubules continually move back and forth along their long axes on radial tracks. Occasionally, two mitochondrial tubules encounter each other and fuse, end to end or head to side (Kay et al., 2000). On the other hand, these tubules can also undergo fission events, giving rise to two or more mitochondrial units. It is important to note that mitochondrial fusion and fission are complicated

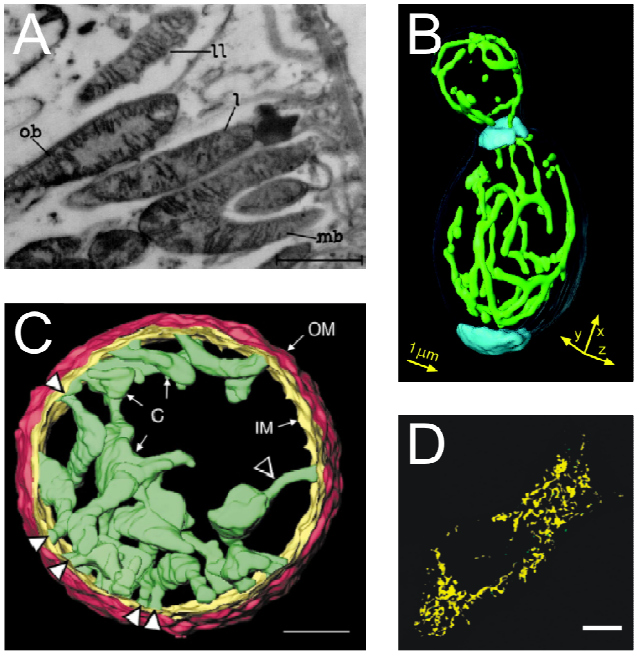

Figure 1 – **The many shapes of mitochondria**. (**A**) Mitochondria of various shapes in the epithelium of a proximal convoluted tubule of rat kidney (Magnification 27,400X; PALADE, 1953) (**B**) Surface rendered 3D stack of the mitochondrial network of *S. Cerivisiae* expressing GFP targeted to the mitochondrial matrix. Adapted from (Egner et al., 2002). (**C**) Three-dimensional reconstructions of isolated rat liver mitochondria obtained by high-voltage (1000 kV) electron microscopic tomography using two-axis tilting. OM: outer membrane, IM: inner membrane, C: selected cristae; arrowheads point to narrow tubular regions that connect cristae to periphery and to each other. □□A□□□□Ī□1□□□□□□□□□□□A□□□□□□□□□ (**D**) Morphology of a mouse embryonic fibroblast transfected with mitochondrially targeted yellow fluorescent protein. Bar, 15µm. Adapted from .

processes, being mitochondria bound by two membranes. Thus, any mechanism of fusion and fission should take into account that the coordinate fusion-division of four lipid bilayers is required to complete the process.

3.1.2 Mitochondria-shaping proteins

3.1.2.1 Proteins involved in mitochondrial fusion

3.1.2.1.1 Fzo/Mitofusin-1,-2

Proteins involved in mitochondrial morphology have been characterized in recent years. The first mediator of mitochondrial fusion to be identified was the *D*. *melanogaster* Fuzzy onions 1 protein (Fzo1), a large transmembrane (TM) guanosine triphosphatase (GTPase) required for the formation of the giant mitochondrial derivative during spermatogenesis (Pelloquin et al., 1998). The *S*. *cerevisae* ortholog of Fzo1 mediates mitochondrial fusion during mitotic growth and mating and is required for long-term maintenance of mitochondrial deoxyribonucleic acid (mtDNA) (Cipolat et al., 2004). In mammals, two widely expressed Fzo1 homologues, Mitofusin (MFN)-1 and -2, exist (Lee et al., 2004a). MFN1 and -2 display high homology (81%), similar topologies and they both reside in the OM (Harder et al., 2004). MFN1 and -2 have a GTPase domain and a coiled coil domain located at the N-terminus of the proteins, protruding towards the cytosol. Two TM regions form a U-shaped membrane anchor, ending in a cytosolic, C-terminal coiled coil motif (Ishihara et al., 2004). The coiled coil is a widespread helical structural motif functioning as oligomerization domain (Oakley and Hollenbeck, 2001). In the case of MFNs, two molecules on opposing membranes can bind in trans to bridge mitochondria, maintaining a distance of 95 Angstrom between the two membranes (Koshiba et al., 2004). Moreover, MFN2 possesses a p21RAS-binding domain at its N-terminal, which is not retrieved in MFN1 (de Brito and Scorrano, 2008) (Figure 2). In silico analysis of MFN2 reveals that this protein also has a proline-rich-domain between aminoacids 576 and 590 which is poorly conserved in MFN1 and Fzo1p. Proline-rich domains are involved in the binding to other proteins (Duvezin-Caubet et al., 2007). In spite of their high homology, MFNs are not functionally redundant. They are both involved in membrane docking, but MFN1 has a higher GTPase activity and is essential to promote OPA1-dependent mitochondrial fusion (Cipolat et al., 2004). MFN2 is

less efficient to fuse mitochondria but it localizes also on ER, regulating its morphology, and has been recently found to directly tether ER to mitochondria. MFN2 overexpression decreases the distance between the two organelles, promoting mitochondrial Ca^{2+} uptake and consequent apoptosis (de Brito and Scorrano, 2008). In cells lacking MFN2, ER loses its shape and appears swollen with separated vesicles clustered in different regions of the cell, suggesting a role for MFN2 in ER tubulation. MFN2 binds to the proto-oncogene Ras through its p21RAS-binding domain, inhibiting the activation of the downstream cascades and inducing cell cycle arrest (Chen et al., 2004a). In cells lacking MFN2, ERK1, that is one of the main downstream effectors of Ras, is hyperphosphorylated (de Brito and Scorrano).

3.1.2.1.2 Mgm1p/Msp1p/OPA1

Optic atrophy 1 (OPA1) is a dynamin-related protein located in the IMM. Mgm1p, the yeast homologue of OPA1, has been identified in a genetic screen for nuclear genes required for the maintenance of mtDNA in *S*. *cerevisae* . Years later, Pelloquin and colleagues isolated Msp1p, the *S*. *pombe* orthologue (Ferre et al., 2005). The human gene OPA1 was identified in 2000 by two independent groups (Kijima et al., 2005). A more detailed analysis showed that Mgm1p, Msp1p and OPA1 are localized in the IMS, tightly associated with the IM (Pozzan et al., 1994). These proteins, albeit they display a sequence identity of approximately 20%, maintain a highly conserved secondary structure, consisting of two predicted coiled coils, one N-terminal to the GTPase domain and the other at the C-terminus. The C-terminal coiled coil domain of OPA1 may function as a GTPase effector domain (GED; Figure 2). On its N-terminal, OPA1 possesses a mitochondrial targeting sequence (MTS) that targets the protein to mitochondria (Rizzuto et al., 1992). Studies in yeast show that MTS of Mgm1p is cleaved by the mitochondrial processing peptidase (MPP) upon import (Satoh et al., 2003).

In budding yeast the GTPase Fzo1p (Hermann et al., 1998; Rapaport et al., 1998), which protrudes towards the cytosol, interplays with the adapter Ugo1p in the outer membrane (Mannella et al., 1992), and associates with the inner membrane Mgm1p to coordinate the fusion of the four membranes of two

juxtaposed mitochondria (Nicholls and Crompton, 1980). Function of OPA1 is unclear as well as its interaction with other mitochondria shaping proteins. It has been proposed that OPA1 participates in a fission/fragmentation pathway (Duchen, 2000) or in the maintenance of the structural integrity of the mitochondrial reticulum (Danial and Korsmeyer, 2004). However OPA1 promotes the formation of a branched network of tubular and interconnected mitochondria, which spans the entire volume of the cytoplasm, as substantiated by 3D-image reconstruction and volumetric rendering of stacks of mitochondrial images. Reduction of OPA1 levels by RNA interference (RNAi) results in globular and fragmented mitochondria as a consequence of reduced fusion, specifically measured by polyethylene glycol (PEG) fusion assays. On the other hand, expression of OPA1 increases mitochondrial fusion rates. A genetic dissection of the determinants of OPA1 function reveals an absolute requirement for MFN1 but not for MFN2. Thus, OPA1 impinges on MFN1-dependent fusion to regulate morphology of the mitochondrial reticulum (Scorrano and Korsmeyer, 2003).

3.1.2.2 Proteins involved in mitochondrial fission

3.1.2.2.1 Dnm1p/DLP1/DRP1

The two proteins fission 1 (FIS1) and dynamin-related-protein 1 (DRP1) are required for mitochondrial fission in mammals. The dynamin-like-protein (Dlp) 1p in yeast, DRP-1 in *C*. *elegans*, and DLP1/DRP1 in mammals are homologues. DRP1 exists largely in a cytosolic pool, but a fraction is found at spots on mitochondria at sites of constriction (Scorrano, 2003). DRP1 contains a dynamin-like-central domain and a GED domain, in addition to its N-terminal GTPase (Figure 2). Intramolecular interaction between the GTPase and GED regions appear to be required for full GTPase activity at fission sites (Rodriguez and Lazebnik, 1999). DRP1 can oligomerize, in vitro, into ring-like structures and intermolecular oligomerization is observed at membrane constriction sites. While classical dynamins tubulate and pinch off endocytic vesicles, DRP1 family members instead encircle tubulated mitochondrial membranes (Hengartner,

2000), ultimately mediating mitochondrial fission upon the binding of particular

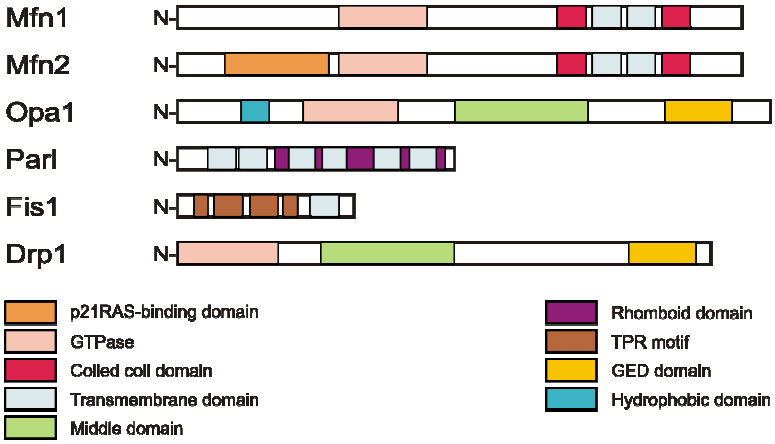

Figure 2 – **Mitochondrial morphology proteins in mammals and their domains**

protein partners and subsequent GTP hydrolysis.

3.1.2.2.2 Fis1p/hFIS1

FIS1 is a tail-anchored OMM protein facing the cytoplasm (Scorrano et al., 2002). Its N-terminal domain is exposed to the cytoplasm and forms a tetratricopeptide (TPR)-like fold (Germain et al., 2005). The C-terminal domain of FIS1 possesses a predicted TM domain and a short stretch of aminoacids facing the IMS (Figure 2). FIS1 is thought to recruit DRP1 to punctuate structures on mitochondria during mitochondrial fusion. It is therefore considered the limiting factor in the fission reaction (Stojanovski et al., 2004).

3.2 Mechanisms of mitochondrial fusion and fission

3.2.1 Yeast

3.2.1.1 Fission

Fission of mitochondrial membranes is accomplished by the recruitment of the dynamin-related large GTPase Dnm1p to the outer membrane, where it complexes with the adapter Mdv1p and the integral outer membrane protein Fis1p (Karbowski et al., 2004a). Another protein , Gag3p, interacts with Dnm1p in a yeast two-hybrid assay and might function as an essential component of the severing machinery (Karbowski et al., 2004b). The role of the GTPase cycle

of Dnm1p is still not completely understood. Since Dnm1p interacts with Mdv1p in a GTPase-dependent manner, it is possible that the GTPase cycle regulates this interaction (Hollenbeck and Saxton, 2005). There is also the possibility that constriction is Dnm1p independent, but generated by local interactions of one or more mitochondrial proteins. Such a function has been proposed for the IM protein Mdm33p (Smith et al., 1977).

How IMM is severed is still unclear, but experimental evidences suggest that separate fission machinery exists. A possible participant is Mdm33p, an IMM protein with predicted coiled-coil domains whose over expression leads to formation of inner membrane septa followed by fission of the mitochondrial reticulum. (Messerschmitt et al., 2003).

3.2.1.2 Fusion

Fusion of mitochondria can be divided in at least 3 steps: docking, fusion of the OM and fusion of the IM. During docking, two or more Fzo1p on juxtaposed mitochondria interact via their coiled coil domains. Fzo1p, Mgm1p and Ugo1p form a fusion complex that connects the IM and the OM (Hollenbeck et al., 1985). This is possible because Ugo1p contains both domains that permit the formation of bridges between Fzo1p and Mgm1p in the fusion complex. An in vitro assay showed that fusion of the OM can be separated from fusion of IM. OM requires GTP and a pH gradient across the IM. On the other hand, fusion of the IM requires the electrical component of the electrochemical gradient and high concentrations of GTP (Cereghetti et al., 2008).

Mitochondrial fusion is regulated by proteolytic processing in yeast. Mgm1p processing by the rhomboid-like protease Pcp1p is required to maintain the tubular network, although only the non-cleaved long form of Mgm1p (l-Mgm1p) is essential for mitochondrial fusion (Sesaki et al., 2003a). Further, Mgm1p processing by Pcp1p depends on mitochondrial membrane potential, meaning that the energetic status of the cell influences mitochondrial morphology (Herlan et al., 2004). In agreement with this, it has been shown that only l-Mgm1p and not its short form (s-Mgm1p) interacts with Fzo1p (Sesaki and Jensen, 2004). This means that s-Mgm1p plays a role that is different from the coupling between IM and OM fusion.

Another regulation mechanism of mitochondrial morphology may be given by the activity of Mdm30p. This protein is localized mostly in the cytoplasm, but can be also retrieved on mitochondria where it regulates mitochondrial fusion. Mdm30p possesses a F-box motif, typical of Skp1-cullin-F-box(SCF)-E3 ubiquitin ligases on its N-terminal (Dimmer and Scorrano, 2006). Mdm30p is able to target Fzo1p for degradation and by doing this it may regulate mitochondrial fusion (Escobar-Henriques et al., 2006).

3.2.2 Mammals

3.2.2.1 Fission

Mitochondrial fission in mammalian cells seems to follow the same mechanism as in yeast. DRP1 is recruited to spots on mitochondria and constriction of the membranes seems to take place via interaction with FIS1, as suggested by the ability of recombinant DRP1 and FIS1 to interact *in vitro* (Altmann et al., 2008). However, this association has never been shown *in vivo* and reduction of FIS1 levels by RNAi does not disrupt DRP1 localization to mitochondria (Linden et al., 1989). Yet, the residual level of FIS1 could still be sufficient to recruit DRP1 to mitochondria. DRP1-dependent mitochondrial fragmentation is controlled by phosphorylation at serine 616 by Cdk1 and dephosphorylation at serine 637 by the Ca^{2+}-dependent phosphatase calcineurin (Chang and Blackstone, 2007; Jahani-Asl and Slack, 2007; Taguchi et al., 2007). DRP1 forms a complex with calcineurin and cyclophilin A in the cytosol. When calcineurin is activated by a mitochondrial depolarization-dependent increase of cytosolic Ca^{2+}, it dephosphorylates DRP1, which translocates to mitochondria and induces fission of the organelle (Cereghetti et al., 2008).

Cells continually adjust the rate of mitochondrial fission and fusion in response to changing energy demands and to facilitate the distribution of mitochondria. (Wozniak et al., 2005). Recent studies have identified post-translational modifications that seem to regulate mitochondrial fission and fusion proteins. For example, DRP1 is modified post-transcriptionally by sumoylation (Garcia and Cleveland, 2001). Sumoylation is a process that involves the covalent binding of the small protein SUMO to the substrate, protecting it from binding to

ubiquitin and therefore from degradation by the proteasome (McConnell and Yaffe, 1993). Along this line, the ubiquitin ligase of the OM MARCH-V regulates targeting of DRP1 for degradation (Fuchs and Cleveland, 1998). Thus, DRP1 turnover is controlled by the equilibrium between ubiquitination and sumoylation, impacting on mitochondrial fission.

3.2.2.2 Fusion

Fusion of mammalian mitochondria is thought to occur in a similar way as in yeast. The mammalian orthologues of Fzo1p, MFN1 and MFN2, are believed to dock two juxtaposed mitochondria via their coiled coil domains (Koshiba et al., 2004). Ability of MFN2 to promote mitochondrial fusion is lower than MFN1, correlating with its GTPase activity (Lane et al., 1983). MFN2 is also localized to the ER (Hirokawa, 1982), and a role of this protein in the formation of the juxtaposition between ER an mitochondria that form the structural basis for interorganellar Ca^{2+} signalling has been proposed and recently demonstrated by our group (Pizzo and Pozzan, 2007).

In yeast, inner membrane fusion requires Mgm1, suggesting that the mammalian orthologue OPA1 is also involved in this process (Cipolat et al., 2004). Proteolytic cleavage *in vivo* releases both Mgm1 and OPA1 from the membrane, producing functionally distinct isoforms. Studies have identified several proteases that might cleave OPA1, including PARL (Frezza et al., 2006), the i-AAA protease YME1L (Frezza et al., 2006) and the human or murine m-AAA protease .

3.3 Diseases of mitochondria-shaping proteins

In the past years, mitochondrial defects have been implicated in a number of degenerative diseases, aging and cancer. Mitochondrial diseases involve mainly tissues with high energetic demands, such as muscle, heart, endocrine and renal systems. More recently, mutations in genes coding for pro-fusion proteins have been associated with genetic disorders.

3.3.1 OPA1

Mutations in OPA1 are the predominant cause of autosomal dominant optic atrophy (DOA), a degeneration of retinal ganglia cells that leads to optic nerve atrophy (Alexander et al., 2000; Delettre et al., 2000). Various pathogenic mutations are dispersed throughout the gene coding sequence, but most occur in the catalytic GTPase domain (Ferre et al., 2005). Almost 50% lead to premature truncation of the protein, and probably haploinsufficiency.

3.3.2 MFN2

In 2004, work by Zuchner et al. mapped the mutations responsible for Charcot-Marie-Tooth 2A (CMT2A), and identified *MFN2* as being the gene responsible for the disorder. CMT is one of the most common inherited disorders in humans, with an estimated prevalence of one in 2500 individuals. It is characterized by muscle weakness and axonal degradation of sensory and motor neurons (Zuchner et al., 2004). CMT neuropathies can be divided into 2 main groups, type 1 and type 2. In CMT1, nerve conduction velocities are considerably reduced. In CMT2, the nerve conduction velocities are normal but conduction amplitudes are decreased, due to the loss of nerve fibres (Zuchner and Vance, 2006).

The symptoms of CMT2A include moderate weakness and wasting of tibial muscles with lower limb hyporeflexia and mild distal sensory loss (Lawson et al., 2005).

Mutations in MFN2 account for around 20% of CMT2 cases, making this the most prevalent axonal form of CMT. Most MFN2 mutations in CMT2A cluster within the GTPase and the p21RAS-binding domains and are missense mutations (Zuchner et al., 2004; Lawson et al., 2005) (Kijima et al., 2005). Recently, a de novo truncation mutation in MFN2 has been associated to CMT2 and optic atrophy (also known as hereditary motor and sensory neuropathy VI, HMSN VI) (Zuchner et al., 2006). The similarity of the symptoms caused by MFN2 and OPA1 mutations supports the idea that these proteins are functionally linked.

MFN2 is also involved in other disorders. Its levels are reduced in obese

patients (Bach et al., 2003). Expression of MFN2 increases 24 hours after endurance exercise (Cartoni et al., 2005), and increased levels of MFN2 in developing muscle tissue correlates with more efficient mitochondrial function and energy transmission from the cell periphery to the cell core (Bach et al., 2003). Furthermore MFN2 overexpression can inhibit neointimal proliferation in rodent models of hypertension (Chen et al., 2004).

3.3.3 DRP1

Mitochondrial fission is a crucial process in polarized cells like neurons, where it regulates the translocation of mitochondria to synaptic terminals and is necessary for synaptic maintenance. Indeed, mutant DRP1 overexpression in hippocampal neurons from rat embryos impairs synaptogenesis (Li et al., 2004). Although no inherited diseases are known to result from mutation of DRP1, a defect of this protein caused one case of neonatal lethality (Waterham et al., 2007). This patient showed symptoms like optic atrophy, microcephalia with abnormal brain development, truncal hypotonia with little spontaneous movement and no tendon reflexes. These defects were accompanied by persistent lactic acidemia in plasma and cerebrospinal fluid, and a mildly elevated plasma concentration of very-long-chain fatty acids. This patient presented a defect in mitochondrial and peroxisomal fragmentation. The peroxisomes appeared fewer and had abnormal shape and mitochondria were extremely elongated, tangled, clustered in the peri-nuclear region. A dominant-negative mutation of DRP1 was responsible for these abnormalities, since the reintroduction of the wild-type protein rescued the normal phenotype. This mutation resulted in the substitution of alanine with aspartic acid at position 395, corresponding to the middle domain of DRP1.

3.4 Ca^{2+} signalling and mitochondria

Calcium ions (Ca^{2+}) control and influence a diverse array of cellular processes such as muscle contraction, gene expression, energy metabolism, proliferation and cell death. Maintenance of physiological levels of intracellular Ca^{2+} depends on the hierarchic interactions between plasma membrane pathways, mediating import and release of Ca^{2+}, and the action of several intracellular organelles, which serve to store and discharge Ca^{2+} in response to a variety of cellular cues. Cells normally maintain a low resting "free" Ca^{2+} concentration in the cytosol ($[Ca^{2+}]_c$) of more or less 100 nM. This contrasts with 1 mM in the extracellular fluid. In order to achieve this low resting $[Ca^{2+}]_c$, cells remove Ca^{2+} using two energy-dependent mechanisms. First, plasma membrane Ca^{2+} ATPases (PMCA) pump Ca^{2+} out of the cell against a concentration gradient, consuming ATP in this process. Second, the Na^+ -Ca^{2+} exchanger (NCX) uses the electrochemical Na^+ gradient to extrude Ca2+. In addition, eukaryotic cells can sequester Ca^{2+} into intracellular organelles. Electron probe analysis provided direct evidence of increased amounts of Ca^{2+} in the ER and mitochondria (Somlyo et al, 1978). Organellar Ca^{2+} sequestration requires either ATP hydrolysis or a favourable electrochemical gradient. Release channels help deliver Ca^{2+} to the required cellular location. This enables the generation of Ca^{2+} signals that can be small or large in amplitude, restricted to a small microdomain or global across the cell.

3.4.1 Ca^{2+} in the endoplasmic reticulum

The ER functions as the main Ca^{2+} store of mammalian cells. It accumulates Ca^{2+} via SERCA pumps and releases it through ryanodine receptors (RYRs) and IP_3 receptors (IP_3Rs). The SERCA pump is encoded by a family of three genes (SERCA1, 2 and 3) that are highly conserved and expressed at various levels in different tissues and stages of development (Clapham, 2007). There are also three isoforms of RyRs and three isoforms of IP_3Rs that are tissue specific and change during development and in disease (Rizzuto, 2006).

Calreticulin, an ER protein, functions as major Ca^{2+} buffer (Pozzan et al., 1994). ER chaperones also bind Ca^{2+} and at least 50 uM Ca^{2+} is required in the ER for protein folding activity. (Gorlach et al., 2006). The concentration of Ca^{2+} in the ER ($[Ca^{2+}]_{ER}$) is estimated to be between 400 and 800 µM (Pinton et al., 1998).

The molecular nature of Ca^{2+} leakage from ER stores is still not completely characterized. It is known that IP_3Rs are activated by inositol-1,4,5-phosphate (IP_3) and ,as RyRs, mediate rapid release of the stored Ca^{2+} (Berridge et al., 2003). There have been proposed leak pathways, that involve other channel candidates, like polycystin-2 (Weber et al., 2008; Koulen et al., 2002), presenilins (Tu et al., 2006) and the ribosome-translocon complex (Lomax et al., 2002; Van Coppenolle et al., 2004).

3.4.2 Ca^{2+}-uptake by mitochondria

During the past decade, the study of mitochondrial Ca^{2+} handling became one of the fastest growing areas of calcium signalling. Targeting of the photoprotein aequorin to mitochondria demonstrated that stimulating a cell with a G-protein-coupled receptor agonist known to release Ca^{2+} from intracellular stores, leads to rapid, large and transient changes in mitochondrial calcium concentration ($[Ca^{2+}]_m$) (Rizzuto et al., 1992). Indeed mitochondria serve as physiological buffers of intracellular Ca^{2+} (Pozzan and Rizzuto, 2000; Bernardi et al., 2001; Ishii et al., 2006). The IP_3R/Ryr-linked $[Ca^{2+}]_c$ oscillations induce activation of the Ca^{2+}-dependent mitochondrial matrix dehydrogenases and ATP production (Jouaville et al., 1999). By taking up Ca^{2+} , mitochondria can both reduce the positive feedback of Ca^{2+} on IP_3-mediated Ca^{2+} release and prevent feedback inhibition of Ca^{2+} on Ca^{2+} release (Landolfi et al., 1998). Mitochondria may also help recycle Ca^{2+} back to the ER, thus facilitating efficient refilling of the Ca^{2+} store (Arnaudeau et al., 2001). In isolated mitochondria Ca^{2+} uptake is driven by the -180 mV membrane potential across the IMM. Since mitochondria accumulate Ca^{2+} via a low-affinity, high-capacity process, rapid elevation of mitochondrial calcium concentration ($[Ca^{2+}]_m$) requires a substantial increase in $[Ca^{2+}]_c$ around the organelle. IP_3-mediated Ca^{2+} release is very efficient at elevating $[Ca^{2+}]_m$ and generation of a transient microdomain of highly elevated

Ca^{2+} at the sites of Ca^{2+} release facilitates the $[Ca^{2+}]_m$ response (Rizzuto et al., 1993; Rizzuto et al., 1998). Targeting of aequorin to the IMS indicates that the Ca^{2+} in the vicinity of the microdomain is at least 10 µM. Ca^{2+} entry into mitochondria involves transport through both the OMM and IMM. The calcium uniporter is responsible for $[Ca^{2+}]_m$ uptake through the IMM. In addition to the uniporter, a Ca^{2+} uptake mechanism, termed the rapid uptake mode (RaM), has been reported to mediate fast uptake of short Ca^{2+} pulses in the range of 400 nM in isolated liver and cardiac mitochondria. The voltage-dependent anion channel (VDAC) has been thought to form large pores that allow free passage of Ca^{2+} through the OMM. Its open configuration is permeable to molecules up to about 5000 Da and so, Ca^{2+} and many small molecules were believed to freely traverse the OMM through the pores formed by the VDAC (Mannella et al., 1992). However, recent studies challenged the idea that the OMM is freely permeable to Ca^{2+} and suggest that Ca^{2+} permeation through the VDAC may be a tightly controlled process in the cells. Since both the IP_3R/RyRs and VDAC are linked to the cytoskeleton, these interactions may also be important in positioning the VDAC between the IP_3R/RyRs and the Ca^{2+} uptake sites in the IMM. Ca^{2+} export occurs via the Na^+-Ca^{2+} and H^+-Ca^{2+} transporters (Nicholls and Crompton, 1980). Mitochondria exhibit $[Ca^{2+}]_m$ activation waves that are propagated throughout the cells. The regenerative mechanism of these waves depends on neighbouring mitochondria and does not require continuity of the mitochondrial membranes and the matrix space (Duvezin-Caubet et al., 2007; Hajnoczky et al., 2001).

Recent evidence suggests there are physical tethers between the ER and mitochondria. Subdomains of the ER membrane are close to the mitochondria and these regions appear to have a major role in calcium signal propagation to the mitochondria. Immuno-electronmicroscopy studies as well as Ca^{2+} transport measurements suggest that IP_3R/RyRs are concentrated and form clusters in the ER membrane aligned with the mitochondria (Hajnoczky et al., 2000). These sites form membrane microdomains of high Ca^{2+} concentration, the mitochondria-associated ER membranes or MAMs (Rizzuto et al., 1993). Disrupting the integrity of the mitochondrial network limits $[Ca^{2+}]_m$ responses to mitochondrial fragments close to the ER. (Szabadkai et al., 2003).

Mitochondrial Ca^{2+} overload is associated with cell death. In the presence of increased ADP, this can lead to opening of the permeability transition pore, collapse of the mitochondrial membrane potential, release of cytochrome *c* and activation of the pro-apoptotic caspase cascade (Duchen, 2000). Pro- and anti-apoptotic protein regulators have a marked effect on the interplay of Ca^{2+} between the ER an mitochondria. Bax and Bak lead to increased $[Ca^{2+}]_{ER}$ which in turn leads to increased $[Ca^{2+}]_m$ uptake whereas anti-apoptotic Bcl-2 tends to reduce the ER load and thereby protect the mitochondria from Ca^{2+} overload (Giacomello et al., 2007).

3.5 Mitochondria and Apoptosis

The term 'apoptosis' was first introduced in 1972 by John Kerr to designate common morphological features of programmed cell death (Kerr et al., 1972). In multicellular organisms, apoptosis ensures the precise and orderly elimination of surplus or damaged cells. Cell death during embryonic development is essential for successful organogenesis and crafting of complex multicellular tissues; during adulthood it ensures the maintenance of normal cellular homeostasis. Conditions that increase or decrease normal cell death levels in different tissues can result in disease: insufficient apoptosis manifests as cancer or autoimmunity, while accelerated cell death is evident in acute and chronic degenerative diseases, immunodeficiency and infertility (Danial and Korsmeyer, 2004). Mitochondria play a key role in the regulation of cell death, and mitochondrial dynamics constitutes an integral part of the pathways leading to the demise of the cell.

3.5.1 The apoptotic cascade

The most studied protein cofactor released by mitochondria in response to an apoptotic stimulus is cytochrome *c* (Liu et al., 1996). Nevertheless, the precise mechanism whereby cytochrome *c* and other mitochondrial intermembrane space proteins are released is still under active investigation. Several

hypothesis have been proposed to explain the egress of cytochrome *c* from mitochondria; these mechanisms may either function on their own or in cooperation: (i) in response to an apoptotic stimulus, BAX or BAK are activated and form pores on the outer mitochondrial membrane, permitting the release of cytochrome *c*. (ii) proapoptotic BCL-2 family members interact with intrinsic proteins of mitochondria, triggering mitochondrial dysfunction and permeability transition. (iii) mitochondrial membrane permeabilization may result from an alteration in membrane curvature or from the formation of lipidic pores in the OM.

Independently from the precise mechanism of cytochrome *c* egress from mitochondria, the BCL-2 family proteins appear as critical death regulators. This family of proteins, consisting of both pro- and anti- apoptotic members, possesses conserved α-helices with sequence conservation clustered in BCL-2 homology (BH) domains. Antiapoptotic members exhibit the homology in all segments from BH1 to 4, while proapoptotic molecules lack stringent sequence conservation of the first α-helical BH4 domain. Proapoptotic molecules can be further subdivided into multidomain and BH3-only proteins. Multidomain proapoptotic members such as BAX and BAK display sequence conservation in BH1-3 domains. BH3-only members display sequence conservation solely in the amphipathic α-helical BH3 region (Scorrano and Korsmeyer, 2003). Nowadays it is clear that the decision to die or not depends on the balance resulting from the activation of proapoptotic and antiapoptotic members of the BCL-2 family (Danial and Korsmeyer, 2004; Szabadkai and Rizzuto, 2004). Once activated, BH3-only proteins function as ligands for the multidomain proapoptotics BAX and BAK, induce their homo/hetero-oligomerization and ultimately release cytochrome *c* from mitochondria (Scorrano, 2003). As mentioned above, other mechanisms (for example: permeability transition or alteration of membrane curvature) may cooperate with multidomain proapoptotics during cytochrome *c* release.

Once released, cytosolic cytochrome *c* binds to APAF-1, increasing its affinity for dATP/ATP. The complex composed by APAF-1, cytochrome c, dATP and ATP forms the apoptosome. The apoptosome is able to recruit procaspase-9, facilitate its auto-activation and subsequently leads to the activation of

downstream executioner caspases, cysteine proteases, that effect cell demise (Zou et al., 1999) (Rodriguez and Lazebnik, 1999). Executioner caspases then cleave other intracellular substrates leading to the characteristic morphological changes in apoptosis such as chromatin condensation, nucloesomal DNA fragmentation, nuclear membrane breakdown, externalization of phosphatidylserine (PS) and formation of apoptotic bodies (Hengartner, 2000).

3.5.2 Mitochondrial morphology and apoptosis

Multiple studies have substantiated a link between mitochondrial dynamics and the classical apoptotic pathway. In mammals loss of MFN1, MFN2 or OPA1 leads to mitochondrial fragmentation and increases sensitivity to cell death stimuli (Olichon et al., 2003; Sugioka et al., 2004; Lee et al., 2004b), while overexpression of these proteins leads to better survival in several cell types. Mitochondrial fragmentation is a classical step that precedes apoptosis in most cell types. Studies in yeast confirm a role for mitochondrial fission and for DRP1 in apoptosis (Fannjiang et al., 2004). In mammals apoptotic DRP1-dependent mitochondrial fragmentation is associated with opening of the cristae structure and mobilization of cytochrome *c*, which can then be rapidly released upon OMM permeabilization (Scorrano et al., 2002). Consequently, interfering with mitochondrial fission using a dominant-negative DRP1 prevents the reorganization of the *cristae*, dampening cytochrome *c* release and caspase activation (Germain et al., 2005). In the last years it has been discovered that the key player in the regulation of cristae remodeling is OPA1 (Cipolat et al., 2006; Frezza et al., 2006; Yamaguchi et al., 2008). OPA1 forms oligomers comprising both the membrane-bound and soluble forms of the protein. Oligomers destabilization precedes cytochrome c release and apoptosis. The rhomboid protease Parl has a crucial role in the proper assembly of these oligomers. Indeed, in cells lacking Parl, oligomerization of OPA1 is impaired, resulting in a higher sensitivity to apoptosis.

Another mitochondria shaping protein linked to apoptosis is Fis1, whose overexpression induces cell death (James et al., 2003), that can be blocked by scavengers of reactive oxygen species and by mutations in the short domain of Fis1 in the IMS (Alirol et al., 2006). However, cell death is not always

consequent and connected to mitochondrial fission. For example MFN2 overexpression can induce apoptosis (Huang et al., 2007), while DRP1 can slow down the amplification of Ca^{2+}-mediated cell death (Szabadkai et al., 2004). In addition, in *C*. *elegans* cell death is amplified by processing of DRP1 by the caspase CED-3 (Breckenridge et al., 2008).

There are evidences that proteins that regulate mitochondrial morphology are connected with Bax/Bak-dependent apoptosis. Indeed, DRP1 and MFN2 have been found located at the same foci formed by BAX and BAK on the OMM (Karbowski et al., 2004a) and Bax translocation increases the percentage of DRP1 that is stably bound to the mitochondrial surface. DRP1 accumulates on mitochondria between completion of fission and initiation of cytochrome c release (Wasiak et al., 2007) and it seems to act downstream of Bax because its silencing has no effect on Bax translocation (Lee et al., 2004b; Karbowski et al., 2002). However there are some evidences that the role of DRP1 in mitochondrial fission is independent from its involvement in Bax/Bak-mediated apoptosis. For example, the use of a novel inhibitor of DRP1 attenuates permeabilization of the OMM in isolated mitochondria, even if fission did not take place in this system (Cassidy-Stone et al., 2008). There are several post-translational modifications of DRP1 that indirectly regulate cell death, among which the phosphorylation of serine 637 by proteine kinase A (PKA), that slows apoptosis, preventing translocation of DRP1 to mitochondria (Cribbs and Strack, 2007). Also MFN2 colocalizes at foci with Bax. It has been observed that when MFN2 is restricted outside these foci, Bax translocation is blocked and MFN2 spreads homogenously in the OMM in Bax/Bcl-2 homologous antagonist killer (Bak) deficient cells (Neuspiel et al., 2005; Karbowski et al., 2006).

Other proteins involved in mitochondrial fusion/fission are linked to apoptosis. For example Endophilin B1 (Bif-1, SH3GLB1), a protein of the endophilin family that plays a role in membrane dynamics, has been shown to regulate both mitochondrial dynamics and activation of BAX (Karbowski et al., 2004b).

3.6 Mitochondrial movement

The cytoskeleton consists of three major protein families, microtubules (MTs), microfilaments (MFs) and intermediate filaments (IFs). Microtubules are polar tubular assemblies formed by tubulin, a globular protein, which constitutes heterodimers composed of two subunits α and β that exhibit cell-specific microheterogeneity (Gozes and Littauer, 1978; Gozes and Sweadner, 1981). MTs are built from 13 to 15 laterally associated tubulin protofilaments. Tubulin is characterized by a nucleotidase activity, so that MTs polymerize spontaneously in vitro in the presence of GTP and Mg^{2+}.

Microfilaments are polar helical filaments made of two linear strands of actin subunits twisted around each other with an axial stagger of half a subunit. There are three types of actin, α, β and γ. α-actin is expressed in muscle cells, β and γ-actin constitute MFs of non-muscle cells.

Intermediate filaments consist of a large group of proteins that are expressed in a tissue-specific manner (Hermann et al., 2007; Kim and Coulombe, 2007) and that constitute the major part of the nucleoskeleton, the nuclear lamina. They are formed by fibrous proteins that consist of a conserved central α-helical rod domain flanked by non-α-helical N-(head) and C-terminal (tail) domains. Intermediate filaments usually adopt a rope-like structure by forming multistranded left-handed coiled coils (Parry et al., 2007).

Studies. in a wide variety of cell types indicate that mitochondria co-localize with all three protein families. However, the mechanisms of mitochondrial trafficking are different in yeast, animals, and plants.

3.6.1 Mitochondrial movement in neurons

The first observations describing differential positioning of mitochondria in cultured cells were reported nearly a century ago (Lewis and Lewis, 1914). Mitochondrial movement and distribution have been studied in details in neurons. It has been appreciated for many years that mitochondria may move rapidly and over relatively long distances (Hollenbeck and Saxton, 2005). In the Fifties, electron microscopy studies showed that mitochondria typically cluster at

synaptic terminals (Palay, 1956), eliminating the concept that the architecture of the mitochondrial network is the outcome of a random distribution process of the organelle, and introducing the possibility that proper mitochondria trafficking and partitioning inside the cell could provide functional support to the execution of key physiological processes (Smith et al., 1977). Mitochondria are typically located at sites of high ATP demand, including synapses, growth cones, nodes of Ranvier and myelination-demyelination interfaces (Hollenbeck and Saxton, 2005). The pool of stationary mitochondria located at synaptic and dendritic terminals likely support bioenergetic and calcium buffering requirements for dendritic development and synaptic plasticity. (Cohen and Greenberg, 2008). Mitochondrial dynamics in neurons are clear and easy to observe. One can develop a scheme that envisages the generation of new mitochondria in the proximity of the neuronal nucleus, the movement of mitochondria to sites of high ATP demand or calcium influx, the functioning of mitochondria at those sites for a finite period of time and then the trafficking of old and dysfunctional mitochondria to a subcellular graveyard for their autophagic demise (Chang and Reynolds, 2006).

Mitochondrial movements occur both away from the nucleus (anterograde transport) and toward the center of the cell and nucleus (retrograde transport). Mitochondria undergo saltatory anterograde and retrograde movement while retaining their identity as discrete organelles. Individual organelles are readily observed to start, stop, move over distances of tens or hundreds of microns at a velocity of several microns per second and to change direction of movement. Among the moving mitochondrial subpopulation 90% of the organelles with high membrane potential move anterogradely. Conversely, 81% of mitochondria showing low membrane potential are transported in the opposite direction, toward the cell body (Miller and Sheetz, 2004). The alternation of saltatory movement and being stationary is presumably a regulated process. This includes the regulation of the attachment of mitochondria to the main motor proteins, and also includes docking or anchoring of mitochondria to static sites such as actin as well as other as yet unidentified cellular entities.

Inhibition of mitochondrial motility has been shown to correlate with altered Na^+, K^+ or calcium ionic balance and application of nerve growth factor (Borgdorff et

al., 2000) (Nicholls et al., 2000; Chada and Hollenbeck, 2003). Mitochondria also respond to synaptic stimulation, where an increase in synaptic activity increases the probability that mitochondria will stop at a post-synaptic site. Conversely, inhibiting synaptic activity with tetrodotoxin results in an overall increase in mitochondrial motility, perhaps reflecting a reduction in calcium mediated docking (Li et al., 2004; Chang et al., 2006; Mironov, 2006). Mitochondrial oxidative phosphorylation uncoupling agents like CCCP also induce calcium transients and inhibit mitochondrial transport. However, this seems to be a non-specific effect, independent of mitochondrial depolarization and calcium release (Hollenbeck et al., 1985) because other uncouplers, such as DNP, FCCP, and PCP, and complex III inhibitors like Antimycin A, increase or have no effect on mitochondrial transport (Bereiter-Hahn and Voth, 1988). Alterations in the activity of fission or fusion proteins clearly has an impact on trafficking of mitochondria (Benard and Rossignol, 2008; Popov et al., 2005; Verstreken et al., 2005), but the nature of the interplay between the formation of mitochondrial networks and the dynamic distribution of mitochondria within neurons remains unclear. Conversely, perturbations of cytoskeleton can alter mitochondrial morphology. For example inhibition of MFs, MTs or IFs causes mitochondrial fragmentation (Kumemura et al., 2007). Recently, a mechanism of regulation of DRP1-mediated fission has been reported which links high calcium levels associated with excitotoxicity and mitochondrial fission. Elevated calcium may activate calcineurin which in turn dephosphorylates DRP1. DRP1 is then translocated to mitochondria where it induces fission (Cereghetti et al., 2008).

Impaired mitochondrial transport is associated with oxidative stress and cellular dysfunction (Stamer et al., 2002). Factors that impact the mobility of mitochondria could impair neuronal viability. There is a growing body of evidence that proteins associated with neurodegenerative disease can impact axonal transport of organelles in general and mitochondria in particular, probably via the formation of aggregates in neuronal processes. One example of this is provided by neurons expressing expanded polyglutamine forms of huntingtin, the protein responsible for Huntington's disease. In these neurons aggregates were invariably associated with mitochondria, and regions of the

neurite around the aggregate displayed less mitochondrial movement (Chang et al., 2006). There are a number of reports that describe other interactions with mitochondrial trafficking, including decreased mitochondrial velocity (Trushina et al., 2004), and an impairment of the association of mitochondria with microtubule-based transport proteins (Orr et al., 2008).

3.6.1.1 Actin

3.6.1.1.1 Yeast

In the budding yeast *S. cerevisiae*, mitochondria predominantly interact with the actin cytoskeleton and use actin tracks for both anterograde and retrograde movements during cell division and for tubulation and DNA inheritance. Numerous mutations in genes encoding actin or factors involved in actin filament dynamics lead to aberrant mitochondrial distribution and morphology (Drubin et al., 1993; Lazzarino et al., 1994; Simon et al., 1995; Smith et al., 1995; Hermann et al., 1997; Simon et al., 1997; Yang et al., 1999; Singer et al., 2000; Boldogh et al., 2001b; Altmann and Westermann, 2005).

A number of yeast mitochondrial morphology proteins have been shown to interact with actin. Mmm1p, Mdm10p, Mdm12p, and Mmm2p, localized on the OMM, assemble to form high molecular weight complexes that might bind mitochondrial DNA to cytoskeleton. Mmm1p crosses both the OMM and IMM and it is necessary for the interaction between mitochondria and actin. Mdm31p and Mdm32p are inner membrane proteins that genetically interact with the OM proteins, and are involved in the binding of actin to mitochondrial DNA (Dimmer and Scorrano, 2006). Mitochondria are propelled by Arp2/3-mediated actin polymerization; Arp2/3 complex colocalizes with mitochondria probably through its interaction with Jsn1p, a peripheral protein of the OM (Boldogh et al., 2001a). Motor proteins of actin are the myosins. The myosin family consists of at least 15 structurally and functionally distinct classes and the class V myosin motor protein, Myo2, seems to play a major role in mitochondrial motility (Altmann et al., 2008).

3.6.1.1.2 Mammals

In neurons, actin MFs assist MTs during short distance mitochondrial movements, in particular in cellular zones where microtubules are absent, and have a role in anchoring mitochondria to specific cellular sites of high energy demand (Hollenbeck and Saxton, 2005). Several forms of myosin are found in neuronal processes, myosin I, II, V and VI, but myosin V may be the most likely form to be involved in mitochondrial attachment and movement along actin fibers. A further confirmation of a role for actin in the regulation of mitochondrial movement came from the recent discovery that depletion of Gα12, a protein which positively regulates actin polymerization through the Rho pathway (Riobo and Manning, 2005), increases mitochondrial motility (Andreeva et al., 2008).

3.6.1.2 **Microtubules**

In some filamentous fungi, in *S*. *pombe* and in higher eukaryotes mitochondrial transport depends on MTs (Yaffe et al., 2003).

3.6.1.2.1 Mammals

The primary mechanism for long-distance movement of mitochondria in neurons requires MTs. Mitochondria move along MTs through specific MTs-associated proteins (MAPs). Some MAPs act as “roadblocks” when an increase in their content inhibited cellular transport (Mandelkow et al., 2004; Ebneth et al., 1998). MAP2 binds to the OMM through the interaction with the porin VDAC (Linden et al., 1989) inducing a physiochemical change in the porin region. Kinases that regulate the affinity to microtubules (MARK) and Par1 are extremely efficient to detach the MAPs from microtubules.

It is clear that anterograde axonal movement of mitochondria is generated by plus end-directed kinesins (KIFs), the molecular motors that convey cargoes along MTs. The members of six KIFs families are involved in organelle transport. Among them, kinesin-1 and kinesin-3 appear to contribute to the mitochondrial movement, in particular KIF5B and KIF1Bα (Hollenbeck and Saxton, 2005). KIF5B has been found to be associated with the OMM. The few mitochondrial proteins that have been shown to anchor the organelle to KIFs

include Miro1 and Miro2, KBP, Syntabulin and Syntaphilin (SNPH). Miro1 and Miro2 are homologues of Drosophila Miro, a mitochondrial Rho-like GTPase protein essential for maintenance of mitochondrial morphology and movement. Miro1 and Miro2 in mammals have been found located on the OMM where they interact with the motor domain of kinesin-1, regulating anterograde movement of mitochondria. KIF1-binding protein (KBP) is a novel protein which colocalizes with mitochondria and binds to KIF1Bα. KBP appears essential for a proper distribution of mitochondria in the cell and increases KIF1Bα motility in vitro. However it is not confirmed that KBP is the direct mediator of mitochondria- KIF1Bα interaction (Wozniak et al., 2005). Syntabulin is a peripheral membrane-associated protein, relatively enriched in the mitochondrial fraction, which seems to play a critical role in the anterograde transport of mitochondria. It appears crucial for mitochondrial trafficking, since knock-down of syntabulin expression or competitive blocking of the syntabulin-kinesin interaction reduces mitochondrial density at synaptic terminals (Cai et al., 2005). A study from the laboratory of Sheng reported a role for axon-targeted SNPH in mitochondrial docking. Axonal mitochondria that contain exogenously or endogenously expressed SNPH lose mobility. Deletion of the mouse *snph* gene results in a substantially higher proportion of axonal mitochondria in the mobile state and reduces the density of mitochondria in axons, a phenotype that is fully rescued by reintroducing the *snph* gene into the mutant neurons. The *snph* mutant neurons exhibit enhanced short-term facilitation during prolonged stimulation, probably by affecting calcium signalling at presynaptic boutons (Kang et al., 2008).

The microtubule associated protein tau interferes with the attachment of cargoes to kinesin-based motors, so that tau overexpression results in the accumulation of mitochondria near the minus end of MTs in the center of the cell (Ebneth et al., 1998). In primary neurons, tau overexpression results in the depletion of mitochondria from neuritis (Stamer et al., 2002). Phosphorylation of tau results in its dissociation from MTs and their subsequent destabilization (Stoothoff and Jhonson, 2005) which would interrupt the delivery of mitochondria to key cellular sites. When tau is hyperphosphorylated it forms neurofibrillary tangles that are one of the hallmarks of Alzheimer's disease

(Garcia and Cleveland, 2001).

Dyneins are the molecular motors that generate minus-end directed mitochondrial movement. There are far fewer dynein in vertebrates compared to the extensive family of KIFs, and cargo specificity is likely provided by a range of accessory proteins. It has been observed that dyneins associate with mitochondria, probably via the interaction with VDAC (Schwarzer et al., 2002).

3.6.1.2.2 D. Melanogaster

In *Drosophila* mitochondrial movement and distribution depend on the microtubule motor as well as on the actin cytoskeleton of the cell (Pereira et al., 1997).

Milton, an essential gene, was previously identified in a mosaic screen for mutants in axonal and synaptic function in the *Drosophila* eye (Stowers et al., 2002). Recently it has been discovered to be a motor adaptor protein that links kinesin-1 to mitochondria. The mammalian orthologues of Milton are $GABA_A$ receptor-interacting factor 1 (GRIF-1) and O-linked N-acetylglucosamine transferase-interacting protein (OIP106) (Brickley et al., 2008). In Milton null flies synapses form normally but they lack mitochondria in axons and presynaptic terminals. Furthermore, once transfected into HEK 293T cells, Milton induces a redistribution of mitochondria within the cell (Stowers et al., 2002), supporting a role in organelle distribution in any cell type. Miro (mitochondrial Rho) is an OMM protein, conserved from yeast to mammals, that is found in complexes with Milton to facilitate the recruitment of Milton to the mitochondria (Glater et al., 2006). Miro belongs to a family of highly conserved eukaryotic proteins required for mitochondrial distribution and morphology (Frederick et al., 2004). Whereas mammals have two Miro family members, Miro-1 and Miro-2 (Fransson et al., 2003), yeast has only one, Gem1p (Frederick et al., 2004). Their structural organization is similar and includes two cytosolic GTPase domains separated by a linker region containing a pair of calcium-binding EF-hand folds and a carboxyl-terminal transmembrane domain for anchoring to the OMM (Wolff et al., 1999). Thus, Miro proteins appear to have bona fide CaM calcium-binding domains, which are known to govern

structural changes and protein activity by coordinated binding to calcium (Lewit-Bentley and Rety, 2000). Indeed Wang and Schwarz showed that KIFs are present on axonal mitochondria, including those that are stationary or moving retrograde, and that the EF-hand motifs of Miro mediate calcium-dependent arrest of mitochondria. Rather than dissociating kinesin-1 from mitochondria, calcium-binding permits Miro to interact directly with the motor domain of kinesin-1, preventing motor/microtubule interactions. Thus, kinesin-1 switches from an active state in which it is bound to Miro only via Milton, to an inactive state in which direct binding to Miro prevents its interaction with MTs. Recently also Pink1, a kinase targeted in part to mitochondria and whose recessive mutations lead to Parkinson disease, has been identified as a member of this multi-protein complex formed by Milton, Miro and kinesin-1 (Weihofen et al., 2009).

3.6.1.3 Intermediate filaments

3.6.1.3.1 Yeast

It is known that mutations of Mdm1p cause an abnormal mitochondrial morphology and defects in mitochondrial growing and movement in yeast. Mdm1p is a protein distributed throughout the cytoplasm and it has a similarity with some proteins of mammals IFs, like vimentin and keratin (McConnell and Yaffe, 1992), although it does not form in vivo a reticulum of filaments (McConnell and Yaffe, 1993).

3.6.1.3.2 Mammals

Mammals posses five types of IFs. The first four are cytoplasmic IFs proteins. Acid (type I) and basic keratins (type II) are found in epithelial cell. Vimentin, desmin, glial fibrillary acidic protein (GFAP) and peripherin (type III) are expressed in mesenchymal, muscle, glial and neuronal cells, respectively. α-internexin and neurofilaments (type IV) are localized in neurons and cells of the peripheral neuroendocrine system. Lamins, which form a meshwork of proteins at the inner layer of the nuclear membrane are type V IFs. The major role of IFs

is to provide a dynamic intracellular scaffolding structure to the cytoplasm and to protect cells and tissues from mechanical stress .

The IFs system has been shown to associate with membranous organelles such as mitochondria, Golgi apparatus and vesicles, as well as with other cytoskeletal components such as actin filaments, microtubules and their associated molecular motors (Herrmann et al., 2007; Tzur et al., 2006; Toivola et al., 2005). Mitochondrial associations with vimentin IFs were first described by electron microscopy (Goldman and Follett, 1969; Goldman, 1971) and a role for IFs in mitochondrial distribution was demonstrated by the disruption of vimentin filaments in CV-1 cells after exposure to cycloheximide, but the relation between the mitochondria and the IFs has been unclear except in the case of desmin (Capetanaki et al., 2007).

Among the various families and subfamilies of IFs proteins, that of the keratins is outstanding due to its high molecular diversity. Keratins (Ks), the IFs proteins of epithelial cells, constitute a family of at least 20 proteins divided into two subclasses, namely K9-K20 and K1-K8 (Moll et al., 1982; Schweizer et al., 2006). They are obligate heteropolymers of members of the two subclasses, co-ordinately expressed as distinct pairs in a differentiation-dependent manner (Coulombe and Wong, 2004). There is evidence that mitochondria interplay with keratins. Mutation of K5 affects mitochondrial distribution (Uttam et al., 1996) and absence of K19 in mice causes skeletal myopathy with mitochondrial and sarcolemmal reorganization (Stone et al., 2007).

K8/K18 are the first IFs proteins to be expressed during embryogenesis (Lane et al., 1983). They are widely distributed among normal epithelial tissues although they are absent in differentiating keratinocytes. K8 and K18 are not strictly epithelium-specific since their expression may occur in rare mesenchymal cells such as certain smooth muscle cells and fibroblastic reticulum cells of lymph nodes as well as various mesenchymal tumors including rhabdo- and leiomyosarcomas (van Muijen et al., 1987; Langbein et al., 1989), where they are co-expressed with other IF types, notably vimentin and desmin. In some epithelial cell types, K8 and K18 are the sole keratins present. The classical example is the liver, with K8/K18 representing the characteristic and only keratin pair of normal hepatocytes. Since the loss of one

keratin normally leads to the degradation of its partner, hepatocytes provide a unique cell model to address the functions of these simple epithelium keratins (Ku and Omary, 2000; Oshima et al., 1996). Most important, there is ample evidence demonstrating an involvement for K8 and K18 in human liver disease development, based on the discovery that single point mutations in K8 and K18 genes lead to IFs disorganization and predispose to cirrhosis, a degenerative condition that largely arises from Fas-induced apoptosis (Oshima, 2002). Structural and mechanical functions are not the key roles of K8/K18. They play a role in protecting the placental barrier function (Jaquemar et al., 2003) and protecting cells from apoptosis (Caulin et al., 2000; Ku et al., 2003), against stress, and from injury (Zatloukal et al., 2000; Ku et al., 2003). Finally, it has been observed that mutation in keratin 18 induces mitochondrial fragmentation in liver-derived epithelial cells (Kumemura et al., 2007)

Desmin, a vimentin-like protein of IFs, is probably the most characterized for its physical and functional interaction with mitochondria, in particular in cardiomyocytes. A desmin knockout mouse shows strong alterations of mitochondrial distribution, number, morphology and function (Milner et al., 2000). This mouse dies of dilated cardiomyopathy and heart failure. Loss of proper mitochondrial positioning in desmin-null cardiomyocytes leads to loss of proximity to other organelles, including endoplasmic/sarcoplasmic reticulum (ER/SR) (Milner et al., 2000). A potential role of desmin or other IFs in ER/SR-mitochondria crosstalk seems likely (Figure 3).

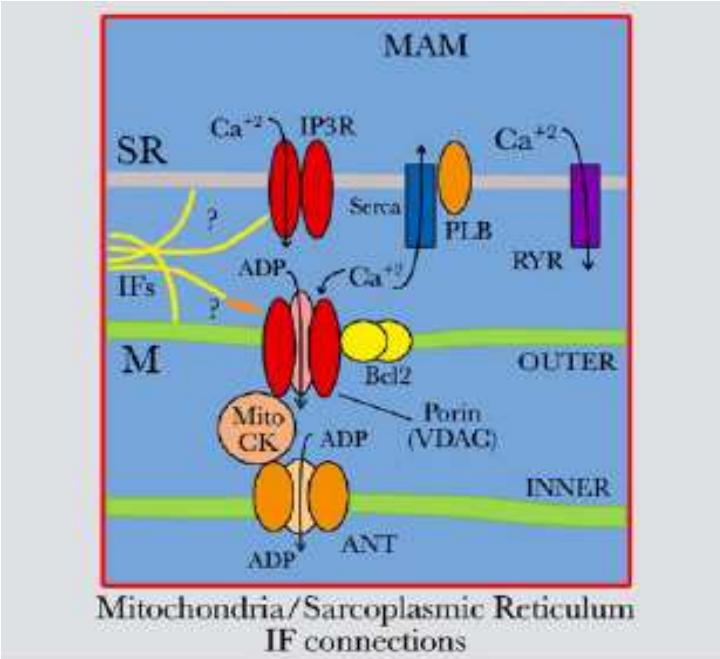

Figure 3. Schematic representation of the IF scaffold in MAMs and mitochondrial contact sites in cardiac muscle (Capetanaki et al., 2007)

A major vimentin- and general IFs-binding protein which constitutes an important organizing element of IF network cytoarchitecture is plectin (Foisner et al., 1988; Tian et al., 2006). Plectin belongs to a group of structurally related proteins, referred to as the plakin protein family (Fuchs and Karakesisoglou, 2001; Sonnenberg and Liem, 2007). It is the most common cytolinker and it plays a role in dynamic cellular processes and as an IFs-based multifaceted scaffolding protein, it recruits a variety of signalling molecules to the cytoskeleton. It associates with vimentin from the early stages of assembly and is required for vimentin motility as well as for the stepwise formation of stable IFs. Being involved in structural as well as dynamic aspects of all three of the major cytoskeletal filament network systems (Rezniczek et al., 2004; Andra et al., 1998), plectin is likely to emerge as a central player in many cellular processes requiring cytoskeletal restructuring and reorganization. Plectin colocalizes with desmin in muscle cells and has been found in proximity with the OMM (Reipert et al., 1999). Plectin's versatility is due in part to complex splicing events in the N-terminal region of its gene giving rise to 11 alternatively spliced isoforms containing different first exons (Fuchs et al., 1999). One of these isoforms, plectin 1b, is targeted to the OMM (Rezniczek et al., 2003), where it acts as a direct linker between IFs and the mitochondrial network. Plectin 1b deficiency leads to elongation of mitochondrial networks without affecting the overall mitochondrial mass. (Winter et al., 2008).

3.7 ER-mitochondria interaction

The analysis of a wide variety of plant and animal tissues revealed close relationships between mitochondria and ER already in the late Sixties (Ruby et al., 1969). The frequency and appearance of these contacts led some researchers to propose that the OMM was an extension of the ER (Bracker and Grove, 1971). In 1973 Lewis and Tata demonstrated that mitochondria are enmeshed or entangled by the ER and that this association might have a functional relevance (Lewis and Tata, 1973).

It is now well documented that ER and mitochondria cooperate with each other in the control of physiological functions like metabolism, calcium signalling and apoptosis. As much as 20% of the mitochondrial surface is in direct contact with the ER, underscoring the dynamic and highly regulated communication between the ER and mitochondria (Rizzuto et al., 1998). This functional association is transient and dynamic (Filippin et al., 2003). Coupling between these two organelles can be weakened by rupture of this interorganellar protein linkage (Csordas et al., 2006). Evidence supports the hypothesis that the movement of mitochondria might occur concomitantly and in synchrony with that of specific ER regions. The mechanism of this reciprocal organelle-docking remains unresolved but it has been proposed that it depends on the expression on both membranes of complementary proteins that link the two organelles together, possibly at specific sites (Pizzo and Pozzan, 2007).

The biochemical site of ER interaction with mitochondria is represented by the mitochondria associated membranes (MAMs), which are ER-contiguous membranes tightly associated with the mitochondria. MAMs co-isolate with mitochondria but can be separated from the latter by centrifugation on a Percoll gradient (Vance, 1990). Several studies proposed that MAMs associate with contact sites between IMM and OMM (Ardail et al., 1991; Ardail et al., 1993; Gaigg et al., 1995). MAMs appear to serve as a nexus, where proapoptotic and antiapoptotic machineries as well as cellular stress sensors converge. They are enriched, compared with the bulk of ER, in several phospholipid- and

glycosphingolipid-synthesizing enzymes, including fatty acid CoA ligase 4 (FACL4), which exchanges the head group of phosphatidylcholine with serine, and phosphatidylserine synthase-1 (PSS-1), and are involved in lipid traffic to and from mitochondria (Vance, 1990) . Furthermore MAMs form membrane microdomains of high calcium concentration (Rizzuto et al., 1993; Filippin et al., 2003) (Wang et al., 2000). Indeed, a major role of MAMs is to propagate calcium signal to mitochondria. Disruption of this network blocks calcium trafficking along ER and mitochondria (Rapizzi et al., 2002) (Rizzuto and Pozzan, 2006). Recently GM1-ganglioside, one of the sialic acid-containing glycosphingolipids (GSLs), has been found accumulated in GSL-enriched microdomains, within the MAMs, where it influences calcium flux between the ER and the mitochondria (Sano et al., 2009). Immuno-electronmicroscopy studies as well as calcium transport measurements suggest that IP_3R/RyRs and SERCA pumps are concentrated in the ER/SR membrane aligned with the mitochondria (Hajnoczky et al., 2000; Csordas and Hajnoczky, 2001). Other specific ER and mitochondrial proteins have been identified to colocalize in the MAMs. These include the molecular chaperone glucose-regulated-protein 75 (grp75), Sigma-1 receptor (Sig-1R), calreticulin, PACS-2 and MFN2 (Simmen et al., 2005) (Szabadkai et al., 2006; Hayashi and Su, 2007; de Brito and Scorrano, 2008). Another protein that seems to be involved in metabolic flow, calcium and cell death signalling between the ER and mitochondrial networks is VDAC. Indeed VDAC has been discovered to be physically linked to the ER calcium release channel IP_3R, through grp75 (Szabadkai et al., 2006).

MAMs are enriched in key chaperones that may play a role in regulating calcium signalling between ER and mitochondria. Specifically, Hayashi et al., identified a new, yet novel ER “ligand-operated” chaperone that specifically targets MAMs, the Sig-1R chaperone. Moreover they noted that under physiological conditions Sig-1R is retained in the MAMs. Upon ER stress, Sig-1Rs redistributes from MAMs to the periphery of the ER. Interestingly, they also found that Sig-1Rs and isoform 3 of IP_3R co-localize and associate at MAMs. Thus, Sig-1Rs forms a calcium-sensitive chaperone machinery with GRP78/BiP and prolongs calcium signalling from the ER to mitochondria by stabilizing IP_3R-3 at MAMs (Hayashi and Su, 2007).

PACS2, a multifunctional sorting protein, indirectly links the ER to mitochondria and controls Bid-mediated apoptosis. It binds to dephosphorylated Bid and it is required to traffic full-length Bid to the mitochondria, where Bid is subsequently cleaved to tBid, leading to the release of cytochrome *c*, the activation of caspase-3, and cell death. (Simmen et al., 2005). Absence of PACS-2 induces the caspase-dependent cleavage of BAP31 to yield the proapoptotic fragment p20, causing mitochondria to fragment and uncouple from the ER. This structural uncoupling also disrupts MAMs and induces ER stress, which is compensated for by increased levels of BiP and ER calcium. Furthermore, PACS-2 mediates the levels of MAM-associated FACL4, thus regulating MAM formation.

The interactions between ER and mitochondria seem to be modulated by the "mitochondria-shaping proteins". DRP1 can alter tethering of the two organelles by causing perinuclear clumping of mitochondria (Pitts et al., 1999). Further, it has recently been discovered by our laboratory that MFN2 directly tethers ER to mitochondria by means of transorganellar homotypic and heterotypic interactions between MFN2 localized on the ER and MFN1 or MFN2 on the surface of mitochondria. Ablation or silencing of MFN2 in mouse embryonic fibroblasts and HeLa cells disrupts ER morphology and loosens ER-mitochondria interactions. The RAS-binding and the GTPase domain of MFN2 result essential to regulate ER shape and ER to mitochondria connection. Tethering ER to mitochondria, MFN2 increases IP_3R calcium uptake to mitochondria (de Brito and Scorrano, 2008).

Alterations in the operation of the ER/mitochondrial couple provide a pathway for activating apoptosis (Pinton et al., 2008). The key process connecting apoptosis to ER-mitochondria interactions is an alteration in calcium homeostatic mechanisms that results in massive and/or a prolonged mitochondrial calcium overload. The switch from a life to a death signal occur when its normal distribution between the ER and the mitochondria is distorted leading to a breakdown of mitochondrial function. Impairment of ER functioning, including depletion of ER calcium stores, induced by protein expression, alteration or by chemical agents (e.g. H_2O_2, arachidonic acid); block of the proteasome that is required to degrade unfolded proteins (e.g. tunicamycin and

brefeldin A); or genetic mutations resulting in proteins that cannot be properly folded, can induce apoptosis (Ferri and Kroemer, 2001). IP_3R-3 plays a selective role in the induction of apoptosis by preferentially transmitting apoptotic calcium signals into mitochondria, whereas IP_3R-1 predominantly mediates cytosolic calcium mobilization (Mendes et al., 2005).

3.8 Trichoplein

Trichoplein was originally identified in a yeast two-hybrid screening of a human liver cDNA library as a K8-binding protein. This association was mediated by the C-terminal portion of the novel protein. Using the same approach, it was found that the same fragment of trichoplein (73-498) binds to K5, K6a, K14, K16 and K18. The full-length protein interacted with KIFs, most strongly with K16 and K18. The association between trichoplein and K8/18 filaments was further supported by a subset of experiments that showed that trichoplein is expressed ubiquitously and is characterized by a punctuate distribution throughout the cytoplasm, which colocalizes with K8/18 filaments. Trichoplein is associated with K8/18 filaments both in interphase and in mitosis (Nishizawa et al., 2005). However, the observation that trichoplein is expressed not only in epithelial tissues but also in non-epithelial tissues where keratins are absent, suggests that the protein may have other functions independent of keratin IFs. The *Trichoplein* gene localizes at 12q24.1 and its open reading frame is constituted by 498 amino acids with a molecular mass of 61 kDa. The name “Trichoplein” derives from its low degree of sequence similarity to trichohyalin, plectin and myosin heavy chain (Nishizawa et al., 2004). Indeed, the region of its sequence residues 259-415, designated the trichohyalin/plectin homology domain (TPHD), shows 23% or 31% amino acid identity with the region of residues 334-471 of human trichohyalin or residues 1365-1460 of murine plectin 1, respectively (Nishizawa et al., 2004). Proteins that show homology to trichohyalin and plectin, AJM-1 (Koppen et al., 2001) and Fbf-1 (Schmidt et al.,

2000) have been identified. AJM-1 is a coiled-coil protein localizing to an apical junctional domain of *C*. *elegans* epithelia basal to the HMR-HMP (cadherin-catenin) complex. In the absence of AJM-1, the integrity of this domain is compromised. Fbf-1 binds to the cytosolic domain of the murine death receptor CD95/APO-1/FAS.

A novel role for trichoplein has been identified by Baffa and coworkers. Designated with a new name, Mitostatin, trichoplein was identified in a screening for growth-arrested gene induced by the leucine-rich proteoglycan decorin, a soluble protein that inhibits migration (Grant et al., 2002), invasion (Xu et al., 2002) and tumorigenicity of a wide variety of tumoral and normal cells. *Trichoplein* was found to be a novel putative tumor suppressor gene (Vecchione et al., 2009). Indeed it is localized in a chromosomal region deleted in a large variety of solid advanced tumours (Aubele et al., 2000; Field et al., 1995; Kimura et al., 1998). Trichoplein affects prostate cancer cell growth and cell death by regulating the level and activation of Hsp27. Its expression is reduced in advanced primary bladder, breast and prostate tumors. It was also observed that trichoplein partially colocalizes with mitochondria in HeLa cells. (Vecchione, 2009) Furthermore, trichoplein was found to inhibit cell migration, invasion and tumorigenicity of prostate cancer.

5 Results

Cerqua C., Anesti V., Baffa R., Dimmer K.S., Scorrano L.
Trichoplein negatively regulates ER-mitochondria juxtaposition

Cerqua C., Scorrano L.
Trak1 participates in melanocyte trafficking

Trichoplein negatively regulates ER-mitochondria juxtaposition

Cristina Cerqua[1], Vassiliki Anesti[1], Raffaele Baffa[2], Kai Stefan Dimmer[1], and Luca Scorrano[1,3]

[1]*Dulbecco-Telethon Institute, Venetian Institute of Molecular Medicine, Via Orus 2, 35129 Padova, Italy;*

[2]*Kimmel Cancer Center and Department of Pathology, Thomas Jefferson University, Philadelphia, PA 19107, USA*

[3]*Department of Cell Physiology and Medicine, University of Geneva, 1 Rue M. Servet, 1211 Geneve, Switzerland*

Address correspondence to

Luca Scorrano. Email: luca.scorrano@unige.ch

Running Title: trichoplein and ER-mitochondria interactions

Character count: 25509

Abstract

Trichoplein is a keratin-binding protein of unclear function that partially colocalizes with mitochondria and is frequently downregulated in epithelial cancers. Here we report that trichoplein is enriched in mitochondria-associated membranes, *i.e.* at the juxtaposition between mitochondria and endoplasmic reticulum, and regulates their tethering. Association of full length trichoplein with the outer mitochondrial membrane requires the mitochondrial protein plectin 1b, but not keratin. Expression of trichoplein loosens mitochondria-endoplasmic reticulum tethering and accordingly inhibits apoptosis by Ca^{2+} dependent stimuli. Our data indicate a role for a cytoskeleton-binding element at the interface between mitochondria and endoplasmic reticulum.

Keywords: mitochondria/ endoplasmic reticulum/ trichoplein/ intermediate filaments/ apoptosis

Introduction

The location of mitochondria in the cytoplasm is controlled by the concerted action of organelle fusion/fission (Anesti and Scorrano, 2006), movement along microtubular tracks (Liu and Hajnoczky, 2009) and anchoring at defined sites (Capetanaki, 2002). Mitochondria can be immobilized via their binding to components of the cytoskeleton such as intermediate filaments (IFs) (Anesti *et al.*, 2006), accomplished by ad hoc mitochondrial molecules, like plectin 1b, the only linker of mitochondria to IFs identified so far (Winter et al., 2008). Such an organization allows for example the dynamic mitochondrial redistribution at sites of greater energy demand (Campello et al., 2006) and permits that mitochondria remain juxtaposed to the endoplasmic reticulum (ER). Mitochondria-ER tethering is required for mitochondrial lipid biosynthesis and delivery, for efficient Ca^{2+} uptake by mitochondria and for the amplification of Ca^{2+} dependent apoptosis (Hayashi et al., 2009).

The molecular basis of ER-mitochondria juxtaposition is starting to be unraveled, thanks to the possibility to purify the Mitochondria Associated Membranes (MAMs), patches of ER attached to the outer mitochondrial membrane (OMM) (Vance, 1990). The ER Ca^{2+} channel inositol triphosphate receptor (IP3R) (Szabadkai et al., 2006) and several enzymes of the lipid biosynthetic pathway (Stone and Vance, 2000) are enriched in MAMs. Chaperones [heat shock protein (HSP) 70 (Szabadkai et al., 2006); the transmembrane protein Sigma-1 (Hayashi and Su, 2007)] and kinases like PACS-2 (Simmen et al., 2005) are also enriched in MAMs. Levels of these proteins impact on the juxtaposition between ER and mitochondria, even if their effect seems indirect (Simmen *et al.*, 2005;Hayashi *et al.*, 2007). On the other hand, the first structural tether identified between the two organelles in mammalian cells is the mitochondria-shaping protein Mitofusin (Mfn) 2, whose ablation loosens the interaction between ER and mitochondria (de Brito and Scorrano, 2008). Components of the cytoskeleton like the IFs could also participate

in the tethering, as suggested by (i) the dynamic nature of the interaction (Rizzuto *et al.*, 1998), compatible with a role for ER and mitochondrial movement along microtubules (Liu *et al.*, 2009;Bola and Allan, 2009) (ii) the increased distance between ER and mitochondria cardiomyocytes lacking the IF desmin (Milner *et al.*, 2000).

Trichoplein (also called Mitostatin, TpMs) is a protein originally identified as a keratin interactor. It displays weak homology to trichohyalin, plectin and myosin and binds to keratins 8 and 18 (Nishizawa *et al.*, 2005), the two major components of the IFs in epithelial cells (Fuchs, 1996). The genomic locus of TpMs (12q24) is a hotspot of allelic deletion in a variety of cancers. A more careful analysis of TpMs subcellular localization revealed that it partially colocalizes with mitochondria, and that cells with higher TpMs levels display reduced growth and an increase in the response to apoptosis by intrinsic stimuli. (Vecchione *et al.*, 2009). The role of IFs in these functions of TpMs is unclear. Here we set out to characterize the mitochondrial role(s) of TpMs. Our results indicate that trichoplein is a previously uncharacterized MAM protein that negatively regulate the interaction between mitochondria and ER.

Results

TpMs localizes at the interface between keratins and mitochondria

TpMs, a keratin-binding protein, is partially retrieved on mitochondria (Vecchione *et al.*, 2009). Given our unsuccessful attempts to immunoprecipitate endogenous TpMs (not shown), we confirmed that TpMs is able to interact with keratins 8/18 (Nishizawa *et al.*, 2005) and that it displays s somehow increased affinity for keratin 8 by immunoprecipitating a TpMs-V5 chimeric protein stably expressed in LnCaP cells (Vecchione *et al.*, 2009) (Fig. 1A). In the reverse immunoprecipitation, we did not retrieve endogenous TpMs interacting with keratins (not sshown), but a small fraction was pulled down by actin (Fig. 1B). As expected (Nishizawa *et al.*, 2005), other IFs (vimentin) and cytoskeletal components (tubulin) did not interact with TpMs (not shown). Since TpMs has the ability to interact at least with two components of the cytoskeleton, we tested whether levels of TpMs affected its organization. Efficient silencing or transient overexpression of TpMs, verified by immunoblotting (Fig. S1), did not affect IFs, actin or microtubules, as judged by specific immunofluorescence (Fig. 1C). Thus, changes in levels of TpMs do not alter the overall cytoskeletal architecture.

Given that endogenous or expressed TpMs displays a punctuate pattern, partially overlapping with mitochondria (Nishizawa *et al.*, 2005;Vecchione *et al.*, 2009) we decided to verify whether these puncta were at the interface between mitochondria and keratin. We coexpressed a mitochondrially targeted cyan fluorescent protein (mtCFP) with TpMs-V5 and we immunostained for V5 and for keratins. A confocal analysis of the immunofluorescence pattern (Fig. 1D) showed that: (i) mitochondria and keratins can colocalize (pale cyan in the magnification); (ii) TpMs and keratins can also colocalize, as judged by the appearance of green areas; (iii) TpMs and mitochondria are often overlapping (magenta areas); (iv) several areas contain the colocalization between mitochondria, TpMs and keratins (white). However, this

experiment also revealed that not all TpMs is on mitochondria, prompting us to investigate the subcellular distribution of the protein in more detail.

Full length TpMs associates with the OMM: role of plectin 1b

TpMs lacks a canonical mitochondrial targeting sequence, or a clear transmembrane domain that could insert it into the mitochondrial membrane(s). Is then TpMs targeted to mitochondria? We analyzed the colocalization pattern of a TpMs-GFP chimera with several organelles. TpMs-GFP partially colocalized with a cotransfected dsRED targeted to mitochondria (mtRFP), with dsRED targeted to the ER, but not with autophagosomes (marked by GFP-LC3) or late endosomes (stained using the specific marker mannose-6-phosphate receptor), two other organelles whose shape could be reminiscent of the TpMs puncta (Fig. 2A). Thus, TpMs partially colocalizes with mitochondria and ER. We next decided to map the part of the protein required for the mitochondrial localization. We constructed a series of chimeras containing fragments of TpMs fused with GFP at the C-terminus: four of them (Δ1 to Δ4) represented increasing length of the N-terminus of the protein, while in the fifth (Δ5) GFP was fused to the trichohyalin-plectin homology domain of TpMs (Nishizawa *et al.*, 2005). In coexpression experiments with mtRFP, Δ1, Δ2 and Δ5 remained completely cytoplasmic, Δ3 and Δ4 displayed a partially punctuate pattern that partially overlapped with mtRFP, as judged by confocal microscopy (Fig. 2B). Subcellular fractions prepared from HeLa cells transfected with Δ1, Δ4 and full length TpMs-GFP confirmed that Δ1 was retrieved mostly in the LDH positive cytoplasmic fraction, while Δ4 and to a greater extent full length TpMs-GFP were present in the MnSOD positive mitochondrial fraction. Of note, Δ4 and full length TpMs were also present in the ER fraction (Fig. 2C). These experiments revealed that the first ~120 or the last ~240 aminoacids are not sufficient for the

punctuate pattern of full length TpMs that colocalizes with mitochondria; and that full length TpMs is mostly mitochondrial, but also found in the ER.

We next addressed the submitochondrial localization of full length TpMs. When purified mitochondria from HeLa cells were treated with proteinase K, TpMs was completely degraded like the OMM marker TOM20, while the inner membrane (IMM) and the matrix markers OPA1 and GRP75 were protected (Fig. 2D), indicating that TpMs is localized on the OMM. When we incubated mitochondria in Na_2CO_3 (pH=11), TpMs, like the loosely attached Bax and actin, were retrieved in the supernatant, while integral proteins like TOM20 remained in the membranous pellet following centrifugation (Fig. 2D). Thus TpMs is loosely attached to the OMM.

How does TpMs associate with mitochondria? Given the presence of a plectin homology domain in TpMs, we reasoned that plectin 1b could represent a candidate to mediate this association. When we efficiently down-regulated plectin 1b levels by siRNA (Fig. 2E), total TpMs levels were unchanged (Fig. 2F), but the amount retrieved in purified mitochondria was reduced (Fig. 2G). Thus, TpMs is a peripheral OMM protein whose mitochondrial localization depends on plectin 1b. However, plectin 1b could play an indirect role in directing TpMs to the OMM that depends on keratin binding. To rule out this possibility we turned to mouse embryonic fibroblasts (MEFs) that do not express keratins 8/18 (not shown). The distribution of Δ1, Δ4 and full length TpMs-GFP expressed in MEFs was perfectly superimposable to that observed in HeLa (Fig. S2A). The pro-fission effect of TpMs were also independent of keratins: mitochondria in MEFs co-expressing TpMs and mtRFP were round-shaped, as opposed to the short rods observed in mock transfected cells (Fig. S2B,C). These data indicate that TpMs can target mitochondria and fragment them independently of keratins and rule out a plectin 1b-keratin interplay in TpMs association to mitochondria.

TpMs is enriched in MAMs and controls ER-mitochondria tethering

A small fraction of TpMs was also retrieved at the ER and the mitochondrial staining of TpMs was patchy, a pattern highly resembling of that of the MAMs component Mfn2 (de Brito *et al.*, 2008). We indeed found that TpMs was almost exclusively in mouse liver MAMs, when we separated them from mitochondria by using a Percoll-gradient (Fig. 3A). Given this subcellular location, we analyzed if TpMs influenced ER morphology. ER structure, judged by three-dimensional (3D) reconstruction and volume rendering of confocal stacks of ER targeted yellow fluorescent protein (ER-YFP) (de Brito *et al.*, 2008), was not affected by levels of TpMs (Fig. 3B and C). We reasoned that TpMs could somehow affect ER-mitochondria tethering and we set out to measure it by our confocal semiquantitative approach (de Brito *et al.*, 2008). Volume-rendered 3D reconstruction of z-axis of confocal images of mitochondria and ER targeted spectral variants of GFP indicated that the areas of tethering (appearing as pseudo-colocalized yellow pixels) were reduced in cells where TpMs was overexpressed. A modest increase in the tethering was appreciated conversely when we down-regulated the levels of TpMs (Fig. 3D). The quantitative Manders' correlation coefficient analysis corroborated the visual impression that levels of TpMs affect ER-mitochondria tethering (Fig. 3E). Crude mitochondria isolated from HeLa cells transfected with TpMs were less contaminated by microsomes than mock transfected ones. *Vice versa*, microsomes were more abundant when TpMs was silenced (Fig. 3F). Finally, the phenotype could be reproduced in HeLa cells stably expressing TpMs (Fig. S3), and in MEFs (not shown), thereby excluding that it could be a consequence of transient transfection or that it requires keratin. In conclusion, TpMs is enriched in MAMs and negatively regulates tethering of ER to mitochondria.

TpMs selectively inhibits death by stimuli that require ER-mitochondria juxtaposition

We next ought to address the functional consequence of TpMs localization, which is likely to impact on ER-mitochondria communication. We therefore decided to test the influence of TpMs levels on the apoptotic response to death triggers that we previously classified according to their requirement for Ca^{2+} transfer between ER and mitochondria: (i) extrinsic stimuli; (ii) intrinsic stimuli that do not require ER Ca^{2+}, like tBID; (iii) "mixed" stimuli that partially require ER Ca^{2+}, like staurosporine; (iv) stimuli that rely on ER Ca^{2+} like H_2O_2 (Scorrano *et al.*, 2003). Expression of TpMs marginally sensitized HeLa cells to apoptosis by staurosporine, etoposide, tBID (Fig. 4A), while it had no effect on the extrinsic stimuli TRAIL and Fas (Fig 4B). On the other hand, cells overexpressing TpMs were specifically resistant to apoptosis by the Ca^{2+}-dependent stimulus H_2O_2, which requires ER-mitochondria Ca^{2+} transfer to cause death (Fig. 4A) (Scorrano *et al.*, 2003). Silencing of TpMs as expected increased killing by H_2O_2 (Fig. 4C), while it did not have any significant effect on the response to the other stimuli tested (not shown). In order to confirm that the function of TpMs in cell death was independent from keratin, we turned to MEFs where we similarly found that overexpression of TpMs specifically inhibited apoptosis by H_2O_2 (Fig. S4). In conclusion, TpMs selectively inhibits death by stimuli that require adequate Ca^{2+} transfer from the ER to mitochondria.

Discussion

Here we identify TpMs as a novel protein localized at the mitochondria-ER interface, regulating the interaction between the two organelles. TpMs was originally described as a keratin binding protein (Nishizawa *et al.*, 2005), but we recently found it partially localized on mitochondria and downregulated in a number of solid tumors (Vecchione *et al.*, 2009), raising questions on its function. TpMs is a protein associated with the OMM, enriched at the points of juxtaposition between mitochondria and endoplasmic reticulum. Levels of mitochondrial TpMs are reduced when plectin 1b, a mitochondrial isoform of the large cytolinker plectin (Winter *et al.*, 2008), is down-regulated. Members of the plectin family can heterodimerize (Fontao *et al.*, 2001): it is tempting to speculate that the association of TpMs with mitochondria is mediated by the interaction between plectin 1b and the plectin homology domain of TpMs. However, a fusion protein of this domain with GFP does not display a mitochondrial pattern, suggesting that other parts of the protein are required for the interaction with plectin 1b.

The composition of the interface between mitochondria and ER is largely unknown, despite the physiological relevance of this compartment in mitochondrial function (Rizzuto *et al.*, 1998;Stone *et al.*, 2000;Scorrano *et al.*, 2003;Simmen *et al.*, 2005;Sano *et al.*, 2009). A handful of proteins are unexpectedly enriched at this site. Most of them are chaperones or play an active role in signaling (Hayashi *et al.*, 2009), with the exception of Mfn2 that in mammalian cells acts as a structural tether (de Brito *et al.*, 2008). Here we extend the components of this compartment to a cytoskeleton-interacting protein and suggest that MAMs have the ability to engage in interactions with the keratins, opening to the possibility that ER-mitochondria interaction are dynamically modulated by the interaction with the cell's architectural modules, even if the relevance of keratins for TpMs is questionable (Vecchione *et al.*, 2009).

TpMs negatively regulate the juxtaposition between ER and mitochondria, albeit at present the mechanism is unclear. Coimmunoprecipitation experiments do not support our prediction that TpMs could sequester Mfn2 (not shown). One possibility is that TpMs anchor mitochondria at specific locations, inhibiting the formation of interactions with the ER. Consistently, we found that motility of mitochondria is reduced by expression of TpMs (not shown).

TpMs is downregulated in several human tumors and higher levels of this protein are associated with a marginal increase in the response to apoptosis by staurosporine (Vecchione *et al.*, 2009). Here we expanded the array of stimuli tested and we found a similar pattern of sensitization to apoptosis by intrinsic stimuli. Why does TpMs sensitize to mitochondria-mediated cell death? We excluded that high levels of TpMs cause mitochondrial depolarization or latent dysfunction, as measured by the oligomycin assay (not shown) (Irwin *et al.*, 2003). Its effects could then be related to the promotion of mitochondrial fragmentation, observed in cells overexpressing TpMs and associated with a greater tendency to apoptosis (Lee *et al.*, 2004). Notably, expression of TpMs is *protective* against the Ca^{2+}-dependent stimulus hydrogen peroxide. This confirms functionally the role of TpMs as a negative modulator of ER-mitochondria juxtaposition and extends the evidence supporting the importance of the interorganellar juxtaposition in cell death (Simmen *et al.*, 2005;Csordas *et al.*, 2006;Sano *et al.*, 2009).

In conclusion, our data support a model in which proteins interacting with IFs can participate in the formation of the tethering between organelles. It will be interesting to investigate the role of the cytoskeleton in the relative spatial organization of organelles that must be juxtaposed for functional reasons, like mitochondria and ER.

Methods

Detailed experimental procedures are described in the supplementary information online.

Molecular Biology

Detailed information of plasmids, cloning and siRNA sequences are available in supplementary information online.

Imaging.

Confocal imaging on fixed and live samples, morphometric and contact analysis were performed as previously described (de Brito *et al.*, 2008) and as detailed in the supplementary information online.

Biochemistry

Subcellular fractionation, MAM isolation, immunoprecipitation and SDS-PAGE/immunoblotting were performed as indicated in the supplementary information online. Proteinase K accessibility and carbonate extraction assays were performed as in (Dimmer *et al.*, 2008). Modifications are detailed in supplementary information online.

Analysis of Cell death

Viability was determined cytofluorimetrically as the percentage of Annexin-V negative cells in the GFP positive population. Details are in supplementary information online.

References

1. Anesti V and Scorrano L (2006) The relationship between mitochondrial shape and function and the cytoskeleton. *Biochim Biophys Acta,* **1757,** 692-699.

2. Bola B and Allan V (2009) How and why does the endoplasmic reticulum move? *Biochem Soc Trans,* **37,** 961-965.

3. Campello S, Lacalle RA, Bettella M, Manes S, Scorrano L, and Viola A (2006) Orchestration of lymphocyte chemotaxis by mitochondrial dynamics. *J Exp Med,* **203,** 2879-2886.

4. Capetanaki Y (2002) Desmin cytoskeleton: a potential regulator of muscle mitochondrial behavior and function. *Trends Cardiovasc Med,* **12,** 339-348.

5. Csordas G, Renken C, Varnai P, Walter L, Weaver D, Buttle KF, Balla T, Mannella CA, and Hajnoczky G (2006) Structural and functional features and significance of the physical linkage between ER and mitochondria. *J Cell Biol,* **174,** 915-921.

6. de Brito OM and Scorrano L (2008) Mitofusin 2 tethers endoplasmic reticulum to mitochondria. *Nature,* **456,** 605-610.

7. Dimmer KS, Navoni F, Casarin A, Trevisson E, Endele S, Winterpacht A, Salviati L, and Scorrano L (2008) LETM1, deleted in Wolf Hirschhorn syndrome is required for normal mitochondrial morphology and cellular viability. *Hum Mol Genet,* **17,** 201-214.

8. Fontao L, Geerts D, Kuikman I, Koster J, Kramer D, and Sonnenberg A (2001) The interaction of plectin with actin: evidence for cross-linking of actin filaments by dimerization of the actin-binding domain of plectin. *J Cell Sci,* **114,** 2065-2076.

9. Fuchs E (1996) The cytoskeleton and disease: genetic disorders of intermediate filaments. *Annu Rev Genet,* **30,** 197-231.

10. Hayashi T, Rizzuto R, Hajnoczky G, and Su TP (2009) MAM: more than just a housekeeper. *Trends Cell Biol,* **19,** 81-88.

11. Hayashi T and Su TP (2007) Sigma-1 receptor chaperones at the ER-mitochondrion interface regulate Ca^{2+} signaling and cell survival. *Cell,* **131,** 596-610.

12. Irwin WA, Bergamin N, Sabatelli P, Reggiani C, Megighian A, Merlini L, Braghetta P, Columbaro M, Volpin D, Bressan GM, Bernardi P, and Bonaldo P (2003) Mitochondrial dysfunction and apoptosis in myopathic mice with collagen VI deficiency. *Nat Genet,* **35,** 367-371.

13. Lee YJ, Jeong SY, Karbowski M, Smith CL, and Youle RJ (2004) Roles of the mammalian mitochondrial fission and fusion mediators Fis1, Drp1, and Opa1 in apoptosis. *Mol Biol Cell,* **15,** 5001-5011.

14. Liu X and Hajnoczky G (2009) Ca^{2+}-dependent regulation of mitochondrial dynamics by the Miro-Milton complex. *Int J Biochem Cell Biol,* **41,** 1972-1976.

15. Milner DJ, Mavroidis M, Weisleder N, and Capetanaki Y (2000) Desmin cytoskeleton linked to muscle mitochondrial distribution and respiratory function. *J Cell Biol,* **150,** 1283-1298.

16. Nishizawa M, Izawa I, Inoko A, Hayashi Y, Nagata K, Yokoyama T, Usukura J, and Inagaki M (2005) Identification of trichoplein, a novel keratin filament-binding protein. *J Cell Sci,* **118,** 1081-1090.

17. Rizzuto R, Pinton P, Carrington W, Fay FS, Fogarty KE, Lifshitz LM, Tuft RA, and Pozzan T (1998) Close contacts with the endoplasmic reticulum as determinants of mitochondrial Ca^{2+} responses. *Science,* **280,** 1763-1766.

18. Sano R, Annunziata I, Patterson A, Moshiach S, Gomero E, Opferman J, Forte M, and d'Azzo A (2009) GM1-ganglioside accumulation at the mitochondria-associated ER membranes links ER stress to Ca^{2+}-dependent mitochondrial apoptosis. *Mol Cell,* **36,** 500-511.

19. Scorrano L, Oakes SA, Opferman JT, Cheng EH, Sorcinelli MD, Pozzan T, and Korsmeyer SJ (2003) BAX and BAK regulation of endoplasmic reticulum Ca^{2+}: a control point for apoptosis. *Science,* **300,** 135-139.

20. Simmen T, Aslan JE, Blagoveshchenskaya AD, Thomas L, Wan L, Xiang Y, Feliciangeli SF, Hung CH, Crump CM, and Thomas G (2005) PACS-2 controls endoplasmic reticulum-mitochondria communication and Bid-mediated apoptosis. *EMBO J,* **24,** 717-729.

21. Stone SJ and Vance JE (2000) Phosphatidylserine synthase-1 and -2 are localized to mitochondria-associated membranes. *J Biol Chem,* **275,** 34534-34540.

22. Szabadkai G, Bianchi K, Varnai P, De SD, Wieckowski MR, Cavagna D, Nagy AI, Balla T, and Rizzuto R (2006) Chaperone-mediated coupling of endoplasmic reticulum and mitochondrial Ca^{2+} channels. *J Cell Biol,* **175,** 901-911.

23. Vance JE (1990) Phospholipid synthesis in a membrane fraction associated with mitochondria. *J Biol Chem,* **265,** 7248-7256.

24. Vecchione A, Fassan M, Anesti V, Morrione A, Goldoni S, Baldassarre G, Byrne D, D'Arca D, Palazzo JP, Lloyd J, Scorrano L, Gomella LG, Iozzo RV, and Baffa R (2009) MITOSTATIN, a putative tumor suppressor on chromosome 12q24.1, is downregulated in human bladder and breast cancer. *Oncogene*, **28,** 257-269.

25. Winter L, Abrahamsberg C, and Wiche G (2008) Plectin isoform 1b mediates mitochondrion-intermediate filament network linkage and controls organelle shape. *J Cell Biol*, **181,** 903-911.

Figure legends

Fig. 1: TpMs interacts with keratins and mitochondria.

(A) Pre-cleared lysates from LnCap cells stably overexpressing TpMs-V5 (Vecchione *et al.*, 2009) were prepared and equal amounts of protein (500 µg) dissolved in RIPA buffer were immunoprecipitated with an anti-V5 antibody, separated by SDS-PAGE and immunoblotted using an anti-K8/K18 antibody. Input represents a 1:10 dilution of the total lysates.

(B) Pre-cleared lysates from HeLa cells were prepared and equal amounts of protein (500 µg) dissolved in CHAPS buffer were immunoprecipitated with the indicated antibodies (input represents a 1:10 dilution) and coprecipitated proteins were separated by SDS-PAGE and immunoblotted with the indicated antibodies.

(C) Representative images of HeLa cells transfected as indicated. Cells were fixed and immunostained with anti-cytokeratin8/18 (K8/K18), rhodamine-conjugated phalloidin or anti-tubulin antibody. Scale bar, 20 µm.

(D) Representative confocal images of HeLa cells cotransfected with mtCFP (cyan) and TpMs-V5. Cells were fixed and immunostained with FITC-conjugated anti-K8/K18 (green) and TRITC-conjugated anti-V5 antibodies (red). The merged image is also shown. The boxed area is magnified 9 folds. Scale bar, 20 µm.

Fig. 2: Full length TpMs is peripherally recruited to the OMM by plectin 1b.

(A) Upper panels: HeLa cells were cotransfected with TpMs-GFP (green) and mtRFP (mito, in red) or ER-RFP (ER, in red). After 24 hrs, cells were fixed and representative confocal images acquired. Lower panels: HeLa cells were cotransfected with TpMs-V5 and empty vector (left) or YFP-LC3 (autophago, right) and after 24 hrs fixed and immunostained with TRITC-conjugated

anti-V5 (red). Left panel, cells were stained with a FITC-conjugated anti-cM6PR (endosomes, green). Bar, 20 μm

(**B**) HeLa cells were cotransfected with mtRFP and the indicated TpMs-GFP chimeras and after 24 hrs representative confocal images were acquired. Scale bar, 20 μm.

(**C**) HeLa cells were transfected with the indicated plasmids and after 24 hrs equal amounts (40 μg) of protein from mitochondrial, ER and cytosolic fractions were separated by SDS-PAGE and immunoblotted using the indicated antibodies. MnSOD, Mn-dependent superoxide dismutase; SERCA, sarco/endoplasmic reticulum Ca^{2+} ATPase; LDH, lactate dehydrogenase.

(**D**) Left: Proteinase K accessibility assay. Purified mitochondria (5 mg/ml) from HeLa cells incubated in isolation buffer were incubated where indicated with proteinase k (100 μg/ml) in 20 mM Hepes, pH 7.4 (swelling) or with Triton X100 (0.1%). Twenty five μg of protein were separated by SDS-PAGE and immunoblotted using the indicated antibodies. GRP-75, glucose regulatory protein 75. Right: Carbonate extraction. Purified mitochondria from HeLa cells were incubated in 0.1 M Na_2CO_3 pH 11.3 for 30 min at 4°C. Soluble and membrane fractions were separated by centrifugation and equal amounts (25 μg) of proteins were separated by SDS-PAGE and immunoblotted with the indicated antibodies.

(**E**) mRNA was isolated at the indicated times and retrotranscribed from HeLa cells transfected with the indicated siRNA. Levels of plectin-1b were quantified by real time PCR.

(**F**) Equal amounts of protein (20 μg) from HeLa cells transfected as indicated were separated by SDS-PAGE and immunoblotted using the indicated antibodies.

(**G**) 5 X 10^5 HeLa cells were transfected as indicated and at the indicated times mitochondria were isolated, lysed and equal amounts of protein (25 μg) were separated by SDS-PAGE and immunoblotted with the indicated antibodies.

Fig. 3: **TpMs is enriched in MAMs and negatively regulates mitochondria-ER juxtaposition.**

(**A**) Equal amounts (40 μg) of protein of subcellular fractions (Cyto, cytosol; LM, light membranes; mito, mitochondria; MAM, mitochondria associated membranes) Percoll-purified from mouse hepatocytes were separated by SDS PAGE and immunoblotted using the indicated andibodies.

(**B**) HeLa cells were cotransfected with ER-YFP and the indicated constructs and after 24 hrs 3D reconstructions of ER were acquired. Bar, 20 μm.

(**C**) Mean ± SE (n=3 independent experiments) of morphometric analysis of ER shape from (B).

(**D**) Three dimensional reconstructions of ER and mitochondria in HeLa cells cotransfected with mtRFP, ER-YFP and the indicated plasmids. Yellow indicates that organelles are closer than ~ 270 nm. Scale bar, 20 μm.

(**E**) Mean ± SE (n = 3, 20 cells per experiment) of interaction data from (D).

(**F**) Twenty-four (plasmids) or 48 hrs (siRNA) after the indicated transfections, mitochondria were isolated from 5 X 10^8 HeLa and equal amounts of protein (25 μg) were separated by SDS-PAGE and immunoblotted with the indicated antibodies.

Fig. 4: **TpMs protects cells from Ca^{2+}-dependent apoptosis.**

(**A**) HeLa cells transfected as indicated were treated with 1 mM H_2O_2, 2 μm staurosporine (STS), 1 μm thapsigargin, or 5 μm etoposide. At the indicated times, viability was determined cytofluorimetrically as the percentage of GFP-positive, annexin-V-Alexa568-negative cells. Where indicated, cells were cotransfected with TpMs-V5 and pEGFP or tBID-GFP and after 48 hr cell death was determined cytofluorimetrically as the percentage of GFP-positive, annexin-V-Alexa568-positive cells. Data represent mean ±SE of five independent experiments.

(B) HeLa cells transfected as indicated were treated with TNF-α (25 ng/ml in the presence of 10 μg/ml cycloheximide) or Trail (50 ng/ml). After 16 h cell death was determined cytofluorimetrically as the percentage of YFP-positive, annexin-V-Alexa568-positive cells. Data represent mean ±SE of three independent experiments.

(C) HeLa cells were transfected as indicated and after 48 hrs treated with H_2O_2 or STS for 6 hr. Cell death was determined cytofluorimetrically as the percentage of FAM-positive, annexin-V-Alexa568-positive cells. Data represent mean ±SE of three independent experiments.

Fig.1

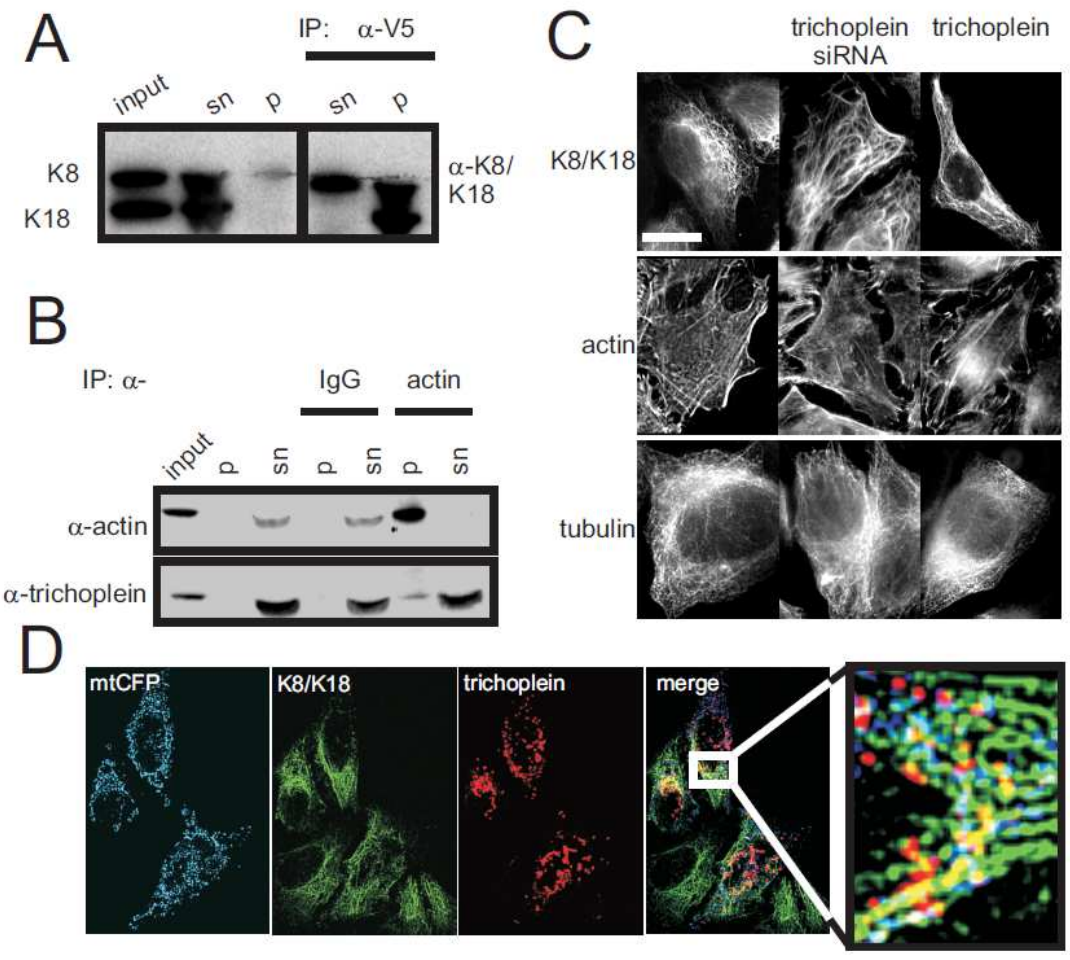
A
IP: α-V5
input
sn
p
sn
p
K8
K18
α-K8/
K18
B
IP: α-
IgG
actin
input
p
sn
p
sn
p
sn
α-actin
α-trichoplein
C
trichoplein
siRNA
trichoplein
K8/K18
actin
tubulin
D
mtCFP
K8/K18
trichoplein
merge

Fig.2

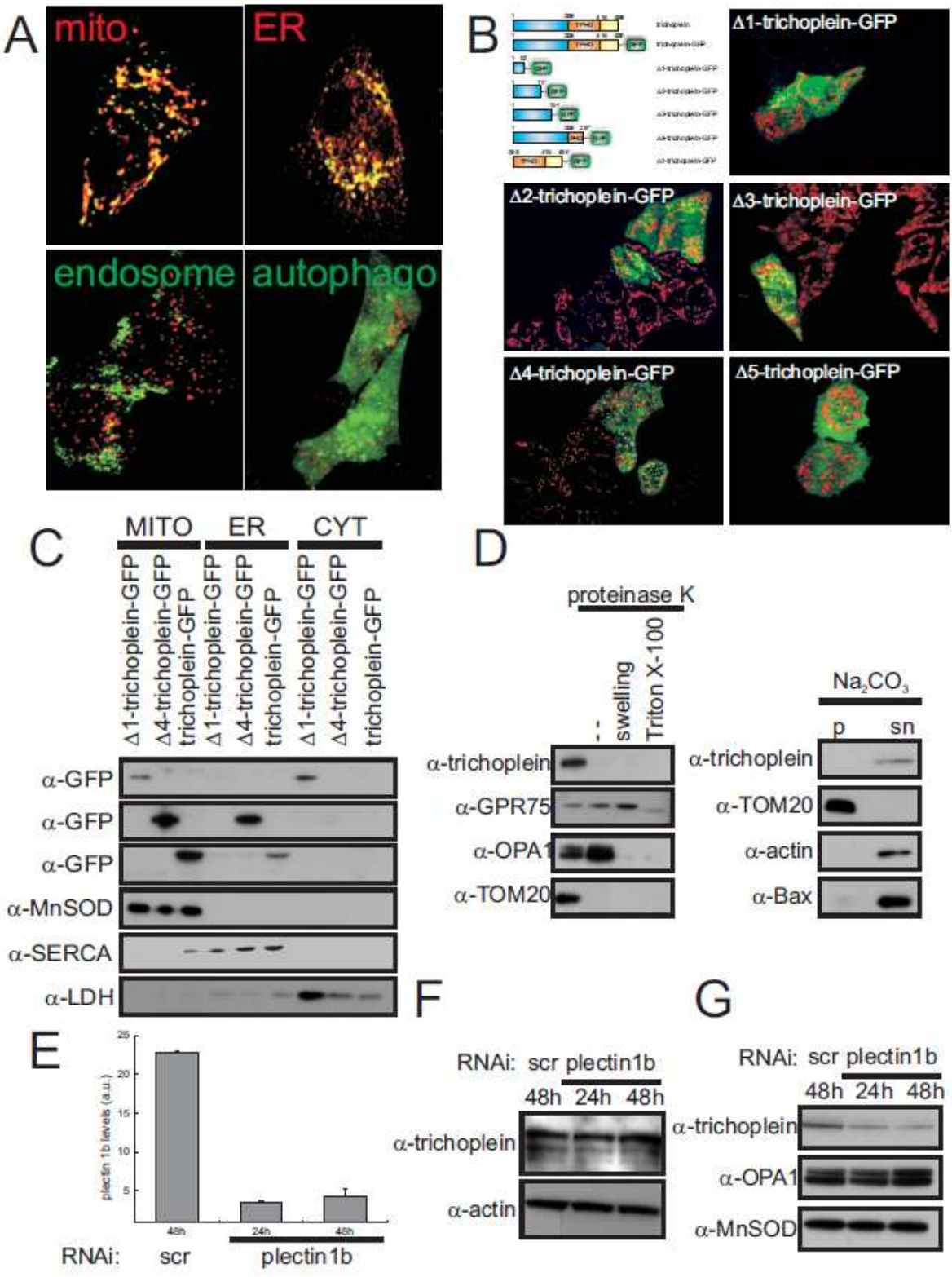
A
mito
ER
endosome
autophago
B
Δ1-trichoplein-GFP
Δ2-trichoplein-GFP
Δ3-trichoplein-GFP
Δ4-trichoplein-GFP
Δ5-trichoplein-GFP
C
MITO
ER
CYT
Δ1-trichoplein-GFP
Δ4-trichoplein-GFP
trichoplein-GFP
α-GFP
α-GFP
α-GFP
α-MnSOD
α-SERCA
α-LDH
D
proteinase K
- -
swelling
Triton X-100
α-trichoplein
α-GPR75
α-OPA1
α-TOM20
Na2CO3
p
sn
α-trichoplein
α-TOM20
α-actin
α-Bax
E
plectin 1b levels (a.u.)
48h
24h
48h
RNAi:
scr
plectin1b
F
RNAi: scr plectin1b
48h 24h 48h
α-trichoplein
α-actin
G
RNAi: scr plectin1b
48h 24h 48h
α-trichoplein
α-OPA1
α-MnSOD

Fig.3

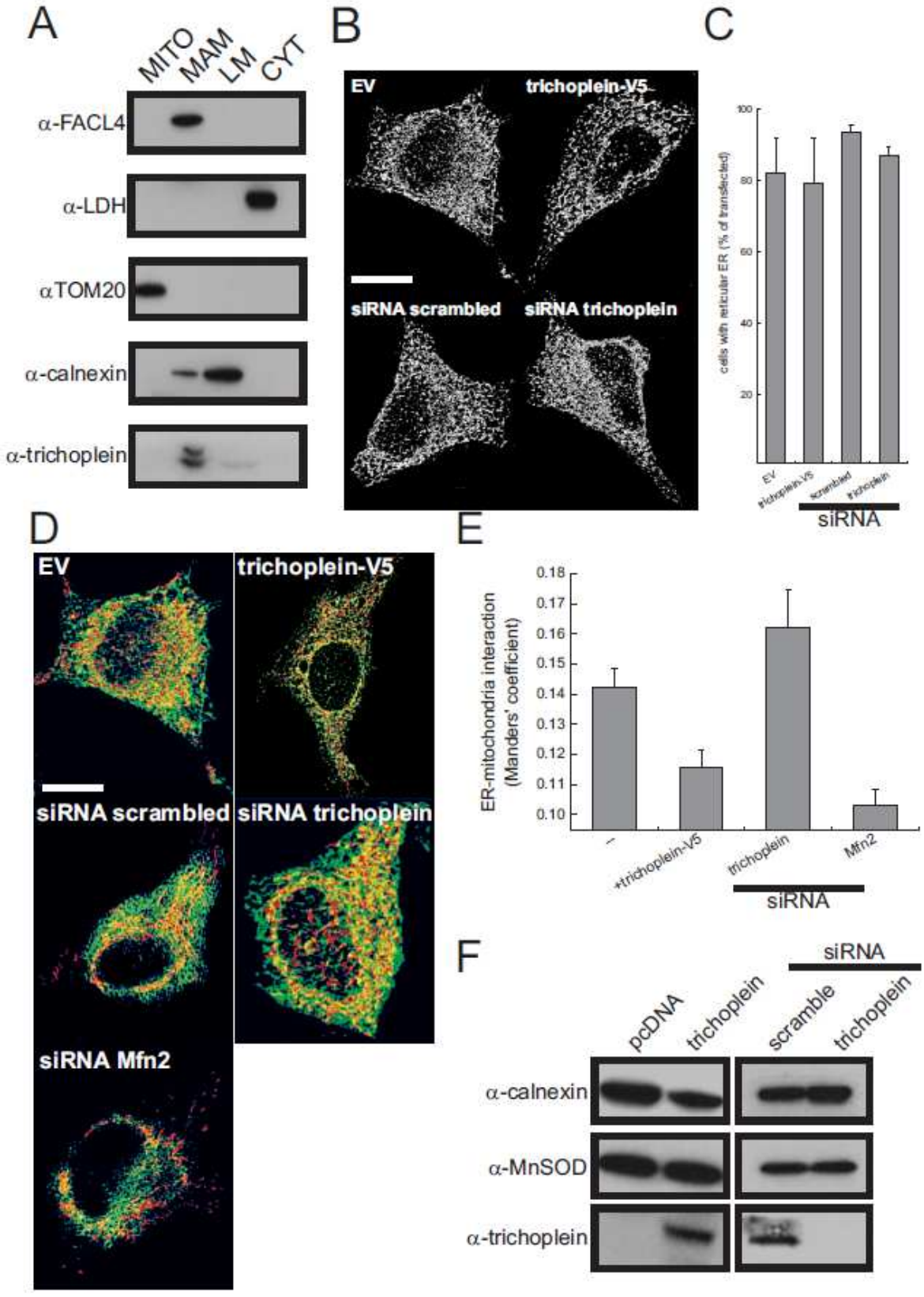
A
MITO
MAM
LM
CYT
α-FACL4
α-LDH
αTOM20
α-calnexin
α-trichoplein
B
EV
trichoplein-V5
siRNA scrambled
siRNA trichoplein
C
cells with reticular ER (% of transfected)
EV
trichoplein-V5
scrambled
trichoplein
siRNA
D
EV
trichoplein-V5
siRNA scrambled
siRNA trichoplein
siRNA Mfn2
E
ER-mitochondria interaction (Manders' coefficient)
–
+trichoplein-V5
trichoplein
Mfn2
siRNA
F
siRNA
pcDNA
trichoplein
scramble
trichoplein
α-calnexin
α-MnSOD
α-trichoplein

Fig.4

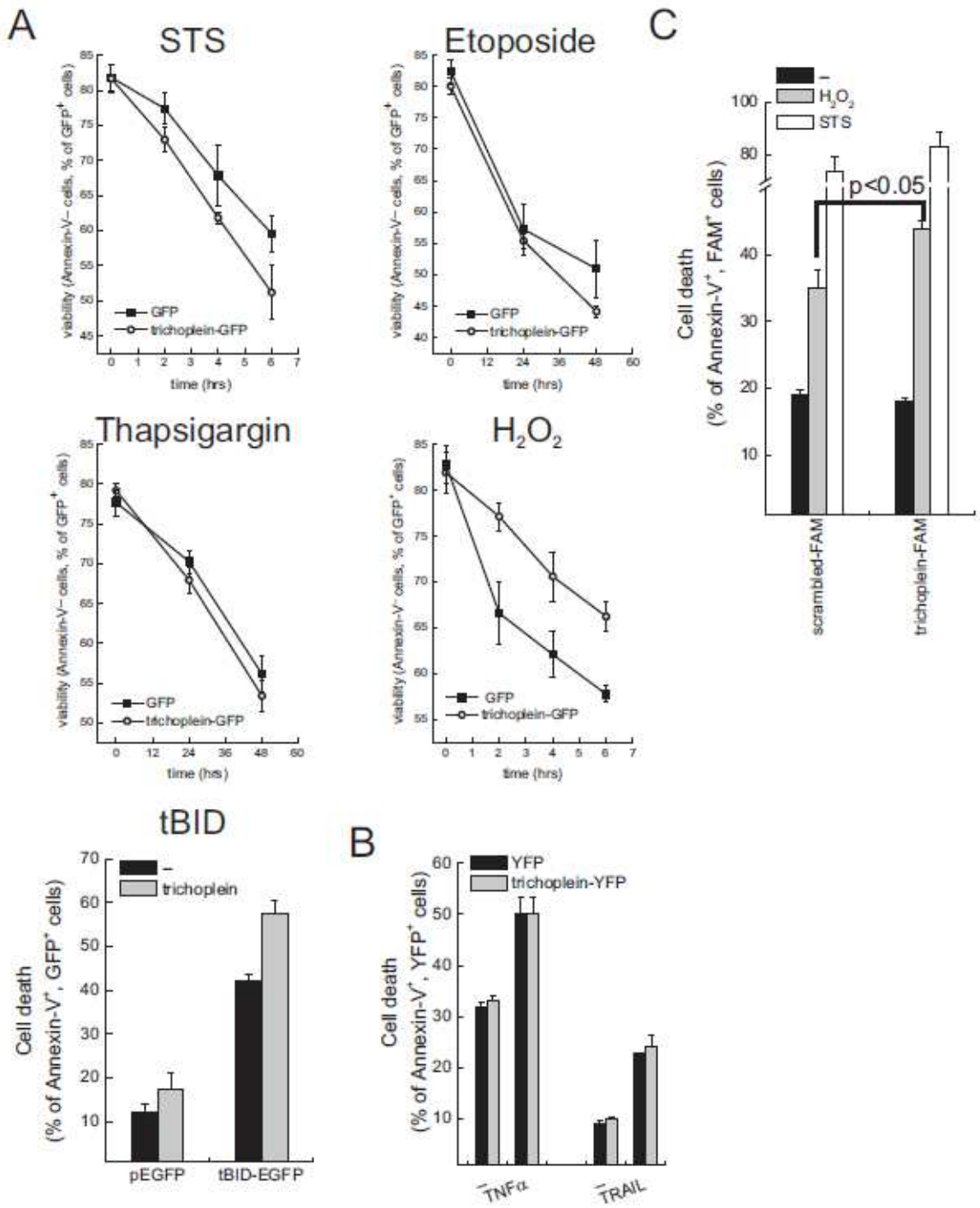
A
STS
Etoposide
Thapsigargin
H_2O_2
viability (Annexin-V− cells, % of GFP+ cells)
time (hrs)
GFP
trichoplein-GFP
tBID
Cell death
(% of Annexin-V+, GFP+ cells)
trichoplein
pEGFP
tBID-EGFP
B
YFP
trichoplein-YFP
(% of Annexin-V+, YFP+ cells)
TNFα
TRAIL
C
H_2O_2
STS
p<0.05
(% of Annexin-V+, FAM+ cells)
scrambled-FAM
trichoplein-FAM

Supplementary online methods

Molecular Biology

Mitochondrially targeted dsRED (mtRFP), pECFP-mt (mtCFP), pDsRed2-ER (erRFP) and pEYFP-ER (erYFP) were previously described (Cipolat *et al.*, 2004;de Brito and Scorrano, 2008). pcDNA/V5-DEST was purchased from Invitrogen. pcDNA-DEST47-TpMs (TpMs-GFP) and pcDNA/V5-DEST-TpMs (TpMs-V5) were generated by standard cloning. YFP-LC3 was kindly provided by T. Yoshimori (National Institute for Basic Biology, Japan).

?1-TpMs, ?2-TpMs, ?3-TpMs, ?4-TpMs, ?5-TpMs-GFP and TpMs-GFP were generated by amplifying the fragments of TpMs by PCR using the following primers : 5'- GGG GAAT TCT ACC ATG GCG CTC CCG ACG CT- 3' and 5'-GGG GGA TCC TGC CTG TTT GGA GCT GCA GAT-3' for ?1-TpMs, 5'-AAA GGA TCC CAA GTT CAT GCT CAG CCT CAG-3' for ?2-TpMs, 5'-AAA GGA TCC CTC CAT CTC TCG AAG TTT CGG-3' for ?3-TpMs, 5'- AAA GGA TCC GCC TGT CTG CCT CCA GCT CCT-3' for ?4-TpMs, 5'- AAA GGT ACC GTT CCA AGC AAT TTT TGG ATG-3' for ?5-TpMs-GFP and 5'- AAA GGT ACC GTT CCA AGC AAT TTT TGG ATG-3' for TpMs-GFP. TpMs also was subcloned into pEGFP-N3, adding a codon stop to block the expression of the GFP, using the following primers : 5'-GGG GAA TTC TAC CAT GGC GCT CCC GAC GCT-3' and 5'-AAA GGT ACC TCA GTT CCA AGC AAT TTT TGG-3'. pEGFP-N3 was mutated to avoid expression of GFP by site directed mutagenesis using the following primers : 5'-TCC ATC GCC ACC TGA GTG AGC AAG GGC GAG-3' and 5'- CTC GCC CTT GCT CAC TCA GGT GGC GAT GGA -3'. To subclone TpMs into pEYFP-C1 (BD Biosciences), TpMs was amplified by PCR using the following primers : 5'- GGGAGATCTATGGCGCTCCCGACGCTGCCG-3' and 5'-AAA GGT ACC TCA GTT CCA AGC AAT TTT TGG-3'.

The siRNA against TpMs was synthesized from the following sequence 5'-GGAGGUGGAGGCGACCAAATT-3' and against plectin-1b from 5'-

GGGGCAUCGGCAGGCAAAGUU -3' (Ambion, UK). The siRNA conjugated to fluorescein (FAM) against TpMs were obtained from Qiagen. The scrambled control was used at the same final concentration.

Real time PCR

For the quantification of plectin-1b expression level by real time RT-PCR, HeLa cells were transfected with scramble or plectin-1b siRNA, as previously described. After the indicated times total RNA was isolated from transfected cells by using the QuickPrep™ Total RNA Extraction Kit (Amersham Biosciences) following manufacturer's instruction. RNA was reverse transcribed into cDNA using the SuperSript™ III Reverse Transcriptase (Invitrogen). The resulting cDNA was used as template for subsequent PCR amplification of a 200 bp fragment in t first exon of the mouse plectin-1b cDNA using the following primers : 5'-GAG CAA GAT GAA CGA GAC CGT GTG -3' and 5'- TCC AGG GCA ATC TGC ACA TTC TGC -3'. A fragment of the mouse ß-actin cDNA was amplified using the following primers : 5'- CTG GCT CCT AGC ACC ATG AAG AT -3' 5'- GGT GGA CAG TGA GGC CAG GAT -3', and used as a control for the extracted RNAs. The RT-PCR was performed by using the Applied Biosystems 7000 Fast System (ABI PRISM 7000).

Cell culture

SV40-transformed wild-type (wt) mouse embryonic fibroblasts (MEFs) were kindly provided by D. Chan and cultured as described before (Chen et al., 2005; Chen et al., 2003).

HeLa cells were a king gift from C. Montecucco (University of Padova, Italy). MEFs and HeLa cells were cultured in Dulbecco's Modified Eagle Medium (DME , Invitrogen) supplemented with 10% foetal bovine serum (FBS, Invitrogen), 2 mM L-glutamine, non-essential amino acids (0.89 g/l L-alanine, 1.32 g/l L-asparagine, 1.33 g/l L-aspartic acid, 1.47 g/l L-glutamic acid, 0.75 g/l glycine, 1.15

g/l L-proline, 1.05 g/l L-serine, Invitrogen), 75 U/ml penicillin, 50 µg/ml stre tomycin (Invitrogen) at 37°C in a 5% CO_2 incubator.

LnCap overexpressing stably TpMs-V5 (LnCaPB3A) were previously described (Vecchione *et al.*, 2009). These cells were cultured in Roswell Park Memorial Istitute (RPMI, Invitrogen) supp emented with 10% foetal bovine serum, 2 mM L-glutamine, non-essential amino acid75 U/ml penicillin, 50 µg/ml streptomycin and 200 µg/ml geneticin (G-418, GIBCO) at 37°C in a 5% CO_2 incubator.

MEFs were transfected using Trasfectin (Biorad) according to the manufacturer's instructions. Transfection of HeLa cells and LnCapB3A with siRNAs and plasmid DNA was performed with Lipofectamine 2000 (Invitrogen) according to the manufacturer's protocol. When indicated in the figure legend, HeLa cells were transfected with siRNA hrs after seeding on glass coverslips and with mtRED/erYFP 48 hrs after plating.

HeLa cells stably overexpressing TpMs were generated by transfecting the cells with the plasmids pEGFP-N3 or TpMs-GFP in which GFP expression was blocked as described previously. Clones were selected by culturing cells in complete medium supplem nted with 1 mg/mL G418 and single cell clones were generated by limiting dilution as previously described (Frezza *et al.*, 2006).

Imaging

For confocal imaging of live cells, cells seeded onto 4-mm round glass coverslips were transfected as indicated and after the indicated time were incubated n Hanks balanced salt solution [HBSS, 0.14 g/l $CaCl_2$, 0.4 g/l KCl, 0.06 KH_2PO_4, 0.1 g/l $MgCl_2 6H_20$, 0.1 g/l $MgSO_4 7H_20$, 8 g/l NaCl, 0.09 g/l $Na_2HPO_4 7H_20$, 1 g/l Glucose, 1 mM HEPES, pH 7.4], and placed on the stage of a Nikon Eclipse TE300 inverted microscope equipped with a spinning-disk PerkinElmer Ultraview LCI confocal system, a piezoelectric z-axis motorized stage (Pifoc, Physik Instrumente, Germa y), and a Orca ER 12-bit charge-coupled device camera (Hamamatsu Photonics, Japan). Ce ls expressing pEGP-N3,

mutant variants of TpMs-GFP (or ER-YFP), (or YFP-LC3) and mtRFP (or ER-RED) were excited using the 488 nm, or the 543 line of the HeNe laser (P inElmer) with exposure times of 50 milliseconds by using a 60x 1.4 NA Plan Apo objective Nikon). For confocal z-axis stacks of ER to mitochondria interaction, stacks of 50 images separated by 0.3 µm along the z-axis were acquired. Total acquisition time for each stack was 1.1 sec to minimize reconstruction artef s caused by movement of mitochondria and ER. 3D reconstruction and volume rendering of the stacks were performed with the appropriate plugins of ImageJ (Nati nal Institutes of Health, Bethesda) as previously described (de Brito *et al.*, 2008).

For immunofluorescence, HeLa cells transfected as indicated, grown on 13 mm round coverslips, were fixed after 24 hrs for 30 min at room temperature with 3.7% (w/V) ice-cold formaldehyde, permeabilized for 20 min with ice-cold Nonidet P40 (GIBCO) and incubated with a rabbit anti-ciM6PR serum 8738 (1:200), kindly provided by M. De Bernard (Venetian Institute of Molecular Medicine, Padua, Italy) or a mouse monoclonal anti-V5 antibody (1:200, Invitrogen), a guinea pig polyclonal anti-cytokeratins 8/18 (1:200, Progen), a rhodamine phalloidin antibody (1:250, Molecular Probes) or a mouse monoclonal anti-a tubulin antibody (1:300, Santa Cruz Biotechnology). taining was revealed incubating with a goat anti-mouse or anti-rabbit IgG conjugated to the fluorochrome fluorescein-isothiocyanate (FITC) or tetramethyl-rhodamine-isothiocyanate (TRITC). For detection, blue, green and red channel images were acquired simultaneously using three separate colour channels on the stage of a laser scanning microscope (TCS SP5, Leica) using the LasAF software (Leica).

Morphometric and Contact Analysis.

Morphometric analysis was performed with Imagetool 3.0 (University of Texas Health Science Center, San Antonio) as previously described (de Brito *et al.*, 2008). Images of cells expressing mtRFP or erYFP were thresholded by using the automatic threshold function. For morphometric analysis of

mitochondria, the major axis length and the roundness x of each identified object were calculated. Cells were scored with elongated mitochondria when >50% of the objects in the image (*i.e.*, mitochondria) displayed a major axis longer than 3 µm d a roundness index below 0.3 (maximum value is 1). For morphometric analysis of ER, major ax s length and the elongation index of each identified object were calculated. Cells were scored with reticular ER when major axis was longer than 5 µm and the elongation index was above 4 of more than 50% of the identified objects. For analysis of the mitochondria to ER interaction, images of cells expressing mtRFP or erYFP were thresholded using the automatic threshold function of ImageJ, followed b deconvolution, 3D reconstruction and surface rendering using the VolumeJ plugin of ImageJ. Analysis of the interaction between ER and mitochondria was performed using Manders' colocalization coefficient (MCC) as described in before (Manders et al., 1993).

Cell Lysates, Subcellular Fractionation, Immunoprecipitation and Immunoblotting.

For analyses of protein of whole cell lysates, 48 hrs after transfection, 10^6 cells were disrupted in RIPA buffer [150 mM NaCl, 1% (V/V) Nonidet P-40 (NP40), 0.25% (w/V) deoxycholate, 1 mM EDTA, 50 mM Tris, pH 7.4], CHAPS buffer [1% (w/V) CHAPS, 100 mM KCl, 50 mM Hepes pH 7.5, 1 mM EGTA] or in NP40 lysis buffer (1% NP40, 150 mM NaCl, 50 mM Tris pH7.4), in the presence of complete protease-inhibitor mixture (5 µg/ml aprotinin, 5 µg/ml leupeptin, 5 µg/ml pepstatin, Sigma.

For subcellular fractionation, 10^9 HeLa or MEFs were transfected as indicated and after h washed once with PBS, suspended in isolation buffer (IB, 200 mM sucrose, 1mM EGTA/Tris, and 10 mM Tris/MOPS), and then disrupted by dounce homogenization. The homogenate was spun at 600 g for 10 min; the supernatant was spun for 10 min at 7000 g. The resulting pellet (mitochondrial fraction) and supernatant (cytosol, ER, Golgi apparatus, peroxisomes, lysosomes and ll the other light membranes) were collected and washed by further centrifugation. T e mitochondrial fraction was collected while

the supernatant was further spun for 45 min at 100,000 g. The 100,000 g pellet (ER fraction) and supernatant (cytosolic fraction) were spun again at 200,000 g to further purify the fractions. The mitochondrial fraction was purified by spinning twice t 7,000 g for 10 minutes. To obtain a pure mitochondrial fraction, the obtained pellet was further purified from ER and MAM contamination by spinning at 95,000 g for 30 min on a 30% Percoll gradient in IB. The obtained mitochondrial layer was washed free of Percoll and resuspended in IB. Alternat vely, subcellular fractions were obtained by differential centrifugation from mouse liver, as descr before (de Brito *et al.*, 2008). Mitochondrial associated membranes (MAM) were identified as an inter ediate layer between the light membranes and the mitochondrial fraction on the Percoll gradient as previously described (Stone and Vance, 0). Protein concentration was determined by using the Brad ord protein assay, based on an absorbance shift in the dye Coomassie for the colorimetric detect and quantitation of the total protein and 25-40 ug of protein per condition, according to the experiment, were loaded on a lane of a SDS-PAGE.

For immunoprecipitation, protein-G or -A were incubated with a mouse anti-actin antibody (1:20), or anti-V5 antibody (1:50) for 3 h at 4°C. The beads/antibody complex was subsequently incubated ON at 4°C with 500 µg of cell extract. Beads were boiled NuPage® LDS Sample buffer (Invitrogen).

For immunoblotting, proteins were transferred onto polyvinylidene difluoride (PVDF, BioRad) by using XCell *SureLock*™. Blot Module (Invitrogen) with NuPage® Transfer Buffer containing 10% methanol. Transfer was performed at RT for 2h at 30V, ing to the manufacturer's instructions. Membranes were probed using the following antibodies: i-GFP (1:200, Invitrogen); anti-actin (1:30000, Chemicon); anti-MnSOD (1:8000, Stressgen); anti- TOM20 (1:4000, Santa Cruz Biotechnology), anti-SERCA2a (1:100, Santa Cruz Biotechnology), anti-LDH (1:2000, Rockland); anti-V5 (1:1000, Invitrogen), anti-OPA1 (1:1000, BD Biosciences); anti-GRP75 (1:1000, Santa Cruz Biotechnology); anti-cytokeratin K8/18 (1:2000, Progen); anti-FACL4 (1:1000, Santa Cruz Biotechnology); anti-calnexin (1:1000, Stressgen) and anti-TpMs (1:100), kindly provided by R. Baffa

(Kimmel Cancer Center and Department of Pathology, Thomas Jefferson University, Phila lphia, PA 19107, USA).

Proteinase K Assay and Carbonate Extraction

Mitochondria (50 µg) isolated from HeLa cells were incubated at 4°C for 30 min in IB, or where indicated in the presence of proteinase k (100 µg/mL, Invitrogen), 20 mM Hepes, pH 7.4 or 0 mM Hepes, pH 7.4 plus 0.1% Triton X100 (SIGMA) in a final volume of 1 mL. To block proteinase k, Phenylmethanesulfonyl fluoride (PMSF, 2 mM, Fluka BioChemica) was added to the reaction for 5 min. Mitochondrial proteins were precipitated using 15% trich etic acid (TCA) 100% for 30 min at 4°C. The samples were denaturated, and 25 µg of protein per condition were separated by SDS-PAGE and immunoblotted.

For carbonate extraction, 200 µg of mitochondrial protein were incubated in IB for 30 min at 4°C in the presence of Na_2CO_3 (0.1M, pH 11.3) in a final volume of 1 mL. The reaction mix was centrifuged for 10 min at 12000 x *g*. The recovered pellet contained the integral proteins of mitochondrial membranes; on the other hand, the supernatant represented the per l ones.

Analysis of Cell Death

$2x10^5$ cells were transfected with the indicated plasmids and after 24 hrs treated as detailed in the figure legends. At the indicated times cells were stained with Annexin-V-Alexa568 (BenderMedSystems) and viability was measured by flow ytometry as the percentage annexin-V, PI-negative cells or as the percentage of annexin-V-negative events in the GFP cotransfected positive population.

HeLa cells stably expressing TpMs were treated as detailed in the figure legends and at the indicated times harvested and stained with propidium iodide (PI) and annexin-V-FLUOS (BenderMedSystems). Viability was measured as described above.

References

1. Cipolat S, de Brito OM, Dal Zilio B, and Scorrano L (2004) OPA1 requires mitofusin 1 to promote mitochondrial fusion. *Proc Natl Acad Sci U S A,* **101,** 15927-15932.

2. de Brito OM and Scorrano L (2008) Mitofusin 2 tethers plasmic reticulum to mitochondria. *Nature,* **456,** 605-610.

3. Frezza C, Cipolat S, Martins dB, Micaroni M, Beznoussenko GV, Rudka T, Bartoli D, Polishuck RS, Danial NN, De Strooper B, and Scorrano L (2006) OP 1 Controls Apoptotic Cristae Remodeling Independently from Mitochondrial Fusion. *Cell,* **126,** 177-189.

4. Vecchione A, Fassan M, Anesti V, Morrione A, Goldoni S, Baldassarre G, Byrne D, D'Arca D, Palazzo JP, Lloyd J, Scorrano L, Gomella LG, Iozzo RV, and Baffa R (2009) MITOSTATIN, a putative tumor suppressor on chromosome 12q24.1, is do nregulated in human bladder and breast cancer. *Oncogene,* **28,** 257-269.

Legends to supplementary figures

Fig. S1: **Expression levels of TpMs.** HeLa cells were transfected as indicated. After 24 h (**A**), or at the indicated times cells (**B**) cells were lysed and protein (20 µg) was analyzed by SDS-PAGE/immunoblotting. (**C**) HeLa cells stably overexpressing empty vector or TpMs were lysed and equal amounts of protein (20 µg) were separated by SDS-PAGE and immunoblotted with the indicated antibodies.

Fig. S2: **Mitochondrial targeting and fragmentation by TpMs does not require keratins.**

(**A**) Subcelhular fractions were prepared from MEFs transfected with the indicated constructs and equal amounts (40 µg) of protein from the indicated fraction were separated by SDS-PAGE and immunoblotted using the indicated antibodies.

(**B**) Representative confocal images of MEFs cotransfected with mtRFP and empty vector or TpMs-GFP. Scale bar, 20 µm.

(**C**) Morphometric analysis of mitochondrial shape. Experi were as in (B). 120 randomly selected images of mtRFP fluorescence were acquired, stored, and c sified as described. Data represent mean ±SE of three independent experiments.

Fig. S3: **Loosened ER-mitochondria interactions in cells stably overexpressing TpMs.** (**A**) Three dimensional reconstructions of ER and mitochondria in HeLa cells stably overexpressing empty vector or TpMs and cotransfected with mtRFP, er-YFP. Yellow indicates that organelles are closer than 70 nm. Scale bar, 20 µm. (**B**) Mean ± SE (n = 3, 20 cells per experiment) of interaction data. Experiments were as in (A).

Fig. S4: **MEFs overexpressing TpMs are protected from hydrogen peroxide induced cell death.** (**A**) MEFs transfected as indicated were treated with 2 µm STS for 6 hrs or 5 µm etoposide for 48 hrs. Cell death was determined cytofluorimetrically as the percentage of YFP-positive, annexin-V-Alexa568-positive cells. Data represent mean ±SE of three independent experiments. (**B**) MEFs were cotransfected with TpMs-V5 and pEGFP or tBID-GFP. After 48 hrs cell death was determined cytofluorimetrically as the percentage of GFP-positive, annexin-V-Alexa568-positive cells. Data represent mean ±SE of three independent experiments. (**C**) MEFs transfected as indicated were treated with 1 mM H_2O_2. At the indicated times, viability was determined cytofluorimetrically as the percentage of YFP-positive, annexin-V-Alexa568-negative cells. Data represent mean ±SE of three independent experiments.

Fig. S1

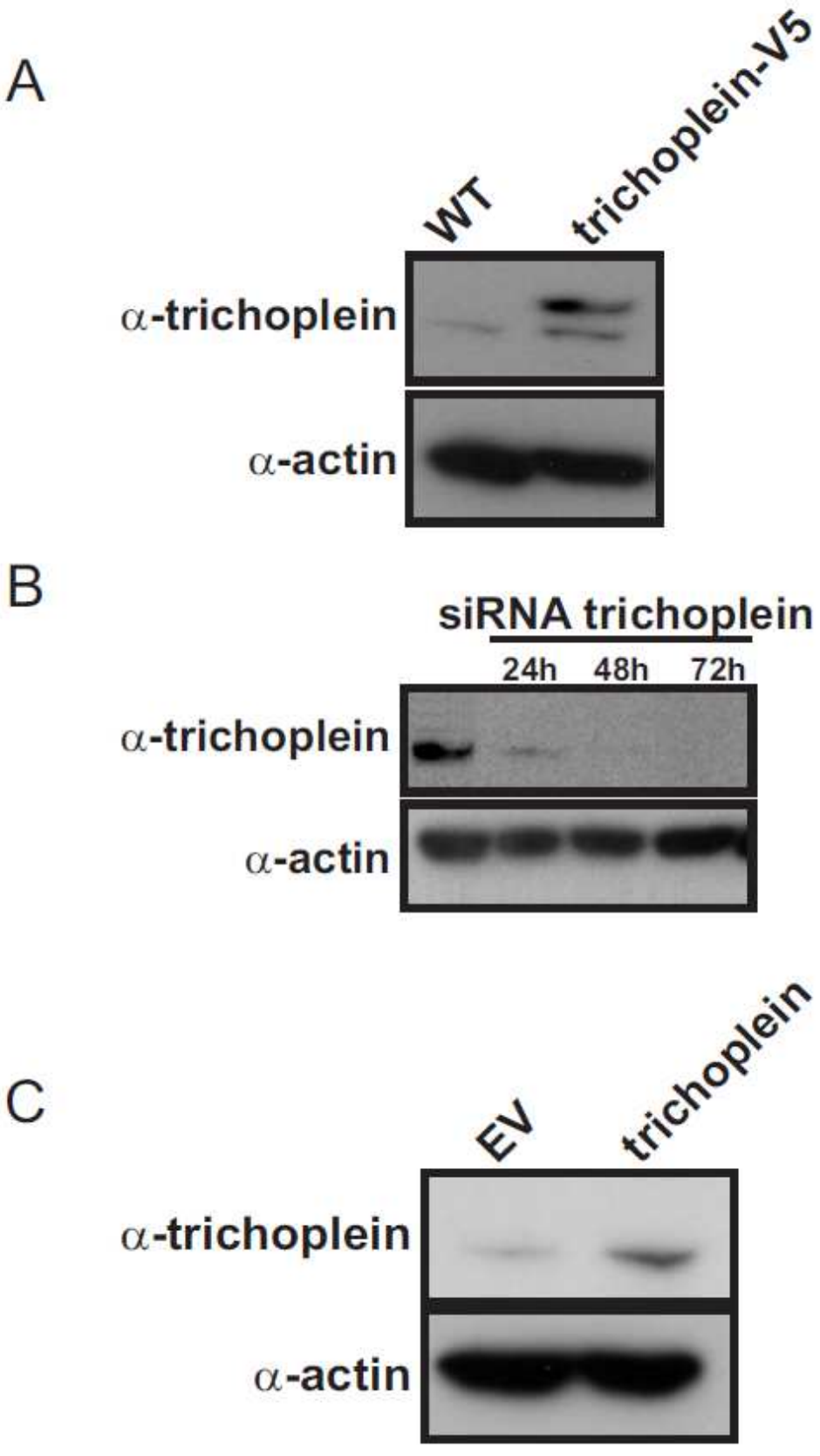
A
WT
trichoplein-V5
α-trichoplein
α-actin
B
siRNA trichoplein
24h
48h
72h
α-trichoplein
α-actin
C
EV
trichoplein
α-trichoplein
α-actin

Fig. S2

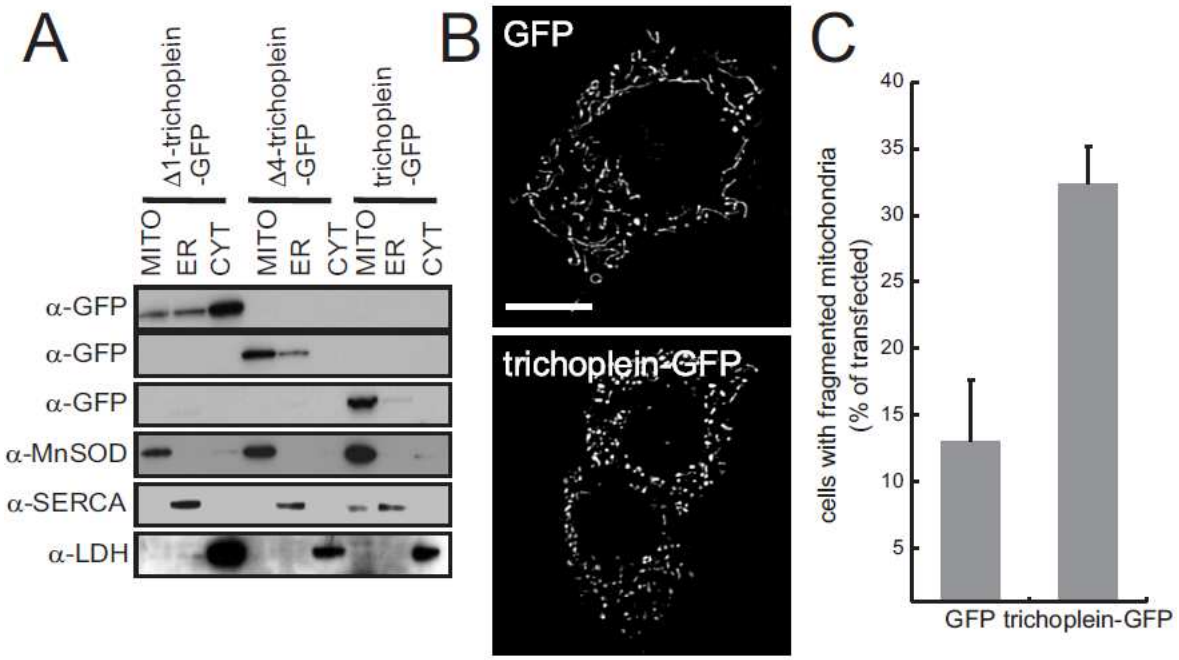
A
Δ1-trichoplein -GFP
Δ4-trichoplein -GFP
trichoplein -GFP
MITO
ER
CYT
MITO
ER
CYT
MITO
ER
CYT
α-GFP
α-GFP
α-GFP
α-MnSOD
α-SERCA
α-LDH
B
GFP
trichoplein-GFP
C
cells with fragmented mitochondria (% of transfected)
40
35
30
25
20
15
10
5
GFP
trichoplein-GFP

Fig. S3

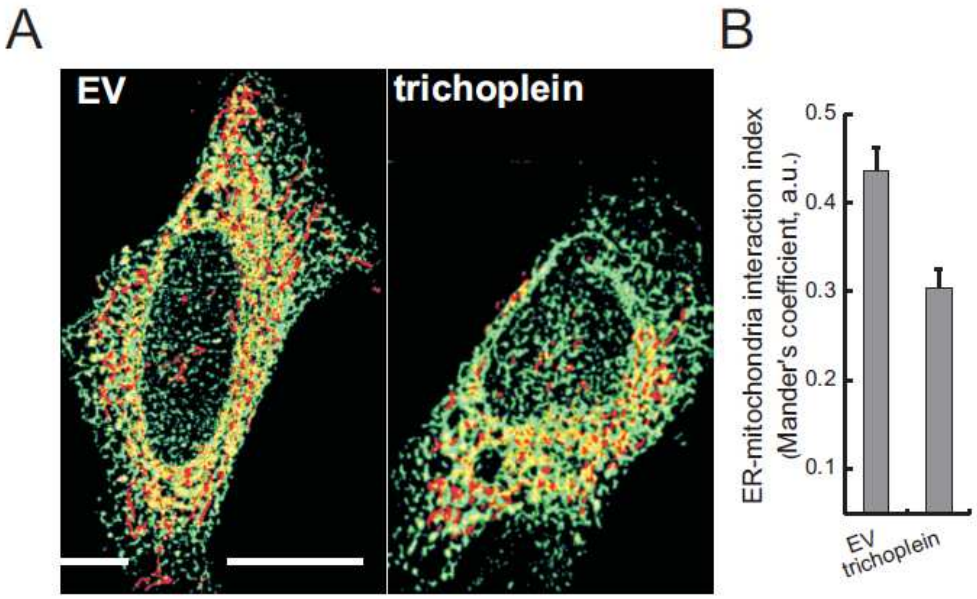
A
EV
trichoplein
B
ER-mitochondria interaction index (Mander's coefficient, a.u.)
0.5
0.4
0.3
0.2
0.1
EV
trichoplein

Fig. S4

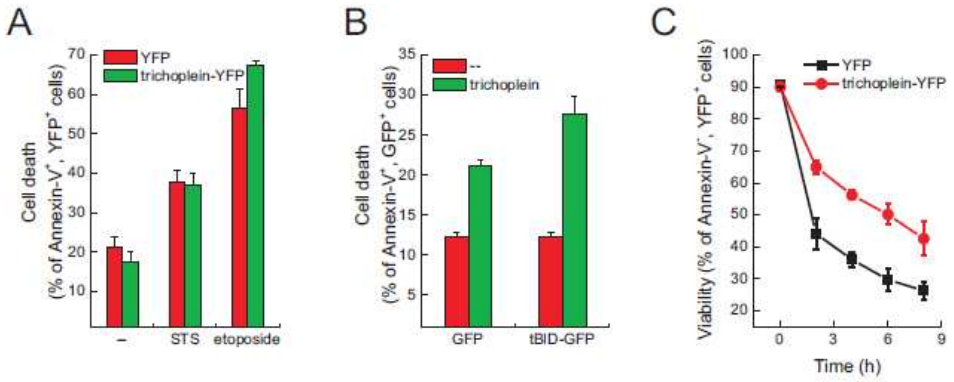
A
YFP
trichoplein-YFP
Cell death
(% of Annexin-V+, YFP+ cells)
70
60
50
40
30
20
10
–
STS
etoposide
B
--
trichoplein
Cell death
(% of Annexin-V+, GFP+ cells)
35
30
25
20
15
10
5
GFP
tBID-GFP
C
YFP
trichoplein-YFP
Viability (% of Annexin-V-, YFP+ cells)
100
90
80
70
60
50
40
30
20
0
3
6
9
Time (h)

TRAK1 participates in melanocyte trafficking

Cristina Cerqua[1] and Luca Scorrano[1,3]

[1]*Dulbecco-Telethon Institute, Venetian Institute of Molecular Medicine, Via Orus 2, 35129 Padova, Italy;*

[3]*Department of Cell Physiology and Medicine, University of Geneva, 1 Rue M. Servet, 1211 Geneve, Switzerland*

Abstract

Trak1 is one of the mammalian homologues of Drosophila Milton, a protein essential for the regulation of mitochondrial movement. Trak1 associates to Miro-1, Miro-2 and kinesin heavy chain, suggesting for this protein a role similar to that of Milton. It was proposed also to have a role in the endosome-to-lysosome transport. We report here a new role for Trak1 in the regulation of the melanosomes trafficking.

Keywords: mitochondrial movement/Milton/microtubules/Trak1

Introduction

Mitochondrial movement

Mitochondria are very mobile organelles. Mitochondrial movement has been characterized mainly in neurons where it is fundamental to transport mitoch ria to specific cellular sites of high energy demand (Hollenbeck and Saxton, 2005). Defects in mitochondrial transport have been associated to a variety of different neurodegenerative diseases (Chang et al., 2006; Ebneth et al., 1998). Mitochondrial movement depends mainly on microtubule m tors. There are two types of motors, kinesins (KIFs) and dyneins. KIFs are involved primari in the anterograde transport of organelles and protein complexes, and are cargo specific, while dyneins regulate the retrograde movements. The KIF is a heterotetramer formed by two heavy chains and two light chains. The heav chain contains a motor domain, an a-helical stalk domain, and a globular tail region. The otor domain has two conserved sequences proximal to a Walker A ATP binding motif and a microtubule binding domain (Miki et al., 2001).

The best characterized protein that regulates mitochon ial movement in Drosophila is Milton, a protein enriched in neuronal tissue. It is essential f r axonal and synaptic function (Stowers et al., 2002). In Milton-null flies mitochondria are not able to reach the axon and the synaptic terminals, while the protein overexpression in HEK 293T cells lea s to repositioning of mitochondria in the cytoplasm. Milton functions forming a complex with Miro to recruit kinesin-1, via its heavy chain, to the OMM (Glater et al., 2006). The mitochondrial protein Miro belongs to the family of Rho GTPases, that play a key role in distribution and morphology of mitochondria (Frederick et al., 2004). Ablation of Miro in Drosophila perturbs mitochondria distribution, causing severe movement problems in the fly and premature death (Guo et al., 2005). Miro is conserved from yeast, where it is designated as Gem1p, to mammals, th posses two Miro family members, Miro-1 and Miro-2 (Fransson et al., 2003). Miro is characterized by two GTPase domains, a calcium-binding EF-hand motif, which is responsible for mitochondrial arrest, and a transmembrane C-terminal domain, essential for its binding to mitochon ria.

The complex formed by Milton and Miro is essential to gulate movement and arrest of mitochondria. When calcium binds to its EF-hands motif, Miro associates with the motor domain of kinesin-1, preventing motor/microtubule interactions (Wang and Schwarz, 2009).

GRIF-1 and OIP106

The closest mammalian orthologues of Milton are $GABA_A$ receptor-interacting factor 1 (GRIF-1) and O-linked N-acetylglucosamine (*O*-GlcNAc) transferase-interacting protein (OIP106) (Brickley et al., 2005). GRIF-1 was first identified in a rat two-hybrid library to bind to the $ß_2$ subunit of the $GABA_A$ receptor-associated protein, and it was shown to be expressed only in excitable tissue (Beck et al., 2002). GRIF-1 was proposed to function as a $GABA_A$ receptor-trafficking protein. Later, it was found that GRIF-1 and OIP106 bind also to the enzyme *β-O*-linked *N*-acetylglucosamine (*O*-GlcNAc) transferase (OGT) (Iyer et al., 2003), whose they seem to be substrates of. This enzyme is a glycosyltransferase essential for the life of ES cells in mice (Shafi et al., 2000). It catalyzes the post-translational modification of proteins by *O*-GlcNAc in the cell cytoplasm. GRIF-1 and OIP106 bind to one of the tetratricopeptides pre ent in the OGT sequence, and OIP106 forms a complex with RNA polymerase II and in the nucleus of HeLa cells. It was observed that these complexes form punctuate structures containing proteins involved in splicing and transcription.

Both GRIF-1 and OIP106 sequences contain very highly identical c ed-coil domains, through which GRIF-1 homodimerizes. Rat GRIF-1 shares 44 % amino acid sequence identity with the human protein OIP106 (Kikuno et al., 1999) and dMilton Mouse OIP106 shares 25 % amino acid identity with dMilton. These proteins have also a comm huntingtin-associated protein 1 (HAP-1) N-terminal homology domain with other proteins, including HAP-1, members of the ezrin-radixin-moesin-merlin family, myosin heavy chain, hook proteins, mito ic checkpoints proteins and intermediate filament proteins. HAP-1 binds to the $p150^{Glued}$ subunit of dynactin, glutamate neurotransmitter receptor-GluR2-interacting protein (GRIP1), the inositol 1,4,5-trisphosphate receptor type 1, and kinesin 5C (Li et al., 1998; Tang et al., 2003; Gauthier et al., 2004), and it was reported to play a role in the regulation of vesicular trafficking from early endosomes to late endocytic compartments, and in the enhancement in vesicular transport of brain-derived neurotrophic factor along microtubules. GRIP-1 was shown to interact directly with kinesin heavy chains to steer to traffic a-amino-3-hydroxy-5-methylisoxazole-4-propionate receptors to dendrites in neurons (Setou et al., 2002). GRIF-1 and OIP106 could have, like Milton, a role in mitochondrial transport, since also these two proteins directly asso iate with kinesin, through their N-terminal domain (124-283) and bind to the first GTPase domain of Miro-1 and Miro-2, colocalizing with mitochondria (Fransson et al., 2006). In particular, GRIF-1 directly binds to KIF5C, but in whole brain tissue predominantly associates with KIF5A and the heart with KIF5B. GRIF-1 and OIP106 associate with KIF5B in HEK 293 cells and their overexpression in mammalian cells lead to a mitochondrial aggregation (Brickley et al., 2005)

TRAK1

The new official approved nomenclature for OIP106 is now trafficking protein, kinesin-binding 1 (TRAK1). Milton has two human orthologs, TRAK1 (OIP106 and TRAK2 (GRIF-1). The TRAK1 sequence is characterized by 16 exons, whose last corresponds to 27% of the entire sequence. This protein is widely expressed, with the higher expressio levels seen in brain, liver and kidney.

TRAK1 was found mutated in a mouse affected by a reces vely transmitted form of hypertonia (Gilbert et al., 2006). The mutation was characterized by a deletion of the final 12 % of the p otein. Hypertonia is a syndrome characterized by rigidity and hypertonicity, observed in many neurological disorders, including cerebral palsy, dystonia, Parkinson's disease, stroke, and spinal cord injury. It is thought to arise from defects in GABA-mediated inhibitory pathways (Lorish et al., 1989). Homozygous *Trak1-/-* mouse was characterized by hypertonicity, stiff gait, unched posture, jerky movements and slight tremor. At the tissue level, this mouse presented aggregates of vesicular structures in the neuronal processes of the gray matte Some of these inclusions were present within cellular processes that harboured postsynaptic ensities juxtaposed with presynaptic terminals. Further, the expression of the a-1 and ß2 subunits of $GABA_A$ receptors was reduced in the CNS, especially in lower motor neurons. TRAK1 seem to partially colocalize with $GABA_A$ receptors a-1 and ß2 subunits and an immunoprecipitation showed th it binds to $GABA_A$ receptors, suggesting a role for TRAK1 in the regulation of endosome-to lysosome trafficking.

Recently this hypothesis was corroborated by the group of Chin (Webber et al., 2008). They found that TRAK1 partially colocalizes with early endosomes its binding to the hepatocyte-growth-factor-regulated tyrosine kinase substrate (Hrs), a component of the endosomal sorting machinery, already decribed to bind to HAP1 and GRIF-1 (Kirk et al., 2006; Li et al., 2002). In particular TRAK1 and GRIF1 interact to Hrs with the domain formed by residues 359-507. It was also shown that TRAK1 is required for degradation of t e epidermal growth factor receptors (EGFRs) that are internalized to reach lysosomes. Also TRAK2 could have a similar role, since its overexpression alters the endosomal distribution.

In order to verify if Trak1 is primarily involved in l sosomal or mitochondrial trafficking, we decided to take a genetic approach and we constructed Trak1-/- mouse by using a gene trap strategy. Our preliminary results indicate a prominent role for Trak1 in pigmentation, supporting a model in which Trak1 participates in melanocyte (hence endosomal) trafficking.

Experimental procedures

Mouse genomic DNA extraction

Mouse pieces of fingers were incubated in lysis buffer (1M Tris-HCl pH 7.5, 10 mg/ml proteinase K) at 57°C for 1 hr. Then samples were placed on ice and incubated at 99°C for 5 min, to inactivate the proteinase K. Samples were stored at -20°C and spinned before using them.

Molecular biology

To find the exact position of the inserted gene trap vector we performed some PCR, using the following primers : a forward primer positioned at 2 kb (5'-ACT CGC CCC GTA GAC ATT TT-3'), 3 kb (5'-GTC AAT GCT CTG CTC ACA CC-3'), 4 kb (5'-GCT TAA GGG TGG GAC AAA CA-3') or 5 kb (5'-GGA TTC TGG GAC ACA TGA GC-3') respectively from the initiation of the intron 14-15, and one reverse primer, complementary to the beginning of the *β-geo* cassette of the gene trap construct (5'-AGG GTT TTC CCA GTC ACG-3'). For genotyping we performed two PCR using the following primers : 5'-GTC TGT CCA TCC ATC CAT CC-3' and 5'-TCT TCC CAT GAA TTC CAA GC-3' to identify the gene-trapped, or 5'-CCA GAA GAG AAG GGG AGC TT-3' to find the wild-type allele.

RESULTS

Generation of a TRAK1 gene-trap mouse

To better characterize the functional role of TRAK1, w turned to a mouse model. To this end we decided to analyse a mouse where TRAK1 was gene-trapped (TRAK1^{gt}), generated by the Sanger Insitute Gene Trap Resource (SIGTR).

Gene trapping is a method of randomly generating embryonic stem cells with sequenced insertional mutations, by inserting a gene trap construct into an ntronic region of genomic DNA with a promoter-less reporter gene and a selectable marker. This technique leads to the ablation of one of the two alleles of the gene-trapped gene.

TRAK1 sequence is characterized by 16 exons. In our system, insertion of the vector containing the *ß-geo* cassette (a fusion of ß-galactosidase and neomycin phosphotransferase II) occu d after the exon 14 of TRAK1 gene (Fig.2), from the residue 659 of the protei , that corresponds to the C-terminal 30 % of the entire sequence. The SIGTR created a TRAK1^{gt} ES cell line (CSH100) and injected these cells into C57BL/6 blastocysts which we then implanted in pseudopregnant females. They obtained two male TRAK1^{gt} chimeras, one with 80 % and the other with 20 % chimerism. We crossed the 80 % chimera (C1) with a wt C57BL/6 female.

Genotyping strategy

The intron 14-15 of TRAK1, in which the gene trap construct inserted, is 8.3 b long. To confirm that our TRAK1^{gt} mice contained the vector in the TRAK1 gene, and to d the exact position of this insertion, we performed some PCR, using the following primers : four forward primers in intron 14-15, positioned at 2 kb (P1), 3 kb (P2), 4 kb (P3) or 5 kb (P4) respectively from the initiation of the intron, and one reverse primer, complementary to the beginning of the *ß-geo* cassette (P5), that amplified 1.5 kb of the gene trap construct (Fig. 3A). We obtained a PCR product of 1.7 kb using the primers P4-P5. This suggested us that the gene trap vector inserted at approximately 6.2 kb from the intron initiation. To genotype our mice we performed two PCR. We used a primer forward in intron 14-15, positioned at 6 kb from the intron initiation, and a primer reverse complementary to the beginning of the gene trap vector, in the splice acceptor sequence/engrailed-2 (En2) exon, to identify the gt allele or a primer reverse positioned at 7 kb from the intron 14-15 beginning, to amplify the wild-type (wt) allele (Fig. 3B). As expected, we

detected a PCR band of approximately 0.2 kb for the gt allele, and one of 1 kb for the wt allele. Finally we sequenced the 0.2 kb PCR to confirm the pre ence of the insertion.

Linkage and phenotype analysis

We detected a heterozygous mouse in the resulting F_2 (Fig.4A). We crossed it with a wt C57/BL6 female and with a heterozygous female of the resulting F_3. In the F_4 we identified a homozygous male. We obtained other two homozygous males, after cr ssing two heterozygous mice of F_4. All homozygous mice did not present gross abnormalities, b t they surprisingly presented a white colour coat and pink eyes (Fig. 4B).

Discussion

TRAK is one of the orthologues of dMilton. It partially colocalizes with mitochondria and binds to Miro-1, Miro-2 and the kinesin heavy chain. It could probable have role in the regulation of mitochondrial movement in mammals. This does not exclude that it could have other different functions. Indeed, a role of TRAK1 in the regulation of endosome-to-lysosome trafficking has been described (Webber et al., 2008). Given the ability of RAK1 to bind to $GABA_A$ receptors, it could have a role also in regulating the endocytic trafficking of these receptors. Indeed, it is known that neuroreceptors undergo a constant flux whereby surface-bound receptors are endocytosed to form an intracellular pool, then recycled back onto the cel surface or shunted toward lysosome-mediated degradation (Luscher and Keller, 2004). This costant f ux helps maintain the appropriate homeostasis of neuroreceptors. In this scenario, TRAK1 might facilitate the targeting of endocytosed $GABA_A$ receptors back to the cell surface, block them from degradation or direct newly sinthesized receptors to the cell surface.

Endosome to lysosome trafficking is not only essential to regulate trafficking of cell surface receptors, but it is fundamental also to control the transport of melanosomes, that are formed in melanocytes, and that are responsible to confer the pi ent to, for example, the skin or the animal coat. Given that mutations in the proteins forming the melanosomes cause albinism in humans or coat-colour dilution in animals (Bennett and Lamoreux, 2003), the mouse phenotype observed in our animal model suggests that TRAK1 could be involved also in the regulation of melanosomes trafficking.

Figure legends

Fig.1 : *TRAK1 is the mammalian orthologue of Drosophila Milton.*

(A) Domain structure of TRAK1 and its homologues. Accession numbers are as follows : mTRAK1, NP_780323; hTRAK1, NP_001036111; hTRAK2, NP_055864; and dMilton, NP_723249. The amino acid identity and similarity of e protein relative to the protein sequence of human TRAK1 are indicated. Each protein contains three predicted coiled-coil domains shown as blue boxes. mTRAK1 : 103-185, 207-356, and 489-529; hTRAK1 : 104-186, 207-356, and 492-532; hTRAK2 : 126-170, 198-354, and 507-519; dMilton : 133-209, 226-377, and 1021-1034. The bracket indicates the location of the HAPN domain. mTRAK1 : 46-353; hTRAK1 : 47-354; hTRAK2 : 47-354; dMilton : 75-376. m, Mus musculus; h, Homo sapiens; d, Drosophila melanogaster.

(**B**) Multalin alignment of mouse TRAK1 and drosophila Milton. The consensus sequence is marked in red.

Fig.2 : *Generation of a TRAK1 gene trap mouse.*

(**A**) Schematic representation of TRAK1 gene in wild-type and gene-trapped allele. Insertion of *β*-Geo cassette is indicated. WT, wild-type.

(**B**) Domain structure of TRAK1 protein sequence in wt and gene-trapped allele.

(**C**) Generation of the TRAK1 gene trap mouse. TRAK1^{gt} ES cells are injected in blastocysts of pregnant mice to obtain TRAK1^{gt} chimeras. gt, gene trapped.

Fig.3 : *Genotyping strategy.*

(**A**) Schematic representation of the intron 14-15 of TRAK1 gene. Position of the relative primers are indicated (upper panel). 1% agarose gel of PCR pro cts obtained using the indicated primers (lower panel).

(**B**) Schematic representation of the intron 14-15 of TRAK1 gene. Insertion of β-Geo cassette and position of the relative primers are indicated (left). 1% agarose gel of PCR products obtained using the indicated primers (right).

Fig.4 : *Mice linkage and phenotype analysis.*

(**A**) Schematic representation of the genotype of the studied mice, consisting of 6 g nerations. Subjects with the homozygous TRAK1^{gt} gene are indicated by closed symbols; heterozygous carriers are indicated by half-shaded symbols.

(**B**) Representative photographs of wt and homozygous TRAK1^{gt} (Trak1$^{-/-}$) mice.

Reference List

Beck,M., Brickley,K., Wilkinson,H.L., Sharma,S., Smith , Chazot,P.L., Pollard,S., and Stephenson,F.A. (2002). Identification, molecular cloning, and characterization of a novel GABAA receptor-associated protein, GRIF-1. J. Biol. Chem. *277*, 30079-30090.

Bennett,D.C., and Lamoreux,M.L. (2003). The color loci of mice--a genetic century. Pigment. Cell Res. *16*, 333-344.

Brickley,K., Smith,M.J., Beck,M., and Stephenson,F.A. 005). GRIF-1 and OIP106, members of a novel gene family of coiled-coil domain proteins: association in vivo and in vitro with kinesin. J. Biol. Chem. *280*, 14723-14732.

Chang,D.T., Honick,A.S., and Reynolds,I.J. (2006). Mitochondrial trafficking to synapses in cultured primary cortical neurons. J. Neurosci. *26*, 7035-7045.

Ebneth,A., Godemann,R., Stamer,K., Illenberger,S., Trinczek,B., and Mand lkow,E. (1998). Overexpression of tau protein inhibits kinesin-dependent trafficking of vesicles, mitochondria, and endoplasmic reticulum: implications for Alzheimer's di ease. J. Cell Biol. *143*, 777-794.

Fransson,A., Ruusala,A., and Aspenström,P. (2003). Atypical Rho GTPases have roles in mitochondrial homeostasis and apoptosis. J Biol. Chem. *278*, 6495-6502.

Fransson,S., Ruusala,A., and Aspenström,P. (2006). The atypical Rho GTPases Miro-1 and Miro-2 have essential roles in mitochondrial trafficking. Bio hem. Biophys. Res Commun. *344*, 500-510.

Frederick,R.L., McCaffery,J.M., Cunningham,K.W., Okamo o,K., and Shaw,J.M. (2004). Yeast Miro GTPase, Gem1p, regulates mitochondrial morphology via a novel pathway. J. Cell Biol. *167*, 87-98.

Gauthier,L.R., Charrin,B.C., Borrell-Pagès,M., Dompierre,J.P., Rangone,H., Cordelières,F.P., De Mey,J., MacDonald,M.E., Lessmann,V., Humbert,S., and S udou,F. (2004). Huntingtin controls neurotrophic support and survival of neurons by enhancing BDNF vesicular transport along microtubules. Cell *118*, 127-138.

Gilbert,S.L., Zhang,L., Forster,M.L., Anderson,J.R., I ase,T., Soliven,B., Donahue,L.R., Sweet,H.O., Bronson,R.T., Davisson,M.T., Wollmann,R.L., and Lahn,B.T. (2006). Trak1 mutation disrupts GABA(A) receptor homeostasis in hypertonic mice. Nat. Genet. *38*, 245-250.

Glater,E.E., Megeath,L.J., Stowers,R.S., and Schwarz,T.L. (2006). Axonal transport of mitochondria requires milton to recruit kinesin heavy ain and is light chain independent. J. Cell Biol. *173*, 545-557.

Guo,X., Macleod,G.T., Wellington,A., Hu,F., Panchumart S., Schoenfield,M., Marin,L., Charlton,M.P., Atwood,H.L., and Zinsmaier,K.E. (2005). The GTPase dMiro is required for axonal transport of mitochondria to Drosophila synapses. Neuron *47*, 379-393.

Hollenbeck,P.J. and Saxton,W.M. (2005). The axonal tra sport of mitochondria. J. Cell Sci. *118*, 5411-5419.

Iyer,S.P., Akimoto,Y., and Hart,G.W. (2003). Identification and cloning of a novel family of coiled-coil domain proteins that interact with O-GlcNAc transferase. J Biol. Chem. *278*, 5399-5409.

Kikuno,R., Nagase,T., Ishikawa,K., Hirosawa,M., Miyaji a,N., Tanaka,A., Kotani,H., Nomura,N., and Ohara,O. (1999). Prediction of the coding sequences of unidentified hum genes. XIV. The complete sequences of 100 new cDNA clones from brain w h code for large proteins in vitro. DNA Res. *6*, 197-205.

Kirk,E., Chin,L.S., and Li,L. (2006). GRIF1 binds Hrs and is a new regulator of endosomal trafficking. J Cell Sci. *119*, 4689-4701.

Li,S.H., Gutekunst,C.A., Hersch,S.M., and Li,X.J. (1998). Interaction of huntingtin-associated protein with dynactin P150Glued. J Neurosci. *18*, 1261-1269.

Li,Y., Chin,L.S., Levey,A.I., and Li,L. (2002). Huntingtin-associated protein 1 interacts with hepatocyte growth factor-regulated tyrosine kinase substrate and functions in endosomal trafficking. J Biol. Chem. *277*, 28212-28221.

Lorish,T.R., Thorsteinsson,G., and Howard,F.M. Jr. (1989). Stiff-man syndrome updated. Mayo Clin. Proc. *64*, 629-636.

Lüscher,B., and Keller,C.A. (2004). Regulation of GABAA receptor trafficking, channel acti ity, and functional plasticity of inhibitory synapses. Phar acol. Ther. *102*, 195-221.

McKernan,R.M and Whiting,P.J. (1996). Which GABAA-receptor subtypes really occur in the brain? Trends Neurosci. *19*, 139-143.

Miki,H., Setou,M., Kaneshiro,K., and Hirokawa,N. (2001). All kinesin superfamily protein, KIF, genes in mouse and human. Proc. Natl. Acad. Sci. U. S. A *98*, 7004-7011.

Setou,M., Seog,D.H., Tanaka,Y., Kanai,Y., Takei,Y., Kawa shi,M., and Hirokawa,N. (2002). Glutamate-receptor-interacting protein GRIP1 directly steers kinesin to d rites. Nature *417*, 83-87.

Shafi,R., Iyer,S.P., Ellies,L.G., O'Donnell,N., Marek, .W., Chui,D., Hart,G.W., and Marth,J.D. (2000). The O-GlcNAc transferase gene resides on the X chromosome an is essential for embryonic stem cell viability and mouse ontogeny. Proc. Natl. Acad. Sci. *23*, 5735-5739.

Stowers,R.S., Megeath,L.J., Gorska-Andrzejak,J., Meinertzhagen,I.A., and Schwarz,T.L. (2002). Axonal transport of mitochondria to synapses depends o milton, a novel Drosophila protein. Neuron *36*, 1063-1077.

Tang,T.S., Tu,H., Chan,E.Y., Maximov,A., Wang,Z., Well ngton,C.L., Hayden,M.R., and Bezprozvanny,I. (2003). Huntingtin and huntingtin-associated protein 1 influence neuronal calcium signaling mediated by inositol-(1,4,5) triphosphate receptor type 1. Neuron. *39*, 227-239.

Wang,X. and Schwarz,T.L. (2009). The mechanism of Ca2+ -dependent regulation of kinesin-mediated mitochondrial motility. Cell *136*, 163-174.

Webber,E., Li,L., and Chin,L.S. (2008). Hypertonia-associated protein Trak1 is a novel regulator of endosome-to-lysosome trafficking. J Mol. Biol. *382*, 638-651.

Fig.1

A

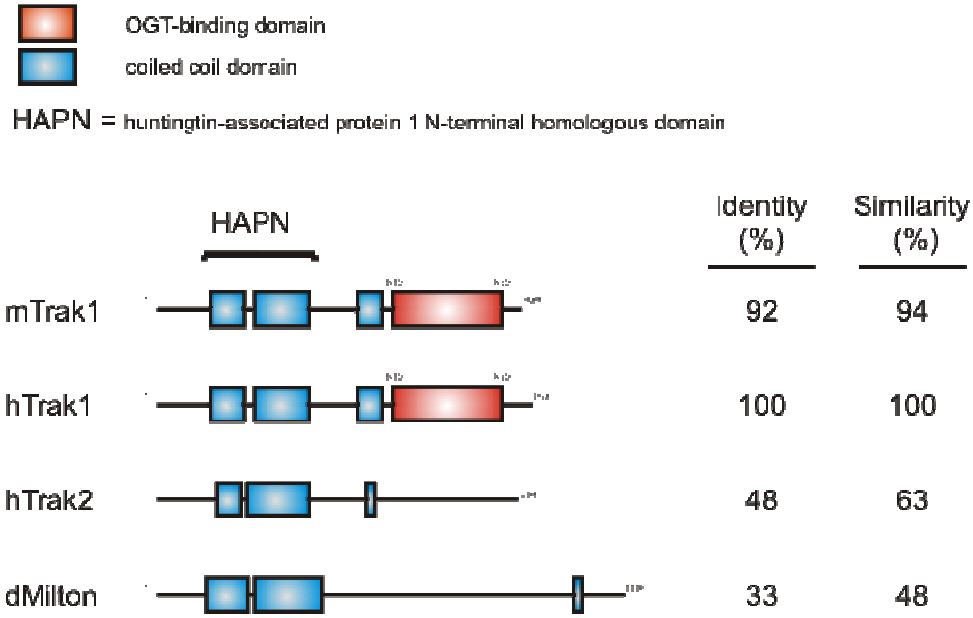
OGT-binding domain
coiled coil domain
HAPN = huntingtin-associated protein 1 N-terminal homologous domain
HAPN
Identity (%)
Similarity (%)
mTrak1
92
94
hTrak1
100
100
hTrak2
48
63
dMilton
33
48

B

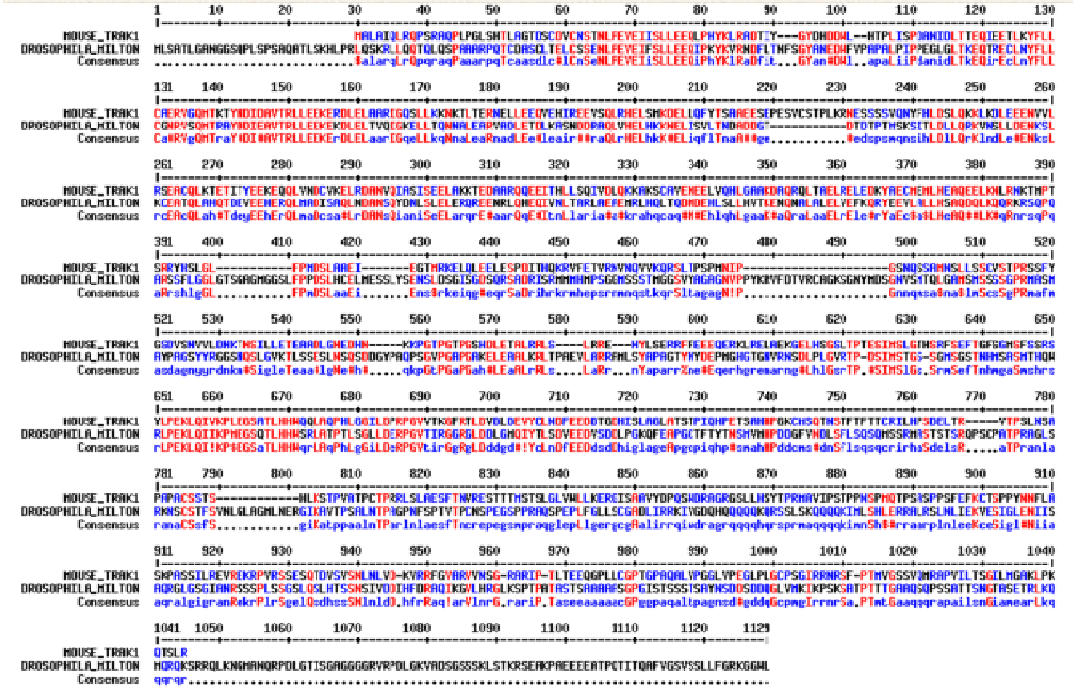

Fig.2

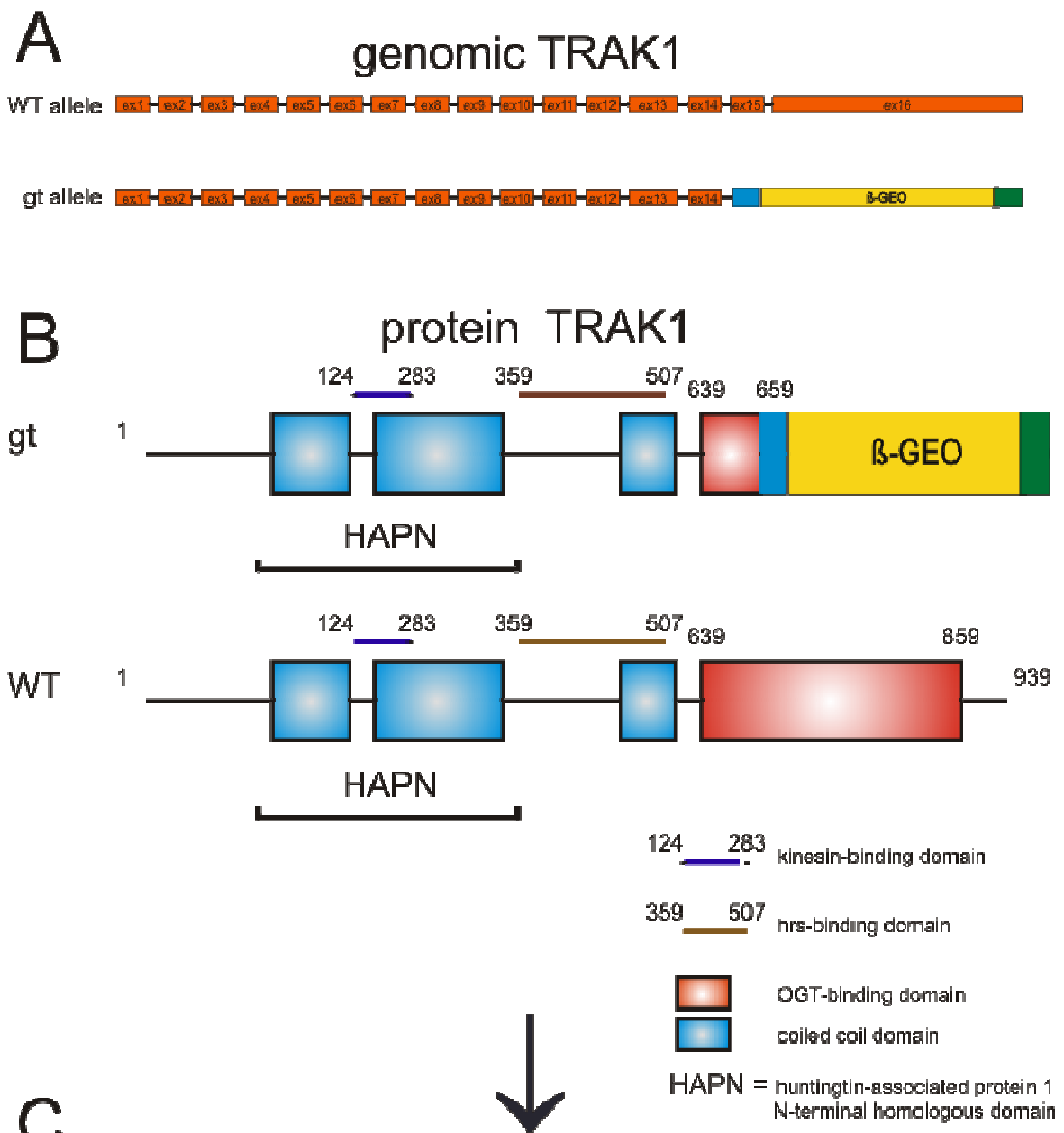
A
genomic TRAK1
WT allele
ex1 ex2 ex3 ex4 ex5 ex6 ex7 ex8 ex9 ex10 ex11 ex12 ex13 ex14 ex15 ex16
gt allele
ex1 ex2 ex3 ex4 ex5 ex6 ex7 ex8 ex9 ex10 ex11 ex12 ex13 ex14 ß-GEO
B
protein TRAK1
124 283 359 507 639 659
gt
1
ß-GEO
HAPN
124 283 359 507 639 859
WT
1
939
HAPN
124 283 kinesin-binding domain
359 507 hrs-binding domain
OGT-binding domain
coiled coil domain
HAPN = huntingtin-associated protein 1 N-terminal homologous domain
C
injection of recombinant ES into blastocysts
chimera 80%
chimera 20%

Fig.3

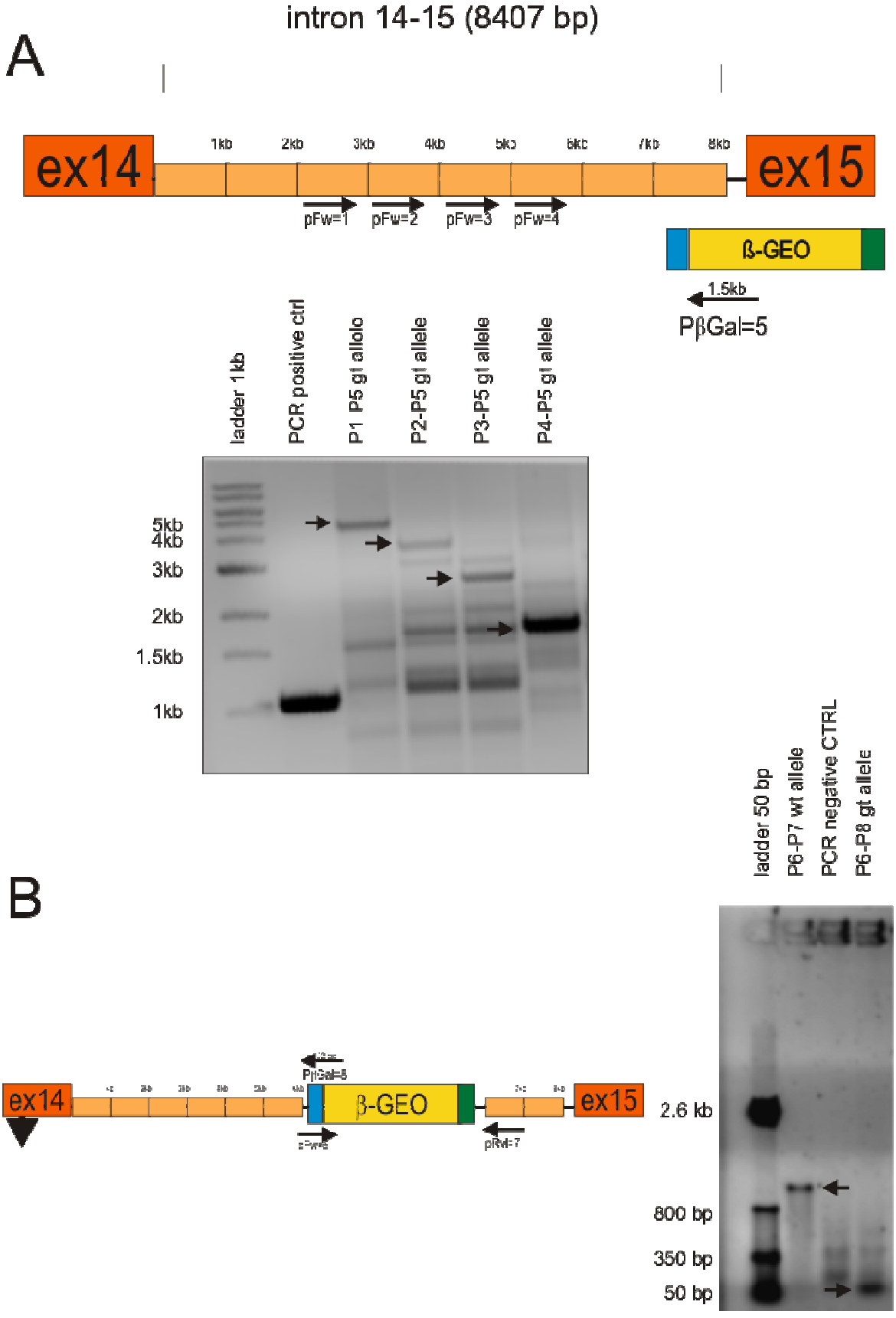
A
intron 14-15 (8407 bp)
ex14
ex15
1kb
2kb
3kb
4kb
5kb
6kb
7kb
8kb
pFw=1
pFw=2
pFw=3
pFw=4
ß-GEO
1.5kb
PβGal=5
ladder 1 kb
PCR positive ctrl
P1 P5 g1 allolo
P2-P5 g1 allele
P3-P5 g1 allele
P4-P5 g1 allele
5kb
4kb
3kb
2kb
1.5kb
1kb
B
ex14
β-GEO
ex15
pRv=7
ladder 50 bp
P6-P7 wt allele
PCR negative CTRL
P6-P8 gt allele
2.6 kb
800 bp
350 bp
50 bp

Fig.4

A

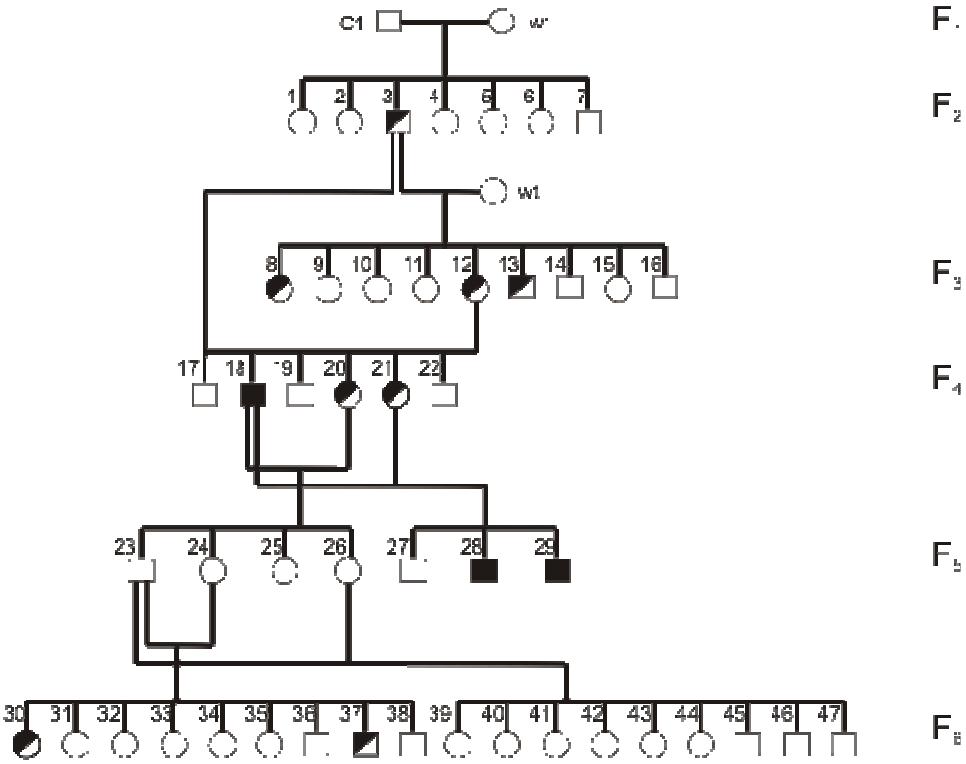
C1
w
1
2
3
4
5
6
7
w1
8
9
10
11
12
13
14
15
16
17
18
19
20
21
22
23
24
25
26
27
28
29
30
31
32
33
34
35
36
37
38
39
40
41
42
43
44
45
46
47
F1
F2
F3
F4
F5
F6

B

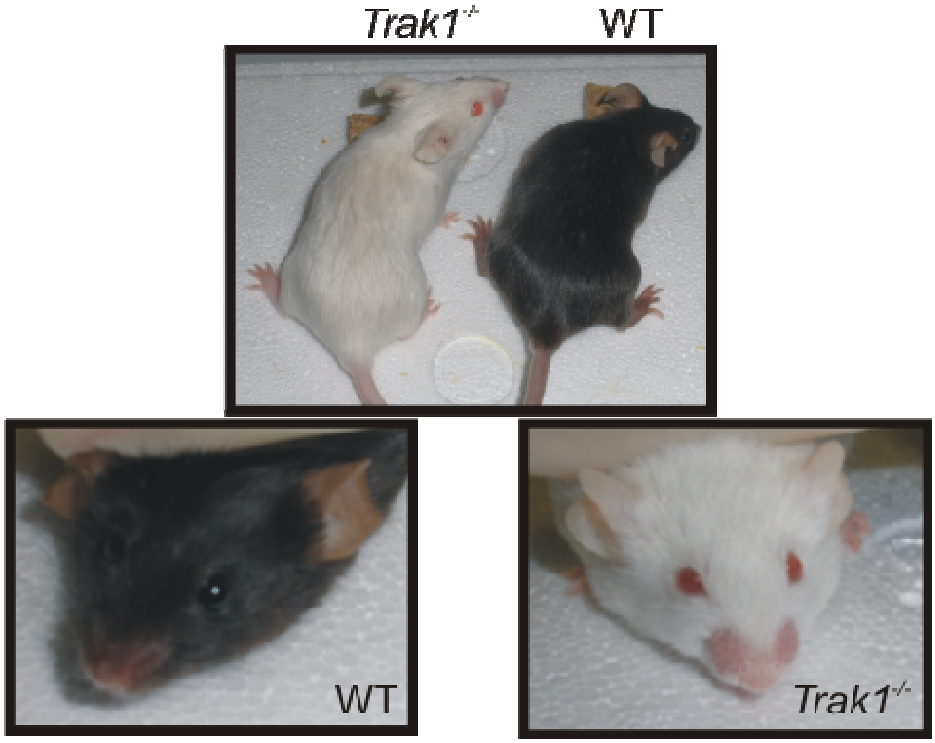
Trak1+/-
WT
WT
Trak1-/-

6 Conclusions

The work presented in the first part of this Thesis described a new role of trichoplein, a keratin-binding protein, and found its precise location in the cell, so far still unknown.

Trichoplein was originally identified as a keratin interactor (Nishizawa et al., 2005), even if its subcellular localization appeared controversial. It was shown to be distributed with a punctuate pattern throughout the cytoplasm, colocalizing with K8/K18. Recently, Baffa and colleagues identified trichoplein as a novel putative tumor suppressor gene, localized in a chromosomal region deleted in a large variety of solid advanced tumors (Aubele et al., 2000; Field et al., 1995; Kimura et al., 1998). Trichoplein was shown to partially colocalize with mitochondria, but the relashionship between the protein and the organelles remained to be clarified

Our results confirmed the interaction between trichoplein and keratins, placing the protein at the interface between mitochondria and K8/K18. We found that trichoplein was relatively enriched in MAMs, where it negatively regulated ER-mitochondria interaction. Overexpression of the protein decreased the proximity between the two organelles. It is known that MAMs form membrane microdomains of high Ca^{2+} concentration (Rizzuto et al., 2003). As a functional consequence of this, our results showed that trichoplein protects against Ca^{2+}-mediated cell death. This suggests that trichoplein could be involved in the Ca^{2+} dynamics between ER and mitochondria, but further investigations are required to better elucidate this function.

The work presented in the second part of this Thesis described a new role for TRAK1, the homologue of the protein dMilton that regulates the mitochondrial movement in the fruit fly (Stowers et al., 2002). TRAK1 has been also identified as a potential itneractor of $GABA_A$ receptors, suggesting a role also in regulating trafficking of cell surface receptors. On the other hand, a role of TRAK1 in the regulation of endosome-to-lysosome trafficking has also been described (Webber et al., 2008). We decided therefore to investigate the role of Trak1 by

generating a gene-trap mouse, where most of the protein (30%) was missing due to the insertion of a B-gal cassette in the intron 14-15. After the successful mapping of the insertion, we bred the mice and obtained homozygous mice for $TRAK^{gt}$. Notably, while they did not display gross neurological abnormalities, their fur was white and their eyes pink. Given that mutations in the proteins forming melanosomes cause albinism in humans or coat-colour dilution in animals (Bennett and Lamoreux, 2003), the mouse phenotype observed in our animal model suggests that TRAK1 could be involved also in the regulation of melanosomes trafficking.

Further studies are required to clarify the mechanism of action of TRAK1, and to analyse the localization and the influence of the protein in our $TRAK^{gt}$ mouse model.

7 Reference List

Alirol,E., James,D., Huber,D., Marchetto,A., Vergani,L., Martinou,J.C., and Scorrano,L. (2006). The mitochondrial fission protein hFis1 requires the endoplasmic reticulum gateway to induce apoptosis. Mol. Biol. Cell *17*, 4593-4605.

Altmann,K., Frank,M., Neumann,D., Jakobs,S., and Westermann,B. (2008). The class V myosin motor protein, Myo2, plays a major role in mitochondrial motility in Saccharomyces cerevisiae. J. Cell Biol. *181*, 119-130.

Altmann,K. and Westermann,B. (2005). Role of essential genes in mitochondrial morphogenesis in Saccharomyces cerevisiae. Mol. Biol. Cell *16*, 5410-5417.

Ardail,D., Gasnier,F., Lerme,F., Simonot,C., Louisot,P., and Gateau-Roesch,O. (1993). Involvement of mitochondrial contact sites in the subcellular compartmentalization of phospholipid biosynthetic enzymes. J. Biol. Chem. *268*, 25985-25992.

Ardail,D., Lerme,F., and Louisot,P. (1991). Involvement of contact sites in phosphatidylserine import into liver mitochondria. J. Biol. Chem. *266*, 7978-7981.

Arnaudeau,S., Kelley,W.L., Walsh,J.V., Jr., and Demaurex,N. (2001). Mitochondria recycle Ca(2+) to the endoplasmic reticulum and prevent the depletion of neighboring endoplasmic reticulum regions. J. Biol. Chem. *276*, 29430-29439.

Benard,G. and Rossignol,R. (2008). Ultrastructure of the mitochondrion and its bearing on function and bioenergetics. Antioxid. Redox. Signal. *10*, 1313-1342.

Bereiter-Hahn,J. and Voth,M. (1988). Ionic control of locomotion and shape of epithelial cells: II. Role of monovalent cations. Cell Motil. Cytoskeleton *10*, 528-536.

Bereiter-Hahn,J. and Voth,M. (1994). Dynamics of mitochondria in living cells: shape changes, dislocations, fusion, and fission of mitochondria. Microsc. Res. Tech. *27*, 198-219.

Bernardi,P., Petronilli,V., Di Lisa,F., and Forte,M. (2001). A mitochondrial perspective on cell death. Trends. Biochem. Sci. *26*, 112-117.

Boldogh,I.R., Yang,H.C., Nowakowski,W.D., Karmon,S.L., Hays,L.G., Yates,J.R., III, and Pon,L.A. (2001a). Arp2/3 complex and actin dynamics are required for actin-based mitochondrial motility in yeast. Proc. Natl. Acad. Sci. U. S. A *98*, 3162-3167.

Boldogh,I.R., Yang,H.C., and Pon,L.A. (2001b). Mitochondrial inheritance in budding yeast. Traffic. *2*, 368-374.

Breckenridge,D.G., Kang,B.H., Kokel,D., Mitani,S., Staehelin,L.A., and Xue,D. (2008). Caenorhabditis elegans drp-1 and fis-2 regulate distinct cell-death execution pathways downstream of ced-3 and independent of ced-9. Mol. Cell *31*, 586-597.

Cai,Q., Gerwin,C., and Sheng,Z.H. (2005). Syntabulin-mediated anterograde transport of mitochondria along neuronal processes. J. Cell Biol. *170*, 959-969.

Capetanaki,Y., Bloch,R.J., Kouloumenta,A., Mavroidis,M., and Psarras,S. (2007). Muscle intermediate filaments and their links to membranes and membranous organelles. Exp. Cell Res. *313*, 2063-2076.

Cartoni,R., Leger,B., Hock,M.B., Praz,M., Crettenand,A., Pich,S., Ziltener,J.L., Luthi,F., Deriaz,O., Zorzano,A., Gobelet,C., Kralli,A., and Russell,A.P. (2005). Mitofusins 1/2 and ERRalpha expression are increased in human skeletal muscle after physical exercise. J. Physiol *567*, 349-358.

Cassidy-Stone,A., Chipuk,J.E., Ingerman,E., Song,C., Yoo,C., Kuwana,T., Kurth,M.J., Shaw,J.T., Hinshaw,J.E., Green,D.R., and Nunnari,J. (2008). Chemical inhibition of the mitochondrial division dynamin reveals its role in Bax/Bak-dependent mitochondrial outer membrane permeabilization. Dev. Cell *14*, 193-204.

Cereghetti,G.M., Stangherlin,A., Martins de,B.O., Chang,C.R., Blackstone,C., Bernardi,P., and Scorrano,L. (2008). Dephosphorylation by calcineurin regulates translocation of Drp1 to mitochondria. Proc. Natl. Acad. Sci. U. S. A *105*, 15803-15808.

Chada,S.R. and Hollenbeck,P.J. (2003). Mitochondrial movement and positioning in axons: the role of growth factor signaling. J. Exp. Biol. *206*, 1985-1992.

Chang,C.R. and Blackstone,C. (2007). Cyclic AMP-dependent protein kinase phosphorylation of Drp1 regulates its GTPase activity and mitochondrial morphology. J. Biol Chem. *282*, 21583-21587.

Chang,D.T., Honick,A.S., and Reynolds,I.J. (2006). Mitochondrial trafficking to synapses in cultured primary cortical neurons. J. Neurosci. *26*, 7035-7045.

Chen,K.H., Guo,X., Ma,D., Guo,Y., Li,Q., Yang,D., Li,P., Qiu,X., Wen,S., Xiao,R.P., and Tang,J. (2004a). Dysregulation of HSG triggers vascular proliferative disorders. Nat. Cell Biol. *6*, 872-883.

Chen,Y.J., Zhang,P., Egelman,E.H., and Hinshaw,J.E. (2004b). The stalk region of dynamin drives the constriction of dynamin tubes. Nat Struct. Mol Biol *11*, 574-575.

Cipolat,S., de Brito,O.M., Dal Zilio,B., and Scorrano,L. (2004). OPA1 requires mitofusin 1 to promote mitochondrial fusion. Proc. Natl. Acad. Sci. U. S. A *101*, 15927-15932.

Cipolat,S., Rudka,T., Hartmann,D., Costa,V., Serneels,L., Craessaerts,K., Metzger,K., Frezza,C., Annaert,W., D'Adamio,L., Derks,C., Dejaegere,T., Pellegrini,L., D'Hooge,R., Scorrano,L., and De Strooper,B. (2006). Mitochondrial Rhomboid PARL Regulates Cytochrome c Release during Apoptosis via OPA1-Dependent Cristae Remodeling. Cell *126*, 163-175.

Cohen,S. and Greenberg,M.E. (2008). Communication between the synapse and the nucleus in neuronal development, plasticity, and disease. Annu. Rev. Cell Dev. Biol. *24*, 183-209.

Cribbs,J.T. and Strack,S. (2007). Reversible phosphorylation of Drp1 by cyclic AMP-dependent protein kinase and calcineurin regulates mitochondrial fission and cell death. EMBO Rep. *8*, 939-944.

Csordas,G. and Hajnoczky,G. (2001). Sorting of calcium signals at the junctions of endoplasmic reticulum and mitochondria. Cell Calcium *29*, 249-262.

Csordas,G., Renken,C., Varnai,P., Walter,L., Weaver,D., Buttle,K.F., Balla,T., Mannella,C.A., and Hajnoczky,G. (2006). Structural and functional features and significance of the physical linkage between ER and mitochondria. J. Cell Biol. *174*, 915-921.

Danial,N.N. and Korsmeyer,S.J. (2004). Cell death: critical control points. Cell *116*, 205-219.

de Brito,O.M. and Scorrano,L. (2008). Mitofusin 2 tethers endoplasmic reticulum to mitochondria. Nature *456*, 605-610.

Dimmer,K.S. and Scorrano,L. (2006). (De)constructing mitochondria: what for? Physiology. (Bethesda.) *21*, 233-241.

Drubin,D.G., Jones,H.D., and Wertman,K.F. (1993). Actin structure and function: roles in mitochondrial organization and morphogenesis in budding yeast and identification of the phalloidin-binding site. Mol. Biol. Cell *4*, 1277-1294.

Duchen,M.R. (2000). Mitochondria and calcium: from cell signalling to cell death. J. Physiol. *529 Pt 1:57-68.*, 57-68.

Duvezin-Caubet,S., Koppen,M., Wagener,J., Zick,M., Israel,L., Bernacchia,A., Jagasia,R., Rugarli,E.I., Imhof,A., Neupert,W., Langer,T., and Reichert,A.S. (2007). OPA1 processing reconstituted in yeast depends on the subunit composition of the m-AAA protease in mitochondria. Mol. Biol. Cell *18*, 3582-3590.

Ebneth,A., Godemann,R., Stamer,K., Illenberger,S., Trinczek,B., and Mandelkow,E. (1998). Overexpression of tau protein inhibits kinesin-dependent trafficking of vesicles, mitochondria, and endoplasmic reticulum: implications for Alzheimer's disease. J Cell Biol *143*, 777-794.

Fannjiang,Y., Cheng,W.C., Lee,S.J., Qi,B., Pevsner,J., McCaffery,J.M., Hill,R.B., Basanez,G., and Hardwick,J.M. (2004). Mitochondrial fission proteins regulate programmed cell death in yeast. Genes Dev. *18*, 2785-2797.

Ferre,M., Amati-Bonneau,P., Tourmen,Y., Malthiery,Y., and Reynier,P. (2005). eOPA1: an online database for OPA1 mutations. Hum. Mutat. *25*, 423-428.

Ferri,K.F. and Kroemer,G. (2001). Organelle-specific initiation of cell death pathways. Nat. Cell Biol. *3*, E255-E263.

Filippin,L., Magalhaes,P.J., Di Benedetto,G., Colella,M., and Pozzan,T. (2003). Stable interactions between mitochondria and endoplasmic reticulum allow rapid accumulation of calcium in a subpopulation of mitochondria. J. Biol. Chem. *278*, 39224-39234.

Frederick,R.L., McCaffery,J.M., Cunningham,K.W., Okamoto,K., and Shaw,J.M. (2004). Yeast Miro GTPase, Gem1p, regulates mitochondrial morphology via a novel pathway. J. Cell Biol. *167*, 87-98.

Frey,T.G. and Mannella,C.A. (2000). The internal structure of mitochondria. Trends. Biochem. Sci. *25*, 319-324.

Frezza,C., Cipolat,S., Martins,d.B., Micaroni,M., Beznoussenko,G.V., Rudka,T., Bartoli,D., Polishuck,R.S., Danial,N.N., De Strooper,B., and Scorrano,L. (2006). OPA1 Controls Apoptotic Cristae Remodeling Independently from Mitochondrial Fusion. Cell *126*, 177-189.

Fuchs,E. and Cleveland,D.W. (1998). A structural scaffolding of intermediate filaments in health and disease. Science *279*, 514-519.

Gaigg,B., Simbeni,R., Hrastnik,C., Paltauf,F., and Daum,G. (1995). Characterization of a microsomal subfraction associated with mitochondria of the yeast, Saccharomyces cerevisiae. Involvement in synthesis and import of phospholipids into mitochondria. Biochim. Biophys. Acta *1234*, 214-220.

Garcia,M.L. and Cleveland,D.W. (2001). Going new places using an old MAP: tau, microtubules and human neurodegenerative disease. Curr. Opin. Cell Biol. *13*, 41-48.

Germain,M., Mathai,J.P., McBride,H.M., and Shore,G.C. (2005). Endoplasmic reticulum BIK initiates DRP1-regulated remodelling of mitochondrial cristae during apoptosis. EMBO J. *24*, 1546-1556.

Glater,E.E., Megeath,L.J., Stowers,R.S., and Schwarz,T.L. (2006). Axonal transport of mitochondria requires milton to recruit kinesin heavy chain and is light chain independent. J. Cell Biol. *173*, 545-557.

Hajnoczky,G., Csordas,G., Krishnamurthy,R., and Szalai,G. (2000). Mitochondrial calcium signaling driven by the IP3 receptor. J. Bioenerg. Biomembr. *32*, 15-25.

Hajnoczky,G., Pacher,P., and Lin,X. (2001). Spatio-temporal organization of the mitochondrial phase of apoptosis. IUBMB. Life *52*, 237-245.

Harder,Z., Zunino,R., and McBride,H. (2004). Sumo1 conjugates mitochondrial substrates and participates in mitochondrial fission. Curr. Biol. *14*, 340-345.

Hengartner,M.O. (2000). The biochemistry of apoptosis. Nature *407*, 770-776.

Hermann,G.J., King,E.J., and Shaw,J.M. (1997). The yeast gene, MDM20, is necessary for mitochondrial inheritance and organization of the actin cytoskeleton. J. Cell Biol. *137*, 141-153.

Hirokawa,N. (1982). Cross-linker system between neurofilaments, microtubules, and membranous organelles in frog axons revealed by the quick-freeze, deep-etching method. J. Cell Biol. *94*, 129-142.

Hollenbeck,P.J., Bray,D., and Adams,R.J. (1985). Effects of the uncoupling agents FCCP and CCCP on the saltatory movements of cytoplasmic organelles. Cell Biol. Int. Rep. *9*, 193-199.

Hollenbeck,P.J. and Saxton,W.M. (2005). The axonal transport of mitochondria. J. Cell Sci. *118*, 5411-5419.

Huang,P., Yu,T., and Yoon,Y. (2007). Mitochondrial clustering induced by overexpression of the mitochondrial fusion protein Mfn2 causes mitochondrial dysfunction and cell death. Eur. J. Cell Biol. *86*, 289-302.

Ishihara,N., Eura,Y., and Mihara,K. (2004). Mitofusin 1 and 2 play distinct roles in mitochondrial fusion reactions via GTPase activity. J. Cell Sci. *117*, 6535-6546.

Ishii,K., Hirose,K., and Iino,M. (2006). Ca2+ shuttling between endoplasmic reticulum and mitochondria underlying Ca2+ oscillations. EMBO Rep. *7*, 390-396.

Jahani-Asl,A. and Slack,R.S. (2007). The phosphorylation state of Drp1 determines cell fate. EMBO Rep. *8*, 912-913.

James,D.I., Parone,P.A., Mattenberger,Y., and Martinou,J.C. (2003). hFis1, a novel component of the mammalian mitochondrial fission machinery. J. Biol. Chem. *278*, 36373-36379.

Jouaville,L.S., Pinton,P., Bastianutto,C., Rutter,G.A., and Rizzuto,R. (1999). Regulation of mitochondrial ATP synthesis by calcium: evidence for a long-term metabolic priming. Proc. Natl. Acad. Sci. U. S. A. *96*, 13807-13812.

Karbowski,M., Arnoult,D., Chen,H., Chan,D.C., Smith,C.L., and Youle,R.J. (2004a). Quantitation of mitochondrial dynamics by photolabeling of individual organelles shows that mitochondrial fusion is blocked during the Bax activation phase of apoptosis. J. Cell Biol. *164*, 493-499.

Karbowski,M., Jeong,S.Y., and Youle,R.J. (2004b). Endophilin B1 is required for the maintenance of mitochondrial morphology. J. Cell Biol. *166*, 1027-1039.

Karbowski,M., Lee,Y.J., Gaume,B., Jeong,S.Y., Frank,S., Nechushtan,A., Santel,A., Fuller,M., Smith,C.L., and Youle,R.J. (2002). Spatial and temporal association of Bax with mitochondrial fission sites, Drp1, and Mfn2 during apoptosis. J. Cell Biol. *159*, 931-938.

Karbowski,M., Norris,K.L., Cleland,M.M., Jeong,S.Y., and Youle,R.J. (2006). Role of Bax and Bak in mitochondrial morphogenesis. Nature *443*, 658-662.

Kay,B.K., Kasanov,J., Knight,S., and Kurakin,A. (2000). Convergent evolution with combinatorial peptides. FEBS Lett *480*.

Kijima,K., Numakura,C., Izumino,H., Umetsu,K., Nezu,A., Shiiki,T., Ogawa,M., Ishizaki,Y., Kitamura,T., Shozawa,Y., and Hayasaka,K. (2005). Mitochondrial GTPase mitofusin 2 mutation in Charcot-Marie-Tooth neuropathy type 2A. Hum. Genet. *116*, 23-27.

Landolfi,B., Curci,S., Debellis,L., Pozzan,T., and Hofer,A.M. (1998). Ca2+ homeostasis in the agonist-sensitive internal store: functional interactions between mitochondria and the ER measured In situ in intact cells. J. Cell Biol. *142*, 1235-1243.

Lane,E.B., Hogan,B.L., Kurkinen,M., and Garrels,J.I. (1983). Co-expression of vimentin and cytokeratins in parietal endoderm cells of early mouse embryo. Nature *303*, 701-704.

Langbein,L., Kosmehl,H., Kiss,F., Katenkamp,D., and Neupert,G. (1989). Cytokeratin expression in experimental murine rhabdomyosarcomas. Intermediate filament pattern in original tumors, allotransplants, cell culture and re-established tumors from cell culture. Exp. Pathol. *36*, 23-36.

Lawson,V.H., Graham,B.V., and Flanigan,K.M. (2005). Clinical and electrophysiologic features of CMT2A with mutations in the mitofusin 2 gene. Neurology *65*, 197-204.

Lazzarino,D.A., Boldogh,I., Smith,M.G., Rosand,J., and Pon,L.A. (1994). Yeast mitochondria contain ATP-sensitive, reversible actin-binding activity. Mol. Biol. Cell *5*, 807-818.

Lee,M.C., Miller,E.A., Goldberg,J., Orci,L., and Schekman,R. (2004a). Bi-directional protein transport between the ER and Golgi. Annu Rev Cell Dev Biol *20*.

Lee,Y.J., Jeong,S.Y., Karbowski,M., Smith,C.L., and Youle,R.J. (2004b). Roles of the mammalian mitochondrial fission and fusion mediators Fis1, Drp1, and Opa1 in apoptosis. Mol. Biol. Cell *15*, 5001-5011.

Li,Z., Okamoto,K., Hayashi,Y., and Sheng,M. (2004). The importance of dendritic mitochondria in the morphogenesis and plasticity of spines and synapses. Cell *119*, 873-887.

Linden,M., Nelson,B.D., and Leterrier,J.F. (1989). The specific binding of the microtubule-associated protein 2 (MAP2) to the outer membrane of rat brain mitochondria. Biochem. J. *261*, 167-173.

Liu,X., Kim,C.N., Yang,J., Jemmerson,R., and Wang,X. (1996). Induction of apoptotic program in cell-free extracts: requirement for dATP and cytochrome c. Cell *86*, 147-157.

Mandelkow,E.M., Thies,E., Trinczek,B., Biernat,J., and Mandelkow,E. (2004). MARK/PAR1 kinase is a regulator of microtubule-dependent transport in axons. J Cell Biol *167*, 99-110.

Mannella,C.A., Forte,M., and Colombini,M. (1992). Toward the molecular structure of the mitochondrial channel, VDAC. J. Bioenerg. Biomembr. *24*, 7-19.

McConnell,S.J. and Yaffe,M.P. (1992). Nuclear and mitochondrial inheritance in yeast depends on novel cytoplasmic structures defined by the MDM1 protein. J. Cell Biol. *118*, 385-395.

McConnell,S.J. and Yaffe,M.P. (1993). Intermediate filament formation by a yeast protein essential for organelle inheritance. Science *260*, 687-689.

Miller,K.E. and Sheetz,M.P. (2004). Axonal mitochondrial transport and potential are correlated. J. Cell Sci. *117*, 2791-2804.

Milner,D.J., Mavroidis,M., Weisleder,N., and Capetanaki,Y. (2000). Desmin cytoskeleton linked to muscle mitochondrial distribution and respiratory function. J. Cell Biol. *150*, 1283-1298.

Mironov,S.L. (2006). Spontaneous and evoked neuronal activities regulate movements of single neuronal mitochondria. Synapse *59*, 403-411.

Neuspiel,M., Zunino,R., Gangaraju,S., Rippstein,P., and McBride,H.M. (2005). Activated Mfn2 signals mitochondrial fusion, interferes with Bax activation and reduces susceptibility to radical induced depolarization. J. Biol. Chem. *280*, 25060-25070.

Nicholls,D., Bernardi,P., Brand,M., Halestrap,A., Lemasters,J., and Reynolds,I. (2000). Apoptosis and the laws of thermodynamics. Nat. Cell Biol. *2*, E172-E173.

Nicholls,D.G. and Crompton,M. (1980). Mitochondrial calcium transport. FEBS Lett. *111*, 261-268.

Nishizawa,M., Izawa,I., Inoko,A., Hayashi,Y., Nagata,K., Yokoyama,T., Usukura,J., and Inagaki,M. (2005). Identification of trichoplein, a novel keratin filament-binding protein. J. Cell Sci. *118*, 1081-1090.

Olichon,A., Baricault,L., Gas,N., Guillou,E., Valette,A., Belenguer,P., and Lenaers,G. (2003). Loss of OPA1 perturbates the mitochondrial inner membrane structure and integrity, leading to cytochrome c release and apoptosis. J. Biol. Chem. *278*, 7743-7746.

Orr,A.L., Li,S., Wang,C.E., Li,H., Wang,J., Rong,J., Xu,X., Mastroberardino,P.G., Greenamyre,J.T., and Li,X.J. (2008). N-terminal mutant huntingtin associates with mitochondria and impairs mitochondrial trafficking. J. Neurosci. *28*, 2783-2792.

Palade,G.E. (1952). The fine structure of mitochondria. Anat. Rec. *114*, 427-451.

Pelloquin,L., Belenguer,P., Menon,Y., and Ducommun,B. (1998). Identification of a fission yeast dynamin-related protein involved in mitochondrial DNA maintenance. Biochem. Biophys. Res. Commun. *251*, 720-726.

Pereira,A.J., Dalby,B., Stewart,R.J., Doxsey,S.J., and Goldstein,L.S. (1997). Mitochondrial association of a plus end-directed microtubule motor expressed during mitosis in Drosophila. J Cell Biol *136*, 1081-1090.

Pinton,P., Brini,M., Bastianutto,C., Tuft,R.A., Pozzan,T., and Rizzuto,R. (1998). New light on mitochondrial calcium. BioFactors *8*, 243-253.

Pizzo,P. and Pozzan,T. (2007). Mitochondria-endoplasmic reticulum choreography: structure and signaling dynamics. Trends Cell Biol. *17*, 511-517.

Popov,V.I., Deev,A.A., Klimenko,O.A., Kraev,V., Kuz'minykh,S.B., Medvedev,N.I., Patrushev,I.V., Popov,R.V., Rogachevskii,V.V., Khutsiyan,S.S., Stewart,M.G., and Fesenko,E.E. (2005). Three-dimensional reconstruction of synapses and dendritic spines in the rat and ground squirrel hippocampus: new structural-functional paradigms for synaptic function. Neurosci. Behav. Physiol *35*, 333-341.

Pozzan,T. and Rizzuto,R. (2000). The renaissance of mitochondrial calcium transport. Eur J Biochem *267*, 5269-5273.

Pozzan,T., Rizzuto,R., Volpe,P., and Meldolesi,J. (1994). Molecular and cellular physiology of intracellular calcium stores. Physiol Rev *74*, 595-636.

Rapizzi,E., Pinton,P., Szabadkai,G., Wieckowski,M.R., Vandecasteele,G., Baird,G., Tuft,R.A., Fogarty,K.E., and Rizzuto,R. (2002). Recombinant expression of the voltage-dependent anion channel enhances the transfer of Ca2+ microdomains to mitochondria. J Cell Biol *159*, 613-624.

Reipert,S., Steinbock,F., Fischer,I., Bittner,R.E., Zeold,A., and Wiche,G. (1999). Association of mitochondria with plectin and desmin intermediate filaments in striated muscle. Exp. Cell Res. *252*, 479-491.

Rizzuto,R. (2006). Microdomains of intracellular Ca2+: molecular determinants and functional consequences.

Rizzuto,R., Brini,M., Murgia,M., and Pozzan,T. (1993). Microdomains with high Ca2+ close to IP3-sensitive channels that are sensed by neighboring mitochondria. Science *262*, 744-747.

Rizzuto,R., Pinton,P., Carrington,W., Fay,F.S., Fogarty,K.E., Lifshitz,L.M., Tuft,R.A., and Pozzan,T. (1998). Close contacts with the endoplasmic reticulum as determinants of mitochondrial Ca2+ responses. Science *280*, 1763-1766.

Rizzuto,R., Simpson,A.W., Brini,M., and Pozzan,T. (1992). Rapid changes of mitochondrial Ca2+ revealed by specifically targeted recombinant aequorin. Nature *358*, 325-327.

Rodriguez,J. and Lazebnik,Y. (1999). Caspase-9 and APAF-1 form an active holoenzyme. Genes Dev. *13*, 3179-3184.

Schwarzer,C., Barnikol-Watanabe,S., Thinnes,F.P., and Hilschmann,N. (2002). Voltage-dependent anion-selective channel (VDAC) interacts with the dynein light chain Tctex1 and the heat-shock protein PBP74. Int. J. Biochem. Cell Biol. *34*, 1059-1070.

Scorrano,L. (2003). Divide et impera: Ca^{2+} signals, mitochondrial fission and sensitization to apoptosis. Cell Death. Differ. *10*, 1287-1289.

Scorrano,L., Ashiya,M., Buttle,K., Weiler,S., Oakes,S.A., Mannella,C.A., and Korsmeyer,S.J. (2002). A Distinct Pathway Remodels Mitochondrial Cristae and Mobilizes Cytochrome c during Apoptosis. Dev. Cell *2*, 55-67.

Scorrano,L. and Korsmeyer,S.J. (2003). Mechanisms of cytochrome c release by proapoptotic BCL-2 family members. Biochemical and Biophysical Research Communications *304*, 437-444.

Simmen,T., Aslan,J.E., Blagoveshchenskaya,A.D., Thomas,L., Wan,L., Xiang,Y., Feliciangeli,S.F., Hung,C.H., Crump,C.M., and Thomas,G. (2005). PACS-2 controls endoplasmic reticulum-mitochondria communication and Bid-mediated apoptosis. EMBO J *24*, 717-729.

Simon,V.R., Karmon,S.L., and Pon,L.A. (1997). Mitochondrial inheritance: cell cycle and actin cable dependence of polarized mitochondrial movements in Saccharomyces cerevisiae. Cell Motil. Cytoskeleton *37*, 199-210.

Simon,V.R., Swayne,T.C., and Pon,L.A. (1995). Actin-dependent mitochondrial motility in mitotic yeast and cell-free systems: identification of a motor activity on the mitochondrial surface. J. Cell Biol. *130*, 345-354.

Singer,J.M., Hermann,G.J., and Shaw,J.M. (2000). Suppressors of mdm20 in yeast identify new alleles of ACT1 and TPM1 predicted to enhance actin-tropomyosin interactions. Genetics *156*, 523-534.

Smith,D.S., Jarlfors,U., and Cayer,M.L. (1977). Structural cross-bridges between microtubules and mitochondria in central axons of an insect (Periplaneta americana). J. Cell Sci. *27*, 255-272.

Smith,M.G., Simon,V.R., O'Sullivan,H., and Pon,L.A. (1995). Organelle-cytoskeletal interactions: actin mutations inhibit meiosis-dependent mitochondrial rearrangement in the budding yeast Saccharomyces cerevisiae. Mol. Biol. Cell *6*, 1381-1396.

Stamer,K., Vogel,R., Thies,E., Mandelkow,E., and Mandelkow,E.M. (2002). Tau blocks traffic of organelles, neurofilaments, and APP vesicles in neurons and enhances oxidative stress. J. Cell Biol. *156*, 1051-1063.

Stowers,R.S., Megeath,L.J., Gorska-Andrzejak,J., Meinertzhagen,I.A., and Schwarz,T.L. (2002). Axonal transport of mitochondria to synapses depends on milton, a novel Drosophila protein. Neuron *36*, 1063-1077.

Sugioka,R., Shimizu,S., and Tsujimoto,Y. (2004). Fzo1, a protein involved in mitochondrial fusion, inhibits apoptosis. J. Biol. Chem. *279*, 52726-52734.

Szabadkai,G. and Rizzuto,R. (2004). Participation of endoplasmic reticulum and mitochondrial calcium handling in apoptosis: more than just neighborhood? FEBS Lett. *567*, 111-115.

Szabadkai,G., Simoni,A.M., Chami,M., Wieckowski,M.R., Youle,R.J., and Rizzuto,R. (2004). Drp-1-dependent division of the mitochondrial network blocks intraorganellar Ca^{2+} waves and protects against Ca^{2+}-mediated apoptosis. Mol Cell *16*, 59-68.

Szabadkai,G., Simoni,A.M., and Rizzuto,R. (2003). Mitochondrial Ca2+ uptake requires sustained Ca2+ release from the endoplasmic reticulum. J Biol Chem. *278*, 15153-15161.

Taguchi,N., Ishihara,N., Jofuku,A., Oka,T., and Mihara,K. (2007). Mitotic phosphorylation of dynamin-related GTPase Drp1 participates in mitochondrial fission. J. Biol Chem. *282*, 11521-11529.

van Muijen,G.N., Warnaar,S.O., and Ponec,M. (1987). Differentiation-related changes of cytokeratin expression in cultured keratinocytes and in fetal, newborn, and adult epidermis. Exp. Cell Res. *171*, 331-345.

Vance,J.E. (1990). Phospholipid synthesis in a membrane fraction associated with mitochondria. J Biol Chem. *265*, 7248-7256.

Vecchione,A., Fassan,M., Anesti,V., Morrione,A., Goldoni,S., Baldassarre,G., Byrne,D., D'Arca,D., Palazzo,J.P., Lloyd,J., Scorrano,L., Gomella,L.G., Iozzo,R.V., and Baffa,R. (2009). MITOSTATIN, a putative tumor suppressor on chromosome 12q24.1, is downregulated in human bladder and breast cancer. Oncogene *28*, 257-269.

Verstreken,P., Ly,C.V., Venken,K.J., Koh,T.W., Zhou,Y., and Bellen,H.J. (2005). Synaptic mitochondria are critical for mobilization of reserve pool vesicles at Drosophila neuromuscular junctions. Neuron *47*, 365-378.

Wang,W., Sacher,M., and Ferro-Novick,S. (2000). TRAPP stimulates guanine nucleotide exchange on Ypt1p. J Cell Biol *151*.

Wasiak,S., Zunino,R., and McBride,H.M. (2007). Bax/Bak promote sumoylation of DRP1 and its stable association with mitochondria during apoptotic cell death. J. Cell Biol. *177*, 439-450.

Waterham,H.R., Koster,J., van Roermund,C.W., Mooyer,P.A., Wanders,R.J., and Leonard,J.V. (2007). A lethal defect of mitochondrial and peroxisomal fission. N. Engl. J. Med. *356*, 1736-1741.

Weihofen,A., Thomas,K.J., Ostaszewski,B.L., Cookson,M.R., and Selkoe,D.J. (2009). Pink1 forms a multiprotein complex with Miro and Milton, linking Pink1 function to mitochondrial trafficking. Biochemistry *48*, 2045-2052.

Wozniak,M.J., Melzer,M., Dorner,C., Haring,H.U., and Lammers,R. (2005). The novel protein KBP regulates mitochondria localization by interaction with a kinesin-like protein. BMC. Cell Biol. *6*, 35.

Yaffe,M.P., Stuurman,N., and Vale,R.D. (2003). Mitochondrial positioning in fission yeast is driven by association with dynamic microtubules and mitotic spindle poles. Proc. Natl. Acad. Sci. U. S. A *100*, 11424-11428.

Yamaguchi,R., Lartigue,L., Perkins,G., Scott,R.T., Dixit,A., Kushnareva,Y., Kuwana,T., Ellisman,M.H., and Newmeyer,D.D. (2008). Opa1-mediated cristae opening is Bax/Bak and BH3 dependent, required for apoptosis, and independent of Bak oligomerization. Mol. Cell *31*, 557-569.

Yang,H.C., Palazzo,A., Swayne,T.C., and Pon,L.A. (1999). A retention mechanism for distribution of mitochondria during cell division in budding yeast. Curr. Biol. *9*, 1111-1114.

Zou,H., Li,Y., Liu,X., and Wang,X. (1999). An APAF-1.cytochrome c multimeric complex is a functional apoptosome that activates procaspase-9. J Biol Chem *274*.

Zuchner,S., Mersiyanova,I.V., Muglia,M., Bissar-Tadmouri,N., Rochelle,J., Dadali,E.L., Zappia,M., Nelis,E., Patitucci,A., Senderek,J., Parman,Y., Evgrafov,O., Jonghe,P.D., Takahashi,Y., Tsuji,S., Pericak-Vance,M.A., Quattrone,A., Battologlu,E., Polyakov,A.V., Timmerman,V., Schroder,J.M., and Vance,J.M. (2004). Mutations in the mitochondrial GTPase mitofusin 2 cause Charcot-Marie-Tooth neuropathy type 2A. Nat. Genet. *36*, 449-451.

Zuchner,S. and Vance,J.M. (2006). Molecular genetics of autosomal-dominant axonal Charcot-Marie-Tooth disease. Neuromolecular. Med. *8*, 63-74.